2023

Investigation of Key Mechanisms of Contact Dependent Growth Inhibition Systems in *Burkholderia cepacia* Complex Species

Zaria K. Elery
University of Kentucky, zaria.elery@uky.edu
Author ORCID Identifier:
https://orcid.org/0009-0004-1206-6426
Digital Object Identifier: https://doi.org/10.13023/etd.2023.346

STUDENT AGREEMENT:

I represent that my thesis or dissertation and abstract are my original work. Proper attribution has been given to all outside sources. I understand that I am solely responsible for obtaining any needed copyright permissions. I have obtained needed written permission statement(s) from the owner(s) of each third-party copyrighted matter to be included in my work, allowing electronic distribution (if such use is not permitted by the fair use doctrine) which will be submitted to UKnowledge as Additional File.

I hereby grant to The University of Kentucky and its agents the irrevocable, non-exclusive, and royalty-free license to archive and make accessible my work in whole or in part in all forms of media, now or hereafter known. I agree that the document mentioned above may be made available immediately for worldwide access unless an embargo applies.

I retain all other ownership rights to the copyright of my work. I also retain the right to use in future works (such as articles or books) all or part of my work. I understand that I am free to register the copyright to my work.

REVIEW, APPROVAL AND ACCEPTANCE

The document mentioned above has been reviewed and accepted by the student's advisor, on behalf of the advisory committee, and by the Director of Graduate Studies (DGS), on behalf of the program; we verify that this is the final, approved version of the student's thesis including all changes required by the advisory committee. The undersigned agree to abide by the statements above.

Zaria K. Elery, Student

Dr. Erin C. Garcia, Major Professor

Dr. Brett Spear, Director of Graduate Studies

Investigation of Key Mechanisms of Contact Dependent Growth Inhibition Systems in *Burkholderia cepacia* Complex Species

---

DISSERTATION

A dissertation submitted in partial fulfillment of the
requirements for the degree of Doctor of Philosophy in the
College of Medicine
at the University of Kentucky

By

Zaria Katrice Elery

Lexington, Kentucky

Director: Dr. Erin C. Garcia, Assistant Professor of Microbiology, Immunology,

and Molecular Genetics

Lexington, Kentucky

2023

ABSTRACT OF DISSERTATION

Investigation of Key Mechanisms of Contact Dependent Growth Inhibition Systems in *Burkholderia cepacia* Complex Species

Burkholderia cepacia complex is a group of closely related environmental bacteria that can exacerbate disease in immunocompromised individuals. *B. cepacia* bacteria are equipped with an arsenal of mechanisms to cooperate and compete for nutrients in various polymicrobial environments. Contact-dependent growth inhibition (CDI) systems are antagonistic mechanisms widespread among proteobacteria. CDI systems consist of Two Partner Secretion pathway proteins that function to deliver the toxic C-terminal portion of the large effector exoprotein (termed 'BcpA' in *Burkholderia*-type CDI systems) to the cytoplasm of a compatible recipient bacterial cell upon direct cell to cell contact. The translocation of BcpA out of the producing cell is mediated by the outer membrane transporter, BcpB. While the production of a cognate immunity protein, BcpI, prevents autotoxicity and mediates the discrimination between kin and non-kin cells. Many *Burkholderia* CDI systems contain an accessory protein, BcpO, that can enhance specific CDI mediated killing, however the precise role remains unknown.

This body of work identifies key factors and mechanisms that influence CDI activity in *Burkholderia* species. Studies contained in this dissertation are outlined into two major sections: (i) the examination of the role the accessory lipoprotein, BcpO, plays in *B. dolosa* AU0158 CDI activity; (ii) the identification of the interaction between CDI systems produced within the same *B. cepacia* complex bacterium.

Previous work identified BcpO as an accessory protein required for maximum CDI activity for two CDI systems; however, the precise function of BcpO remains to be understood. Work done to understand the role of BcpO demonstrates that the accessory protein likely functions in a system specific manner. Immunoprecipitation and mass spectrometry analysis was used to identify potential binding partners of BcpO.

Though unsuccessful in elucidating the role of BcpO, inquiry into BcpO led to the discovery of relaxed specificity among the BcpB transporters. This work shows that various *B. cepacia* complex BcpB proteins can secrete cognate and non-cognate BcpA substrates. The promiscuity among BcpB transporters influences the interplay between CDI systems produced within the same *B. cepacia* complex bacterium. This work demonstrates that genes that encode the

CDI systems of *B. dolosa* AU0158 may not function independently. Instead, the presence of multiple CDI system proteins is required to induce specific BcpA mediated CDI killing. The examination of BcpB flexibility also led to the identification of a fourth *B. dolosa* CDI system capable of mediating interbacterial competition.

All together this dissertation adds valuable information that drives the field of CDI forward. Understanding the interactions that occur between distinct CDI systems provides further insight into the complexity of bacterial antagonism.

KEYWORDS: contact-dependent growth inhibition, *Burkholderia cepacia* complex, interbacterial antagonism, toxin-antitoxin system

Zaria Katrice Elery

(Name of Student)

06/26/2023

Date

Investigation of Key Mechanisms of Contact Dependent Growth Inhibition Systems in *Burkholderia cepacia* Complex Species

By

Zaria Katrice Elery

Dr. Erin C. Garcia
Director of Dissertation

Dr. Brett Spear
Director of Graduate Studies

06/26/2023
Date

DEDICATION

To my mom and dad, whose love has no end.

ACKNOWLEDGMENTS

I first must thank God for blessing me with such wonderful family, friends, and opportunities. To my parents (Reggie and Shayla Elery) from the small towns of Springfield KY and Port St. Joe FL, thank you for your unconditional love and encouragement. Thanks for always answering the phone just to listen to me talk about nothing. To my brother (Xavier Elery), thank you for your love and support even though I can be annoying at times.

Thank you Dr. Erin Garcia for taking a chance on me. You have given me endless support and truly made me feel valued in the lab. I especially want to thank Tanya Myers-Morales for her assistance, support, and friendship. To my committee members (Drs. Ken Fields, Brian Stevenson, and Konstantin Korotkov) thank you for the feedback and assistance throughout this process.

Finally, I must thank all the amazing friends I have made along the way. I would not have made it this far without all of you: Jamila Tucker-Worley, Mackenzie Ryan, Gabriella Kalantar, Beth Oates, Alexis Smith, Tiara Starks, Wesley Saintilnord, Brittany Rice, Nerina Jusufovic, Tatiana Castro-Padovani, Erica Phillips, Svetlana Zamakhaeva, and everyone else who has crossed paths with me along this journey.

TABLE OF CONTENTS

LIST OF TABLES

LIST OF FIGURES

CHAPTER 1. Introduction

1.1 Burkholderia genus

The genus *Burkholderia* consists of Gram-negative bacteria ubiquitously found in a diverse range of ecological niches, though often found in soil and aqueous environments (1,2). In soil, *Burkholderia* bacteria typically act as plant symbionts and prevent fungal infections (3,4). Attempts have been made to use *Burkholderia* bacteria for biological control, plant growth promotion, and bioremediation by preventing fungal infections (5). However, advancements on commercialization have been limited given that some *Burkholderia* spp. can be pathogenic to commercial crops and humans (4,6,7). Even though *Burkholderia* bacteria exist ubiquitously in nature, the first *Burkholderia* bacterium identified was isolated from an onion infection in 1950 but was classified as *Pseudomonas cepacia* (4,6,8). The *Burkholderia* genus has since been separated from the *Pseudomonas* genus based on 16S rRNA sequencing, DNA-DNA hybridization techniques, and phenotypic characteristics (9).

1.2 *Burkholderia cepacia* complex

Despite the beneficial capabilities *Burkholderia* spp. have for promoting plant growth and reversing pollution, certain *Burkholderia* spp. have been classified into the *Burkholderia cepacia* complex (Bcc) based on their ability to cause opportunistic infections in immunocompromised individuals (1). Patients with cystic fibrosis (CF) are most susceptible to Bcc infections, but these infections can also be problematic for individuals suffering from chronic

granulomatous disease (CGD). CGD is an inherited primary immune disorder that impairs the oxidative killing response of neutrophils. This allows for the survival of Bcc pathogens in the respiratory tracts of these immunocompromised patients (1,10). Similarly, due to the dysfunctional mucociliary clearance and immune response in the lungs of patients with CF, Bcc pathogens can establish long term infections (11,12). Bcc bacteria were not known to be CF pathogens until an epidemic occurred during the 1980s at the Hospital for Sick Children in Toronto. These patients experienced more severe symptoms and increased lung function decline compared to patients infected only with *Pseudomonas aeruginosa* (13). Bcc infections resulted in necrotizing pneumonia, septicemia, and rapid death; this condition is now referred to as “cepacia syndrome” (1,14). Cepacia syndrome rarely occurs in patients infected by canonical CF pathogens, such as *P. aeruginosa* and *Staphylococcus aureus.* Cepacia syndrome occurs in approximately 10% of *Burkholderia* infections (15). However, Bcc infections are of great concern among this patient population especially since Bcc bacteria are more frequently associated with person-to-person spread (15-18).

Notable Bcc pathogens are *Burkholderia cenocepacia*, *Burkholderia dolosa*, and *Burkholderia multivorans. B. cenocepacia* and *B. multivorans* have been the most virulent pathogens over the past few decades (14,19,20). *B. cepacia* complex bacteria and *P. aeruginosa* co-infections are common, but Bcc pathogens can also be the predominant organism in the CF respiratory tract during infections (21). For unknown reasons, Bcc pathogens only infect older CF

patients, typically teenagers and adults, with a median age at first induction of 20 years (22).

One of the major concerns for patients infected with Bcc bacteria is their intrinsic resistance to antibiotics, which makes Bcc infections difficult to treat clinically (1,23). Antibiotic resistance is typically mediated by drug efflux pumps, decreased outer membrane (OM) permeability to antibiotics, and degradative enzymes such as β-lactamases (21,24-26). *Burkholderia* pathogens can use penicillin and other derivatives as a sole carbon source which leads to antibiotic resistance (27). In addition to their antibiotic resistance potential, *Burkholderia* pathogens produce a variety of classical virulence factors, though roles in pathogenesis have not been demonstrated for all (1). Compared to other Gram-negative bacteria Bcc bacteria produce a unique lipopolysaccharide (LPS) layer on the outer membrane. Distinct chemical moieties that attach to Lipid A of LPS inhibit the activity of antimicrobial peptides produced during the innate immune response (28,29). Bcc LPS is also highly endotoxic and likely promotes inflammatory pathology during pneumonia and septicemia (30,31). Given that Bcc pathogens typically reside in host cells during infection, flagella are also important virulence factors (21,32,33). Interestingly, in a CF lung environment Bcc bacteria can displace other pathogenic species as the predominant organism. The precise mechanism underlying this behavior remains unknown, but some evidence suggests that a cell-cell contact dependent secretion system is responsible for this phenomenon (21,34-36).

1.3 Microbial communities

Bacteria rarely exist in single-species planktonic forms, instead they coexist in complex polymicrobial communities (37,38). Polymicrobial communities are typically described as biofilms, that can attach to biotic and abiotic sites. The microbial cells within the biofilm are usually encased in an extracellular matrix composed of self-secreted or host derived macromolecules including polysaccharides, (e)DNA, proteins, and lipids (37-39). The extracellular matrix provides protection against external environmental factors, such as antimicrobials and host immune factors. Additionally, the matrix provides space for community-coordinated gene expression, whether through direct cell-cell contact or via secreted molecules (39-41).

The ubiquity of microbial communities in the natural world suggests that living in complex groups is critical for not only bacterial ecology and evolution but also for plant and animal ecology and evolution (37). Microbial community colonization at several human body sites including, skin, oral cavity, intestinal tract, and the female reproductive tract are essential for proper host health (42-45). However, human-associated microbial communities can promote disease and have detrimental effects on their hosts. Polymicrobial infections form at sites naturally colonized by microbial communities, such as the periodontal cavity (46) and in the vagina (43,47). Additionally, these infections can occur on medical device implants (48) and in chronic wounds (49). The intrinsic nature of antibiotic resistance that occurs with biofilms makes it difficult to treat polymicrobial infections (50).

1.4 Microbial cooperation

Even though polymicrobial communities provide protection against external insults, bacteria residing in these communities are often competing for limited nutrients and space (51). To survive, bacteria use a range of strategies to mediate intra-and inter-species competition and communication. Many bacteria tend to use mechanisms such as quorum sensing (QS) to develop synergistic or antagonistic relationships within their environment. Quorum sensing, prevalent among Gram-negative and Gram-positive bacteria, is a density-dependent mechanism of intercellular communication and behavioral coordination (52,53). QS relies on the interaction of a small diffusible signal molecule (autoinducer) with a sensor or transcriptional activator to initiate gene expression for coordinated activities such as virulence factor production or biofilm formation (52-56). QS provides a benefit at the group level, but exploitative individuals could avoid the cost of producing the QS signal or performing the cooperative behavior that was mediated by QS (54,57-59). This allows non-cooperators to spread in the population. Therefore, bacteria need to employ other mechanisms to induce kin selection, to prevent non-cooperators from exploiting the public goods. Bacteria secrete antibiotics, often regulated by quorum sensing, to harm competitors which allows for the discrimination between kin and non-kin cells (57-59).

1.5 Microbial competition

Competitive behaviors are predicted to have a greater influence, compared to cooperative behaviors, on the diversification and evolution of microbial

communities (60). Bacteria have evolved to gain various antagonistic strategies to mediate interbacterial competition. In addition to antibiotics, bacteria can also secrete bacteriocins (or colicins when produced in *Escherichia coli*), small proteins or peptides that have bactericidal activity against related bacterial species (50,61). Bacteriocins can disrupt cytoplasmic cell membranes or exhibit endonuclease activity once inside the target cell. Bacteriocins are not active against the producing bacteria due to the presence of a specific immunity protein (61-63). Bacteriocin entry into target cells is dependent upon their binding to a specific surface receptor (64). Therefore, bacteriocins are not broad spectrum like some antibiotics.

In addition to secreted interbacterial factors, bacteria employ cell-cell contact dependent mechanisms to mediate competition. Specialized secretion systems, including type IV, type Vb, type VI, and type VII secretion systems (T4SS, T5bSS, T6SS, and T7SS, respectively) also act as potent antibacterial effectors. The T4SS, T5bSS, and T6SS are widespread throughout Gram-negative bacteria (65,66), while T4SS and T7SS are found in Gram-positive bacteria (67). T4SSs are ancestrally related to bacterial DNA conjugation systems, and therefore T4SSs can transfer DNA and protein substrates to recipient cells, by contact-dependent or -independent mechanisms. T7SS is a newly characterized tactic of interbacterial competition; this mechanism of activity is less characterized compared to other secretion systems (65,68). Compared to the other specialized secretion systems that mediate contact dependent interbacterial competition, the T5bSS and T6SS are the most characterized.

T6SSs consist of a group of proteins that form a double membrane spanning translocator that delivers effector proteins to recipient cells (65,66,68). T6SS provides a survival advantage and enhances pathogenicity of producing bacteria, including *Burkholderia* spp., by delivering toxins to neighboring bacteria and translocating effector proteins into host cells (69-71).

1.6 Type V secretion systems

The Type V secretion system (T5SS) secretes large exoproteins that function as adhesins, cytolysins, proteases, or contact dependent growth inhibitors (72-76). The mechanistic simplicity of T5SSs, requiring only a small set of proteins (two to three) for effector secretion, makes T5SSs unique compared to other multi-subunit secretion systems. Though T5SSs share several general features T5SSs have been divided into different families, a-e, based on domain organization and structural features. These families consist of classical auto transporter (Va), two-partner secretion (Vb), trimeric autotransporter (Vc), autotransporter phospholipases (Vd), and intimins/invasins (Ve) (75,77,78). Generally, in T5SSs the passenger domain or protein forms a long filamentous structure that frequently contain repeated sequences (79-82). The transporter component forms a transmembrane β-barrel pore that is plugged after passenger translocation (77,83,84). The process of secretion and folding is predicted to be coupled, given that no known hydrolysable energy source or electrochemical gradient is available in the periplasm to drive secretion across the outer membrane (85,86). The lack of an energy source led to the name

“autotransporter” (AT), which suggests a completely self-sufficient system for secretion (87).

Classical ATs are translated as a single polypeptide that contains an N-terminal extended signal peptide region (ESPR) followed by the passenger domain (88). The passenger domain adopts a β-helical fold and contains the functional domain that mainly acts as an adhesin, protease, or esterase (77). In families Va, Vc, Vd, and Ve, the effector (“passenger”) domain is fused to the membrane domain and is autonomously secreted. For the Vb family, the passenger protein (generically named “TpsA”) is distinctly separated from the transporter (TpsB). Therefore, Vb subtype is not considered an autotransporter, instead the Vb subtype is generically referred to as the Two-Partner secretion (TPS) pathway (75,89,90). TpsA proteins most closely parallel the passenger domains of ATs. TpsA proteins contain extended N-terminal signal peptide and filamentous repeats that form long β-helical structures (90,91). The TpsB transporter protein contains two N-terminal polypeptide transport associated (POTRA) domains that are necessary for substrate recognition (80,91,92). The Vc family consist of trimeric autotransporters (TATs), like ATs, TATs begin with an N-terminal ESPR followed by the passenger domain which contains the functional and structural domains (88). However, unlike ATs, the passenger domain of an individual TAT polypeptide only contains one-third of the fully functional passenger domain. Similarly, the β-barrel domains trimerize to assemble a complete integral OM β-barrel (93,94). Trimeric autotransporters are thought to be adhesins that mediate biofilm formation and adherence of the

bacteria to host tissues (93-95). The Vd family is a recently discovered class of ATs that resembles a hybrid of Va and Vb systems. Most studies examining the Vd family focus on the prototypical members PlpD from *P. aeruginosa* and FplA from *Fusobacterium nucleatum* (96,97). The C-terminal β-barrel domain consist of 16 β-strands similar to TpsB proteins, although Vd ATs only contain one POTRA domain instead of the two found in TpsB (78). So far the only identified function of Vd passenger domains has been lipase/esterase activity (97,98). The Ve family consist of intimins and invasins that have a domain organization that differs from ATs and TATs. Intimins/invasins have a reverse order in which the β-barrel domain is N-terminal to the C-terminal passenger domain (99,100). Proteins of the intimins/invasins Ve family are commonly thought to be adhesins that are important for host cell invasion during infection (101-103).

1.7 Overview of Two-Partner Secretion

The Two-Partner Secretion (TPS) system, consist of two distinct proteins; the secreted passenger protein and its outer membrane transporter (75,90). The genes coding for a TPS system are typically a part of the same operon but other genetic arrangements have been observed (90). The specificity of a TpsB transporter for its cognate partner varies between systems. Many TpsB transporters can only secrete one cognate TpsA while others are more promiscuous and can secrete several TpsA proteins (75,104). The mechanism that leads to the variation in TpsB specificity seems to be dependent on specific domains in both TpsA and TpsB proteins. The TpsA proteins consist of a N-

terminal ESPR followed by the Two Partner Secretion domain (TPS domain), which is a hallmark feature of TpsA proteins that is important for protein secretion across the OM (75,105). Beyond the TPS domain, the TpsA polypeptide content varies drastically, but there is a great deal of evidence that suggest a conserved β-helical structure (80,81,91).

The TpsB protein is an integral OM β-barrel transporter, resembling the C-terminal β-domain of ATs (75,106). The TpsB proteins belong to the Omp85 superfamily, along with BamA, the major subunit of the β-barrel assembly machinery (BAM). Omp85-like proteins are one of the most widely distributed classes of OMPs across nature, as they are present in mitochondria, chloroplasts, and Gram-negative bacteria (107,108). Proteins belonging to Omp85 superfamily have between one to five N-terminal POTRA domains that play a role in substrate secretion (107-109). Despite the limited conservation of amino acids sequences, these domains typically consist of a conserved secondary structure that arranges into a globular conformation (104,110). TpsB proteins contain in an N-terminal signal peptide followed by two POTRA domains which are required for translocation of TpsA proteins across the OM (92,109-112). The recognition of a TPS domain by TpsB transporters seems to be dependent on specific motifs within the TPS domains and not on the overall sequence homology between these domains (104,110). A ~300 aa β-barrel domain follows the POTRA domain. Generally, the TpsB β-barrel consists of 16 anti-parallel β-strands with both the N- and C- termini facing into the periplasm. The β-strands are connected by a series of short periplasmic turns and longer

extracellular loops (108,109,111,113). The loop 6 (L6) typically occupies the pore and forms a “lid-lock” structure through interactions with the β-strands (113,114). The flexibility of the β1-β16 strands has also been shown to be essential for substrate secretion (114).

A major question that remains to be answered is how the folding of the T5SS proteins is controlled and what is the energy source or mechanism driving translocation? To date two models of translocation have been proposed. The first postulates that the TpsA protein forms a hairpin in the pore. Throughout the process of secretion TPS domain remains bound to the POTRA domains, while the rest of the protein is progressively translocated and folds at the cell surface (106). An alternative model predicts that the TPS domain reaches the surface first and nucleates the folding of the rest of the protein (115). Several pieces of evidence suggest that both mechanisms are at play depending on the TpsA substrate being translocated (81,116-118). Therefore, the mechanism of translocation is likely specific to each TpsA protein and is probably dependent on its function. One aspect of secretion that is consistent between both models is the role of the ESPR, which is present in many TpsA proteins. The N-terminal ESPR is necessary for TpsA secretion across the IM via the Sec machinery. The ESPR does not mediate secretion across the OM. However, it has been hypothesized to slow down export of T5SS proteins and prevent TpsA from misfolding in the periplasm prior to translocation across the OM through TpsB (119-121).

Though T5SS are generally considered self-sufficient, other factors are involved in secretion and activity of these systems. As with other OM proteins, the T5SS transporter domains or proteins are inserted into the OM via the BAM complex (122,123). Additionally, periplasmic chaperones and proteases have been demonstrated to interact with unfolded ATs and other T5SS effectors; presumably to prevent premature protein secretion or misfolding (121,124,125).

Even though the specific function of many TpsA proteins have not been determined, some studies provide insight into how TPS and other T5SSs may be regulated. Many TPS operons have been described to be upregulated upon bacterial entry into the host (95,126). Signal transduction systems have been the most identified regulators for *tps* operons in several bacterial species. In *B. pertussis* the *fhaBC* TPS system has been shown to be under the control of the BvgAS two-component system (127). In *P. aeruginosa*, the *cdrAB* TPS operon is regulated by the intracellular levels of c-di-GMP (128).

Based on work examining two well characterized TPS system, the FHA of *Bordetella pertussis* and the HMW1 system of *Haemophilus influenzae,* many TpsA proteins have been identified to serve as adhesins, cytolysins, iron sequesters, and regulators of host responses (72-75). However, other systems have been identified to mediate interbacterial competition among closely related bacteria (76). This has led to the identification of a new class of TpsA effectors that function as contact dependent growth inhibitors (CDI) (76). The effects of CDI systems are based on kin vs non-kin recognition mediated by specific immunity proteins (76,129,130). With these toxin-antitoxin systems, the range of

TPS effector functions has been extended to include interbacterial killing and interbacterial signaling (76,131).

1.8 Contact dependent growth inhibition systems

Contact dependent growth inhibition (CDI) systems, which consist of TPS proteins, was first discovered in an *E. coli* strain EC93 isolated from commercial rat fecal pellets. The EC93 strain had a competitive advantage over the *E. coli* K12 strain, that was not mediated by soluble factors but instead required direct cell-to-cell contact (76). Further bioinformatic analysis revealed genes predicted to encode CDI systems are widespread in Proteobacteria (130,132). Moreover, this investigation revealed that a key component of these systems are immunity proteins, which protect against CDI toxins (76,132).

CDI systems are separated into two major classes: the *E. coli*-type and the *Burkholderia*-type systems. *E. coli*-type systems are found in α-,β-, and γ-proteobacteria, whereas *Burkholderia*-type systems, to date, are limited to members of the *Burkholderia* genus (130,132). The major difference between the two CDI classes is the operon gene order. *E. coli*-type systems are encoded by *cdiBAI* loci (76), while *Burkholderia*-type systems are encoded by *bcpAI(O)B* loci (130) **(Fig. 1.1A).** Another difference between the CDI classes is the presence of *bcpO* genes in some *Burkholderia*-type CDI loci (130,133,134).

1.9 *Burkholderia* CDI classification

The *Burkholderia*-type CDI systems are further divided into two phylogenetic groups based on the homology of the amino acid sequence of the

BcpB and BcpO proteins, and the N-terminal domain of the BcpA proteins (130). The amino acid sequence of the class I and class II BcpO proteins have no similarities to each other or any characterized proteins or protein domains. The class I *bcpO* genes are predicted to encode for an outer membrane lipoprotein, based on the presence of a lipobox in the signal peptide (130,133). No clear role exists for BcpO proteins, however *Burkholderia thailandensis* strain E264 and *Burkholderia dolosa* strain AU0158 mutants lacking the class I *bcpO* genes exhibit a reduced level of CDI mediated killing against recipient cells (130,133).

1.10 CDI mechanism

Despite the differences in genetic make-up, *E. coli*-type and *Burkholderia*-type CDI systems generally function in a similar manner **(Fig. 1.1B)**. The CdiA/BcpA proteins are large exoproteins (typically >3000 amino acids) containing filamentous hemagglutinin (FHA) repeats. The C-terminal portions of CdiA/BcpA (CdiA-CT/BcpA-CT) contains the antibacterial toxins of CDI systems (76,130,132,135). Typically, the highly variable toxin domain is marked by conserved amino acid motifs, VENN in *E. coli*-type systems and Nx(E/Q)LYN in *Burkholderia*-type systems (130,132). However, exceptions to these demarcations have been identified as more CDI systems have been characterized (134). To date most of the characterized CdiA-CTs/BcpA-CTs have been shown to be or are predicted to function as nucleases, degrading DNA or tRNA within recipient cells (136,137). The conserved N-terminus of CdiA/BcpA contains the FHA domains that extend into the extracellular milieu and are capped by the receptor binding domain (RBD), while the toxic CdiA-CT/BcpA-CT

domain remains in the periplasm. The CdiB/BcpB (TpsB) proteins are OM β-barrel proteins that allow for the translocation of the CdiA/BcpA (TpsA) passenger proteins. Consistent with other TPS, the CdiA/BcpA proteins are likely progressively folded at the cell surface during translocation through CdiB/BcpB (135). Additionally, a key component of CDI systems are the CdiI/BcpI immunity proteins, which provide protection against CDI toxins. The immunity proteins function to block autotoxicity in cognate CDI protein producing cells, as well as protect cells from CDI-mediated killing by the same CDI system encoding locus produced in a different bacterium (76,132). The amino acid sequence of the CdiA-CT/BcpA-CT toxins and their cognate CdiI/BcpI proteins co-vary, resulting in system specific recognition, which likely leads to kin vs non-kin discrimination (130,132).

1.11 Recipient cell CDI receptors

In addition to the proteins encoded by the CDI locus, BcpA-CT/CdiA-CT intoxication is dependent upon specific recipient cell surface exposed and internal receptors (138-141). Studies examining *E. coli* CDI systems suggest that the donor cell CdiA interacts with a specific outer membrane receptor on the recipient cell surface, triggering CdiA-CT release from the donor cell (135,140). *E. coli*-type CDI systems are divided into different classes (class I-V) based on their predicted recipient cell receptors. The amino acid sequence variations that separate the class I, II, and III CdiA proteins are mainly found in the receptor-binding domain, which is located between FHA repeats (138,140,142). The well characterized class I $CdiA^{EC93}$ binds to major subunit of the β-barrel assembly

machinery complex, BamA (138). The Class II CdiA proteins, consisting of $CdiA^{EC536}$, recognize heterotrimers of the osmoporins OmpF and OmpC (139). The class III CdiA proteins, including $CdiA^{STEC3}$, recognize the nucleoside transporter, Tsx (140). The CdiA proteins from the fourth *E. coli* class contain divergent FHA-1 and RBD regions suggesting the use of different recipient cell receptors (140). The core oligosaccharide of LPS is used as a sensor or receptor for the class IV $CdiA^{STEC4}$ effector (142). The cell surface receptor for class V *E. coli* CdiA proteins, has yet to be identified. Outer membrane receptors have not been identified for *Burkholderia*-type CDI systems. Although alterations to the LPS on *B. dolosa* led to recipient cell resistance to two distinct BcpA proteins (143). Additionally, alterations to the *B. thailandensis* LPS has been shown to disrupt entry of a *Burkholderia pseudomallei* BcpA-CT toxin (144).

Translocation of the CdiA-CT region from the periplasm into the recipient cell cytoplasm is likely dependent on the uncharacterized CdiA-CT entry domain, which recognizes a specific inner membrane protein. Majority of the identified *E. coli* CDI IM receptors are inner membrane components of multidrug transport complexes. The ABC transporter membrane permease, AcrB, is the recipient cell IM receptor necessary for $CdiA^{EC93}$ intoxication (138). The filamenting temperature-sensitive H (FtsH) protein is the IM receptor required for $CdiA^{EC536}$ (145,146).The permease components, GltJ/GltK of a glutamate/aspartate transporter have been shown to be inner membrane receptor for multiple CDI toxins (146,147). Fewer inner membrane transporters have been identified for *Burkholderia*-type CDI systems. The inner membrane permeases Bth_II059 and

GltJ/GltK have been shown to mediate the import of the $BcpA_{II}$-CT^{1026b} and BcpA-2 from *B. pseudomallei* and *B. multivorans*, respectively (146,147).

1.12 CDI recipient cell permissive factors

Additional recipient cell permissive factors have been shown to be required for some CdiA-CT/Bcp-CT toxin activity (141). This phenomenon was first identified for the uropathogenic *E. coli* 536 CdiA-CT^{EC536} toxin, which requires an enzyme involved in cysteine biosynthesis, CysK (O-acetylserine sulfhydrylase A), for toxin activation (148,149). Several *E. coli* CDI toxins, including CdiA-CT^{Kp342}, require the translation Elongation Factors Thermo-Unstable (EF-Tu) and Thermo-Stable (EF-Ts) proteins as well as the nucleotide guanosine 5' – triphosphate (GTP) for CDI activity (150,151). Additionally, proton motive force energy produced in recipient cells is required for the delivery of several different classes of CdiA-CT toxins to the cytoplasm of the recipient cell (145). Currently, there are no known recipient cell toxin activators for *Burkholderia*-type CDI systems. Although, evidence suggest that metabolic and regulatory networks many directly or indirectly influence CDI efficiency of two *B. dolosa* CDI systems, though the mechanism is unknown (143). The limited success in identifying *Burkholderia*-type CDI recipient cell factors, highlights the importance of further examination of the mechanisms of CDI outside of *E. coli* strains. Especially since current evidence suggests that there are some differences between the mechanisms of *E. coli*-type and *Burkholderia*-type CDI systems.

1.13 CDI regulation

A major area of unknown regarding the mechanisms of CDI systems pertains to the regulation of CDI encoding loci. The *E. coli* EC93 *cdi* system is unique, in that under laboratory conditions bacteria constitutively express this system, while *cdi* encoding genes are tightly regulated in other bacteria (76,130,152). However, many *cdi* systems found in other *E. coli* strains, and other proteobacteria, are not expressed under the same laboratory growth conditions (133,134,153,154). A variety of plant pathogens, such as *Erwinia chrysanthemi* EC16 and *Dickeya dadantii* 3937, selectively express their *cdi* genes only during specific host colonization (132,153). As with some CDI systems in *E. coli* strains, several *Burkholderia cdi* loci are not active under native expression or only exhibit low levels of activity (133,134). Examination of *BtE264* regulation revealed that *bcpA* is differentially expressed within a population of bacteria. It was observed that *bcpA* was only expressed in a small portion of bacteria, ~1:1,000. However, *bcpA* was highly expressed in these cells under laboratory conditions (130). Additionally, it was observed that the *bcpAIOB* genes were expressed in a stochastic manner under planktonic conditions. In *P. aeruginosa* PAO1, a transcriptional repressor, RsmA, was identified as a negative regulator of two distinct CDI systems (155). Future work examining the regulation of *cdi* encoding loci will aid in the understanding of how and why CDI systems differ.

1.14 Other roles of CDI systems

In addition to the growth inhibitory activity of CdiA/BcpA proteins, other functions have been implicated for these proteins. The *E. coli* EC93 CdiA promotes intraspecies intracellular adhesion by binding to BamA or by forming CdiA-CdiA interactions, thus promoting biofilm formation (138,156). In *B. thailandensis,* the gene expression of sisters cells can be altered via delivery of BcpA toxins to these immune cells. These phenotypic changes lead to enhanced biofilm formation and other cooperative behaviors; this phenomenon has been termed contact-dependent signaling (CDS) (131). However, to date, CDS has not been observed with any other *Burkholderia* CDI systems. Many *Burkholderia* CDI systems are not activate under typical laboratory conditions, therefore further evaluation of the regulation of these systems may reveal alternative functions for these systems. Some CDI systems in other pathogenic bacteria, such as *P. aeruginosa* and *A. baumannii,* have been described to act as virulence factors. These CDI systems can coordinate group behaviors and facilitate competition with other bacteria present in the host (157,158). For most CDI systems, it is not known when these systems are active and provide a fitness advantage. Therefore, further elucidation of the mechanisms and regulation of CDI systems may lead to the discovery of new functions for CDI proteins.

1.15 Objectives of this Dissertation

As more CDI systems are continuously being identified in pathogenic bacteria, it is becoming more apparent that CDI systems are likely involved in many aspects of bacterial interactions, ranging from antagonistic interactions to coordinating group behaviors. Therefore, investigating both well characterized and newly identified CDI systems is necessary to understand the contributions CDI systems provide in shaping polymicrobial communities. Since the mechanism of BcpA delivery out of the donor cell and into a recipient cell is incompletely understood. We used the pathogenic *Burkholderia dolosa* AU0158 strain as model organism to address the following aims:

Aim 1: Characterize the role the *B. dolosa* accessory BcpO protein plays in BcpA-1 mediated CDI activity.

Aim 2: Examine the interplay between CDI systems produced within the same *B. cepacia* species.

Figure 1.1 Diversity of CDI systems and *Burkholderia*-type CDI model

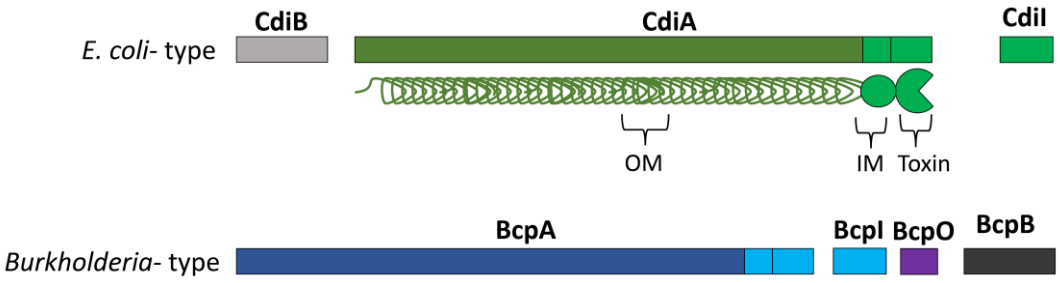

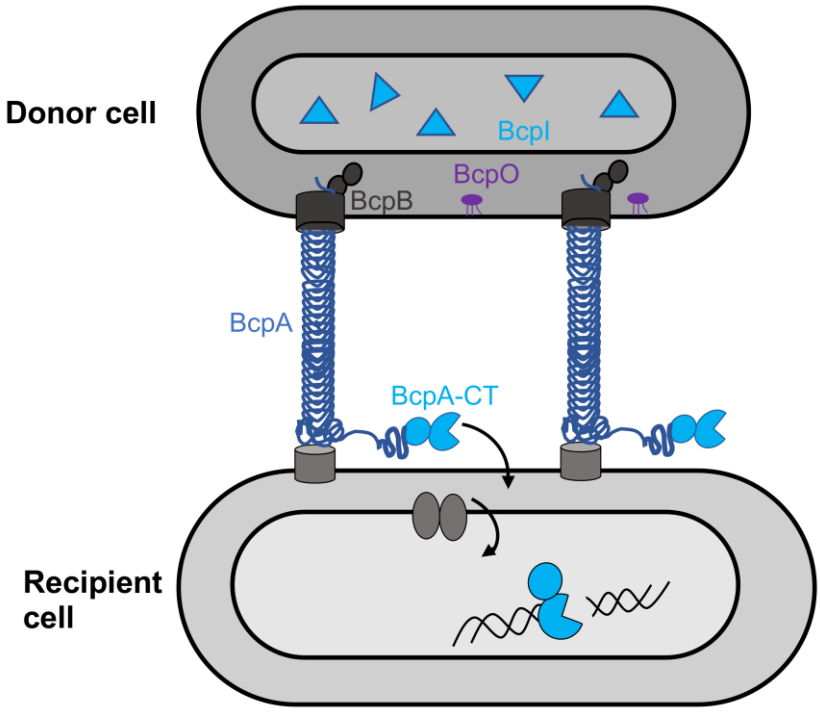

(A) Schematic of CDI proteins encoded by *cdiBAI* and *bcpAIOB* loci for *E. coli*-type and *Burkholderia*-type CDI systems, respectively. Cartoon structure of CdiA marks the CdiA-CT effector domain and the domains that are predicted to interact with the recipient cell OM and IM receptors. Adapted from Ruhe et al., 2017. **(B)** The CDI system-producing cell (donor cell) displays BcpA on the cell surface by translocation through BcpB. The toxic CT domain (BcpA-CT) remains within the periplasm of the donor cell before delivery to the recipient cell. Once the BcpA receptor binding domain interacts with the recipient cell OM receptor the BcpA-CT is delivered to the target cell. The BcpA-CT toxin will act to inhibit the growth of the recipient cell unless the recipient produces the cognate immunity protein. The BcpI immunity proteins remain in the cytoplasm of the donor cell and protects against autotoxicity. The accessory protein BcpO, is a predicted OM lipoprotein that may assist in the secretion or stability of BcpA. Model adapted from Ruhe et al., 2018.

CHAPTER 2. Methods and materials

2.1 Bacterial strains and growth conditions

All strains used in this body of work are listed in Table 2.1. All *Burkholderia* strains were maintained in low salt Luria-Bertani media (LSLB, NaCl concentration of 5 g/L). Antibiotics were added to select for growth of *Burkholderia dolosa* AU0158 (*Bd*AU0158) and *Burkholderia multivorans* CGD2M (*Bm*CGD2M) strains at the following concentrations: 250-500 µg/ml kanamycin or 50-125 µg/ml tetracycline. Plasmids were maintained in *Escherichia coli* DH5α and delivered to *Burkholderia* strains using a conjugation donor strain *E. coli* RHO3, a 2,6 Diaminopimelic acid (DAP) auxotroph. *E. coli* strains were maintained in LSLB, and antibiotics were added at the following concentrations when appropriate: 100 µg/ml ampicillin, 50 µg/ml kanamycin, 25 µg/ml tetracycline, or 200 µg/ml DAP. All strains were grown overnight with aeration at 37°C, unless otherwise indicated.

2.2 Genetic manipulation

All plasmids used in this body of work are listed in Table 2.2. Plasmid inserts were confirmed by DNA sequencing (Eurofins Genomics or ACGT, Inc.) and bacterial mutant strains verified by PCR. Plasmids to deliver cassettes to a neutral *att*Tn7 site on the *Bd*AU0158 and *Bm*CGD2M chromosomes were constructed using the pUC18Tmini-Tn7T backbone (159). Cassettes for generating antibiotic resistant strains were delivered to the *Bd*AU0158 or *Bm*CGD2M chromosome via triparental mating with *E. coli* RHO3 strains

harboring either pUC18T-miniTn7-Km (for kanamycin resistance) or pUC18T-miniTn7-Tet (for tetracycline resistance) and the *E. coli* RHO3 strain harboring the transposase-encoding helper plasmid pTNS3 (130). The pEXKm5 allelic exchange vector (160) was used to generate unmarked, in-frame deletion mutations in *Burkholderia* spp. Briefly, ~500 nucleotides 5' to and including the first three to seven codons of the gene to be deleted were fused to ~500 3' to and including the last three to last 20 codons of the gene by overlap extension PCR and cloned into pEXKm5. To complement *Bd*AU0158 and *Bm*CGD2M deletion mutants, genes of interest were cloned into pUCS12Km or pUCS12Tet (pUC18T-miniTn7-Km plasmid with the promoter of the *Burkholderia thailandensis* constitutive ribosomal S12 subunit gene cloned immediately 5' to the multiple cloning site) and these P_{S12}-driven constructs were delivered to a neutral *att*Tn7 site on the chromosome via triparental mating with *E. coli* RHO3 harboring pTNS3.

For in-frame deletion of *Bd*AU0158 *bcpB-1,* fragments containing a region of 560 bp 5' to the ORF (including the first 3 codons of *bcpB-1*) and 522 bp 3' to the ORF (including the last 7 codons) were constructed. For deletion of *Bd*AU0158 *bcpB-2,* fragments containing a region of 552 bp 5' to the ORF (including the first 3 codons of *bcpB-1*) and 522 bp 3' to the ORF (including the last 7 codons) were constructed. For deletion of *Bd*AU0158 *bcpB-2,* fragments containing a region of 552 bp 5' to the ORF (including the first 3 codons of *bcpB-2*) and 549 bp 3' to the ORF (including the last 6 codons) were constructed. For deletion of *Bd*AU0158 *bcp-4,* fragments containing a region of 446 bp 5' to the

ORF (including the first 7 codons of *bcpA-4*) and 495 bp 3' to the ORF (including the last 20 codons of *bcpB-4*) were constructed. For deletion of *Bm*CGD2M *bcpB-2,* fragments containing a region of 507 bp 5' to the ORF (including the first 7 codons of *bcpB-2*) and 505 bp 3' to the ORF (including the last 11 codons) were constructed. The fragments for *Bd*AU0158 *bcpB-1*, *bcpB-2, bcp*-4, and *Bm*CGD2M *bcpB-2* were joined by overlap PCR cloned into pEXKm5 by restriction digestion, resulting in plasmids pZKE12, pZKE11, pEDP03, and pTMM078, respectively.

For deletion of *Bd*AU0158 *bcpB-3* and *bcpB-4,* the deletion fragments were flanked by restriction sites and purchased from ThermoFisher (GeneArts Strings Gene Synthesis). For *bcpB-3* the region contained 576 bp 5' to the ORF (including the first 3 codons of *bcpB-3*) and 528 bp 3' to the ORF (including the last 6 codons of *bcpB-3*). For *bcpB-4* the region contained 238 bp 5' to the ORF (including the first 58 codons of *bcpB-4*) and 546 bp 3' to the ORF (including the last 6 codons of *bcpB-4*). These fragments were cloned into pEXKm5 by restriction digestion, resulting in plasmids pZKE16 and pZKE24, respectively.

To generate complementation plasmids for *Bd*AU0158 *bcpB-1*, *bcpB-2*, *bcpB-3,* and *bcpB-4,* the ORFs were cloned by restriction digestion into pUCS12 (130), 3' to the strong, constitutive promoter P_{S12} (*B. thailandensis* E264 *rpsL* gene promoter), resulting in plasmids pZKE13, pZKE14, pZKE15, and pEDP02, respectively. Similarly, *Bm*CGD2M *bcpB-1* and *bcpB-2* were PCR amplified and cloned into pUCS12, resulting in plasmids pZKE18 and pZKE19, respectively. *Bd*AU0158 *bcpO* was cloned with a 3' primer that added either one or three (3x)

FLAG epitopes to the C-terminus, resulting in plasmids pZKE02 and pZKE06, respectively. All complementation plasmids were delivered to *att*Tn7 in the *Bd*AU0158 or *Bm*CGD2M genome via triparental mating with helper plasmid pTNS3 as previously described (143,161). To complement the *bcp-4* locus deletion mutant with *bcpI* genes, the *Bd*AU0158 *bcpI-4* and *Bm*CGD2M *bcpI-2* genes were PCR amplified and cloned 3' P_{S12} in pUCTet (130), resulting in plasmids pEDP01 and pECG70, respectively.

For strains constitutively expressing *bcpA-4*, approximately 500 nucleotides 3' to the *bcpA-4* translational start site was PCR amplified and cloned immediately 3' to the P_{S12} promoter of plasmid pUCS12, resulting in plasmid pTMM086. Similarly, plasmids for constitutive expression of *bcpA-1* (pS12AP6), *bcpA-2* (pS12AP7), and *bcpA-3* (pAP29) were generated as previously described (133,143). These plasmids were mated into *Bd*AU0158 strains without the pTNS3 helper plasmid (to prevent *att*Tn7 site delivery). Kanamycin-resistant colonies that carried pS12AP6, pS12AP7, pAP29, or pTMM086 cointegrated 5' to *bcp-1*, *bcp-2*, *bcp-3,* or *bcp-4* were obtained and confirmed by PCR, resulting in the positioning of the P_{S12} immediately 5' to the chromosomal copy of each *bcp* locus, similar to previously described strains (133,143). These strains were routinely cultured with kanamycin to select for plasmid retention.

DNA fragments corresponding to *bcpO* containing two nucleotide changes (GAG to GCA) to generate $bcpO_{E22A}$ and one nucleotide change to generate $bcpO_{C21S}$ (TGC to TCC) point mutants, were purchased from ThermoFisher (GeneArts Strings Gene Synthesis). The $bcpO_{E22A}$ and $bcpO_{C21S}$ fragments were

inserted into the pUCS12 backbone resulting in plasmids pZKE04 and pZKE05, respectively.

To construct the β-galactosidase reporters, a ~500 bp fragment upstream of *bcpA-1*, *bcpA-2*, *bcpA-4, or bcpB-4* ORF were PCR-amplified and cloned 5' to a promoterless *lacZ* in pUC*lacZ*, resulting in plasmids, pECG99, pECG100, pZKE20, and pZKE21, respectively. The reporter cassettes were delivered to an *att*Tn7 site in the *Bd*AU0158 genome as described above. Control reporters P_{neg}-*lacZ* and P_{S12}-*lacZ* and the previously generated *bcp-3* reporter, pAP24 (133), were also delivered to an *att*Tn7 site in the *Bd*AU0158 genome.

For cloning of the TpsA constructs, nucleotides encoding the N-terminus, including the signal sequence, TPS domain, and part of the FHA repeats, of *bcpA-1* (nucleotides 1-1,602) and *bcpA-2* (nucleotides 1-1,713) were amplified with a 3' primer that added a FLAG epitope tag. Fragments were cloned into pUCS12 via restriction digestion resulting in plasmids pZKE22 and pZKE26.

DNA fragments containing chimeric *bcpB-1* of *Bd*AU0158 were ordered from ThermoFisher (GeneArts Strings Gene Synthesis). Chimeric gene *bcpB-1*^{Chim1} consists of *Bd*AU0158 *bcpB-1* coding sequence with nucleotides 283-495 replaced with nucleotides 280-492 from *Bd*AU0158 *bcpB-2*. Chimeric gene *bcpB-1*^{Chim2} consist of *Bd*AU0158 *bcpB-1* coding sequence with nucleotides 283-495 and 499-657 replaced with nucleotides 280-492 and 496-654 from *Bd*AU0158 *bcpB-2*, respectively. Chimeric gene *bcpB-1*^{Chim3} consists of *Bd*AU0158 *bcpB-1* coding sequence with nucleotides 76-207 replaced with nucleotides 94-279 from *Bd*AU0158 *bcpB-2*. Chimeric gene *bcpB-1*^{Chim4} consists of *Bd*AU0158 *bcpB-1*

coding sequence with nucleotides 76-207, 283-495, and 499-657 replaced with nucleotides 94-279, 280-492, and 496-654 from *Bd*AU0158 *bcpB-2*, respectively. Restriction digestion was used to clone *bcpB-1*^{Chim1}, *bcpB-1*^{Chim2}, *bcpB-1*^{Chim3}, and *bcpB-1*^{Chim4} into pUCS12 downstream of P_{S12}, resulting in plasmids pZKE23, pZKE29, pZKE30, and pZKE31, respectively.

2.3 Growth curves

One milliliter of *Bd*AU0158 cells from an overnight culture were pelleted at 15,000 x g for 2 min and resuspended in sterile phosphate- buffered saline (PBS). Twenty-five milliliters of LSLB were inoculated to an OD_{600} = 0.025. Cultures were grown at 37°C on a shaker for 28 h with OD_{600} measurements taken periodically (~2 h first 10 h). Two independent experiments were performed in triplicate.

2.4 Interbacterial competition assays

Interbacterial competition assays were performed as previously described (133,134,143) with modifications. *Bd*AU0158 or *Bm*CGD2M strains carrying antibiotics resistance markers at *att*Tn7 sites were cultured overnight without antibiotics and resuspended in sterile PBS to an OD_{600} of 2, unless otherwise indicated. The donor and recipient bacteria were marked with Kan and Tet resistance markers, respectively. Donor and recipient bacteria were mixed at a 1:1 or 10:1 ratio, and 5 µl or 20 µl spots of the mixture was plated in triplicate on LSLB agar without antibiotic selection. The competition plates were incubated at 37°C for 24-48 h, unless otherwise indicated. The input ratio (donor to recipient)

was determined by plating the co-culture inoculum on antibiotic plates (LSLB Kan_{250} or Tet_{50}). Following 24-48 h, co-culture whole colony spots or cells sampled from the edge of the colony biofilms were resuspended in 1 ml of sterile PBS and serially diluted. Spots (20 µl) of serial dilutions were plated on antibiotic plates (LSLB Kan_{250} or Tet_{50}) and incubated at 37°C for 48 h. Colony counts for donor and recipient bacteria at the start (0 h) and 24 h or 48 h time points were used to determine the competitive index (C.I.). The competitive index was calculated as a ratio of donor strain to recipient strain at 24 h (or 48 h) divided by the input (donor to recipient) ratio at 0 h. A positive $\log_{10}$ C.I. indicates the donor strain outcompeted the recipient strain. A negative $\log_{10}$ C.I. indicates the recipient strain outcompeted the donor strain and a $\log_{10} \approx 0$ C.I. indicates no competitive advantage for either strain. At least two to three independent experiments were performed in triplicate (with three biological replicates), unless otherwise noted.

2.5 Reverse Transcriptase qualitative PCR (RT-qPCR)

*Bd*AU0158 strains cultured in LSLB overnight were spotted in triplicate at 2 OD/ml (20 µl) onto LSLB agar plates and incubated overnight at 37°C. Total RNA was extracted from colony spots using the RNaesy Protect Bacteria Minikit (Qiagen), DNA Free Kit (ThermoFisher), and Zymo RNA Clean and Concentrator, according to manufacturer's protocols with minor modifications. Approximately 800 ng of subsequent RNA was used to prepare a cDNA library using the SuperScript IV (SSIV) First-Strand synthesis system (Invitrogen) according to the manufacturer's protocol. No Reverse Transcriptase controls (no

RT) were set up for DNA contamination. cDNAs were then diluted 1:10 (or 1:5) in nuclease-free water prior to qPCR analysis. RT-qPCR reactions containing iTaq Universal SYBR Green Supermix were performed in 96 well plates in the CFX Opus real-time PCR system (BioRad). Samples lacking reverse transcriptase enzyme (NRT), or no template controls (NTC) were prepared and assayed in tandem to ensure efficient depletion of contaminating DNA. Melting curves were generated to validate the presence of single products. Results were analyzed using CFX Maestro software. Comparisons were made using the $\Delta\Delta C_T$ method (162) normalized against the *recA* (163) housekeeping gene in the wild-type strain.

2.6 Subcellular fractionation and secretion assay

Subcellular fractionation of *Bd*AU0158 was perform as previously described (147) with modifications. Bacterial strains were cultured overnight at 37°C with agitation in LSLB. Cells were harvested by centrifugation at 12,000 x g for 15 min at 4°C. The resulting pellet was resuspended to 8 OD/ml in Tris resuspension buffer (50 mM Tris, pH 8 supplemented with Roche Complete Mini EDTA-free Protease Inhibitor Cocktail and Pierce Universal Nuclease) and incubated on ice ~30 min. For TpsA secretion assays, proteins were precipitated from the culture supernatants with 15% Trichloroacetic acid (TCA), washed with acetone, and resuspended in 10 mM Tris, pH 8 with 2% sodium dodecyl sulfate (SDS) (Tris/SDS buffer).

For subcellular fractionation, cells were broken by three passages through a chilled French Pressure cell (40,000 lb/in^2), and unbroken cells and large debris were removed by two centrifugations at 12,000 x g at 4°C for 15 min. Total membranes were separated by ultracentrifugation for 15 min at 100,000 x g at 20°C and supernatants collected to analyze the cytoplasmic fractions. Total membranes were washed with Tris resuspension buffer and the resulting pellet was resuspended in Tris/SDS buffer.

For selective detergent fractionations, total membrane pellets were resuspended in Tris resuspension buffer + 2% Triton X-100, incubated at room temperature for 30 min, then separated by ultracentrifugation for 15 min at 100,000 x g at 20°C. The supernatant containing the soluble inner membrane fraction was collected and concentrated. The insoluble outer membrane pellet was washed in Tris resuspension buffer + 2% Triton X-100, centrifuged, and then resuspended in Tris/SDS buffer.

For sucrose density gradient fractionations, total membrane pellets were resuspended in TE (50 mM Tris, pH 8 + EDTA) + 20% sucrose, and loaded on top of a 2.5 ml sucrose gradient prepared with 0.7 ml of 70% sucrose and 1.8 ml of 53% sucrose. The gradient was centrifuged at 100,000 x g for 2 h. The inner membrane fraction was collected from the top band and the outer membrane fraction was collected from the bottom band. The fractions were washed in TE buffer, centrifuged for 30 min at 100,000 at 20°C, and solubilized in 4X sample buffer.

The whole cell lysate, cytoplasmic fractions, and Triton X-100 soluble inner membrane fractions were concentrated by methanol-chloroform precipitation, and resulting pellets were suspended in Tris/SDS buffer. Protein concentrations were determined by microplate Bicinchoninic Acid (BCA) assay using Bovine serum albumin (BSA) standards (Pierce).

2.7 Pulldown assay

Cells from overnight Δ*bcpO and* Δ*bcpO::bcpO-*$_{3xFLAG}$ cultures were pelleted and resuspended in Tris HCl + 2% Triton X-100 supplemented with nuclease and EDTA-free protease inhibitor to 20 OD/ml. Cells were broken via French press and unbroken cells were removed, as previously described. Cleared lysate was mixed with M2 FLAG Magnetic Beads (Sigma) and incubated on a rotator for 1 h and 45 min at room temperature. Beads were pulled down by magnet, decanted, and washed four times with Tris Buffered saline (TBS). The remaining bound proteins were eluted from the beads by boiling for 5 min in ~35 µl of 4X sample buffer. Samples were divided in to four wells and resolved on an Invitrogen Novex™ 10-20% Tricine 1.0 mm gel stained with SYPRO Ruby (ThermoFisher). Unique bands were excised from the gel using fresh razors. Bands were stored at -20°C until submitted to the University of Kentucky Mass Spectrometry Core.

2.8 Immunoblotting

Following fractionations, pulldown, or secretion assays, the resulting samples were set to equal protein amounts in SDS/Tris and 4X sample buffer. The samples were boiled and loaded onto an Invitrogen Novex™ 10-20% Tricine

1.0 mm gel. Gels were electrophoresed at 125 v for 90 min. Proteins were electroblotted onto Novex™ 0.2 μM polyvinylidene fluoride (PVDF) low fluorescence membranes at 25 v for 1 h. Membranes were blocked with 5% milk in PBS-T for 1 h at room temperature. Immunoblots were probed with primary mouse monoclonal anti-FLAG M2 (Sigma) or anti-*E. coli* RNA polymerase β (Biolegend) antibodies overnight at 4°C with agitation. Membranes were washed with PBS-T four times with agitation for 5 min. Membranes were probed with anti-mouse secondary antibodies coupled to IRDye 800CW and incubated with agitation for 1 h at room temperature. Membranes were washed with PBS-T four times with agitation for 5 min. Images were acquired on a BioRad ChemiDoc MP imagining system or Gel Doc EZ Imager.

2.9 Liquid Chromatography Tandem Mass Spectrometry (LC-MS/MS)

All Mass Spectrometric analysis was performed by the Proteomics Core Facility of the University of Kentucky. The protein gel slices were subjected to dithiothreitol reduction, iodoacetamide alkylation, before trypsin or chymotrypsin (Band E only) digestion. MS data sets were searched in MASCOT against a custom database containing BcpO-$_{3xFLAG}$ as well as the *Burkholderia dolosa* AU0158 database from NCBI.

2.10 β-galactosidase assay

The following β-galactosidase assay protocol was adapted from Garcia et al., 2016 (131). *Bd*AU0158 reporter strains were grown overnight at 37°C in LSLB. Cells from overnight cultures were washed in PBS and diluted to an OD_{600}

= 2. The cells were spotted (20 µl) on LSLB agar plates and incubated overnight at 37°C. Following incubation, entire colony biofilms were resuspended in 1 ml PBS, diluted 1:10 in Z-buffer + 0.27% β-mercaptoethanol (β-ME), and 250 µl were removed to measure OD_{600}. Cells were permeabilized by adding 50 µl chloroform and 10 µl 0.1% SDS to the remaining 750 µl cell suspensions, samples were vortexed, and allowed to settle. Fifty microliters of permeabilized cells and 50 µl of 4 mg/ml ortho-nitrophenyl-β-galactoside (ONPG) was added to 150 µl Z-buffer. Over a 10-min time course OD_{420} values were measured every minute using a SpectraMax 5M plate reader (Molecular Devices). Three independent experiments were performed, each with three technical replicates. To calculate β-galactosidase activity OD_{420} values for two time points within a linear range and the corresponding change in time (Δt) were used in the following formula:

$$\text{β-galactosidase assays (Miller Units)} = \frac{\Delta OD_{420}}{(\Delta t)(OD_{600})(\text{ml of cells})}$$

β-galactosidase assay controls include promoterless *lacZ* in the pUC backbone (P_{neg}-*lacZ*) and overexpressed *lacZ* under the S12 constitutive promoter in pUCS12 backbone (P_{S12}-*lacZ*).

2.11 Bioinformatics and statistics

Burkholderia homologs of *bcpAIOB* genes were identified using the *Burkholderia* Genome Database and the NCBI BLAST suites. Protein alignments were performed using the Clustal W alignment feature of Geneious Prime

(2022.2.1.) and phylogenetic trees generated using the associated Geneious Tree Builder. Domain predictions were performed using NCBI Conserved Domain search. Predicted *B. dolosa* BcpB-1 structure generated by AlphaFold (164-166) and structure visualized and shaded using UCSF ChimeraX v1.6.1 (167). Data were analyzed by one-way ANOVA with Tukey *post hoc* test or Student's *t* test using the statistical package in GraphPad Prism (v.9).

Table 2.1 *Burkholderia dolosa* AU0158 and *Burkholderia multivorans* CGD2M strains used in this study

Strain	Description	Reference
B. dolosa AU0158	Wild-type strain	
B. multivorans CGD2M	Wild-type strain	
AU0158 Δ*bcp-1*	In-frame deletion of *bcpAIOB-1*	(133)
AU0158 Δ*bcp-2*	In-frame deletion of *bcpAIOB-2*	(133)
AU0158 Δ*bcp-3*	In-frame deletion of *bcpAIOB-3*	(133)
AU0158 Δ*bcp-4*	In-frame deletion of *bcpAIOB-4*	This study
AU0158 Δ*bcpO-1*	In-frame deletion of *bcpO-1*	(133)
AU0158 *bcp-3*^{C}	pAP29 replaces native *bcpA-3* promoter with P_{S12} to constitutively *bcp-3*	(133)
AU0158 *bcp-4*^{C}	pTMM086 replaces native *bcpA-4* promoter with P_{S12} to constitutively *bcp-4*	This study
AU0158 Δ*bcpB-1*	In-frame deletion of Δ*bcpB-1*	This study
AU0158 Δ*bcpB-2*	In-frame deletion of Δ*bcpB-2*	This study
AU0158 Δ*bcpB-3*	In-frame deletion of Δ*bcpB-3*	This study
AU0158 Δ*bcpB-4*	In-frame deletion of Δ*bcpB-4*	This study
AU0158 Δ*bcpB-1* Δ*bcpB-2* Δ*bcpB-3* Δ*bcpB-4* (Δ*bcpB1-4)*	In-frame deletion of *bcpB-1, bcpB-2, bcpB-3,* and *bcpB-4*	This study

Table 2.1 continued

AU0158 Δ*bcpB-2* Δ*bcpB-3* Δ*bcpB-4 (bcpB-1)*	In-frame deletion of *bcpB-2, bcpB-3,* and *bcpB-4*	This study
AU0158 Δ*bcpB-1* Δ*bcpB-3* Δ*bcpB-4 (bcpB-2)*	In-frame deletion of *bcpB-1, bcpB-3,* and *bcpB-4*	This study
AU0158 Δ*bcpB-1* Δ*bcpB-2* Δ*bcpB-4 (bcpB-3)*	In-frame deletion of *bcpB-1, bcpB-2,* and *bcpB-4*	This study
AU0158 Δ*bcpB-1* Δ*bcpB-2* Δ*bcpB-3 (bcpB-4)*	In-frame deletion of *bcpB-1, bcpB-2,* and *bcpB-3*	This study
AU0158 Δ*bcpB-1* Δ*bcpB-2*	In-frame deletion of *bcpB-1* and *bcpB-2*	This study
AU0158 Δ*bcpB-1* Δ*bcpB-2* *bcp-1*^{C}	Δ*bcpB-1* Δ*bcpB-2*::pS12AP6 replaces native *bcpA-1* promoter with P_{S12} to constitutively *bcp-1*	This study
AU0158 Δ*bcpB-1* Δ*bcpB-2* *bcp-2*^{C}	Δ*bcpB-1* Δ*bcpB-2*::pS12AP7 replaces native *bcpA-2* promoter with P_{S12} to constitutively *bcp-2*	This study
AU0158 Δ*bcp-1* Δ*bcpB-2*	In-frame deletion of *bcpB-2* in Δ*bcp-1* mutant	This study
AU0158 Δ*bcp-2* Δ*bcpB-1*	In-frame deletion of *bcpB-1* in Δ*bcp-2* mutant	This study
CGD2M Δ*bcp-1*	In-frame deletion of *bcpAIOB-1* in CGD2M	(133)
CGD2M Δ*bcp-2*	In-frame deletion of *bcpAIB-2* in CGD2M	(133)
CGD2M Δ*bcp-1* Δ*bcp-2*	In-frame deletion of *bcpAIOB*-1 and *bcpAIB-2* in CGD2M	(147)
CGD2M Δ*bcp-1* Δ*bcpB-2*	In-frame deletion of *bcpB-2* in CGD2M *bcpAIOB-1* mutant	This study
CGD2M Δ*bcpB-2*	In-frame deletion of *bcpB-2* in CGD2M	This study

Table 2.2 Plasmids used in this study

Plasmids	Backbone	Description	Antibiotic Resistance	Reference
pEXKm5		Allelic exchange vector	Kan	(160)
pUC18Tmini - Tn7T-Km		To deliver Kan resistance cassette to *att*Tn7 site	Amp, Kan	(138)
pUC18Tmini - Tn7T- Tet	pUC18Tmini - Tn7T-Km	To deliver Tet resistance cassette to *att*Tn7 site	Amp, Tet	(130)
pTNS3		Helper plasmid to deliver cassettes to *att*Tn7	Amp	(76)
pUCS12km	pUC18Tmini - Tn7T-Km	To deliver P_{S12}-driving cassettes to *att*Tn7 site	Amp, Kan	(130)
pECG103	pUC18Tmini - Tn7T-Tet	To deliver constitutively-expressed (P_{S12}) *bcpI-1* to *att*Tn7 site	Amp, Tet	This study
pECG104	pUC18Tmini - Tn7T-Tet	To deliver constitutively-expressed (P_{S12}) *bcpI-2* to *att*Tn7 site	Amp, Tet	This study
pAP42	pUC18Tmini - Tn7T-Tet	To deliver constitutively expressed (P_{S12}) *bcpI-3* to *att*Tn7 site	Amp, Tet	(133)
pECG69	pUC18Tmini - Tn7T-Tet	To deliver *Bm*CGD2M constitutively expressed (P_{S12}) *bcpI-1* to *att*Tn7 site	Amp, Tet	(130)
pECG70	pUC18Tmini - Tn7T-Tet	To deliver *Bm*CGD2M constitutively expressed (P_{S12}) *bcpI-2* to *att*Tn7 site	Amp, Tet	(134)
pAP6	pUC18Tmini - Tn7T-Km	To integrate random DNA 5' to *bcp-1*	Amp, Kan	(133)

Table 2.2 continued

pZKE02	pUC18Tmini - Tn7T-Km	To deliver constitutively expressed (P_{S12}) *bcpO*-$_{FLAG}$ to *att*Tn7 site	Amp, Kan	This study
pZKE04	pUC18Tmini - Tn7T-Km	To deliver constitutively expressed (P_{S12}) *bcpO*-$_{E22A}$ to *att*Tn7 site	Amp, Kan	This study
pTMM041	pUC18Tmini - Tn7T-Km	To deliver constitutively expressed (P_{S12}) *gltK* to *att*Tn7 site	Amp, Tet	(147)
pZKE05	pUC18Tmini - Tn7T-Km	To deliver constitutively expressed (P_{S12}) *bcpO*-$_{C21S}$ to *att*Tn7 site	Amp, Kan	This study
pZKE06	pUC18Tmini - Tn7T-Km	To deliver constitutively expressed (P_{S12}) *bcpO*-$_{3XFLAG}$ to *att*Tn7 site	Amp, Kan	This study
pZKE08	pUC18Tmini - Tn7T-Km	To deliver constitutively expressed (P_{S12}) *bcpOB* to *att*Tn7 site	Amp, Kan	This study
pEDP04	pEXKm5	To generate in-frame deletion of *bcp-4*	Kan	This study
pZKE09	pEXKm5	To generate in-frame deletion of *bcpOB-1*	Kan	This study
pZKE11	pEXKm5	To generate in-frame deletion of *bcpB-2*	Kan	This study
pZKE12	pEXKm5	To generate in-frame deletion of *bcpB-1*	Kan	This study

Table 2.2 continued

pZKE16	pEXKm5	To generate in-frame deletion of *bcpB-3*	Kan	This study
pZKE24	pEXKm5	To generate in-frame deletion of *bcpB-4*	Kan	This study
pZKE10	pUC18Tmini - Tn7T-Km	To deliver constitutively expressed (P_{S12}) *bcpOB-1* to *att*Tn7 site	Amp, Kan	This study
pZKE13	pUC18Tmini - Tn7T-Km	To deliver constitutively expressed (P_{S12}) *bcpB-1* to *att*Tn7 site	Amp, Kan	This study
pZKE14	pUC18Tmini - Tn7T-Km	To deliver constitutively expressed (P_{S12}) *bcpB-2* to *att*Tn7 site	Amp, Kan	This study
pZKE15	pUC18Tmini - Tn7T-Km	To deliver constitutively expressed (P_{S12}) *bcpB-3* to *att*Tn7 site	Amp, Kan	This study
pEDP02	pUC18Tmini - Tn7T-Km	To deliver constitutively expressed (P_{S12}) *bcpB-4* to *att*Tn7 site	Amp, Kan	This study
pTMM078	pEXKm5	To generate in-frame deletion of *Bm*CGD2M *bcpB-2*	Kan	This study
pZKE18	pUC18Tmini - Tn7T-Km	To deliver *Bm*CGD2M constitutively expressed (P_{S12}) *bcpB-1* to *att*Tn7 site	Amp, Kan	This study
pZKE19	pUC18Tmini - Tn7T-Km	To deliver *Bm*CGD2M constitutively expressed (P_{S12}) *bcpB-2* to *att*Tn7 site	Amp, Kan	This study

Table 2.2 continued

pZKE22	pUC18Tmini - Tn7T-Km	To deliver constitutively expressed (P_{S12}) TPS domain of *bcpA-1* to *att*Tn7 site	Amp, Kan	This study
pZKE26	pUC18Tmini - Tn7T-Km	To deliver constitutively expressed (P_{S12}) TPS domain of *bcpA-2* to *att*Tn7 site	Amp, Kan	This study
pZKE25	pUC18Tmini - Tn7T-Tet	To deliver constitutively-expressed (P_{S12}) *bcpI-4* to *att*Tn7 site	Amp, Tet	This study
pZKE23	pUC18Tmini - Tn7T-Km	To deliver constitutively expressed (P_{S12}) *bcpB-1* chimera 1 to *att*Tn7 site	Amp, Kan	This study
pZKE29	pUC18Tmini - Tn7T-Km	To deliver constitutively expressed (P_{S12}) *bcpB-1* chimera 2 to *att*Tn7 site	Amp, Kan	This study
pZKE30	pUC18Tmini - Tn7T-Km	To deliver constitutively expressed (P_{S12}) *bcpB-1* chimera 3 to *att*Tn7 site	Amp, Kan	This study
pZKE31	pUC18Tmini - Tn7T-Km	To deliver constitutively expressed (P_{S12}) *bcpB-1* chimera 4 to *att*Tn7 site	Amp, Kan	This study
pS12AP6	pUC18Tmini - Tn7T-Km	To integrate P_{S12} promoter 5' to *bcp-1*	Kan	(143)
pS12AP7	pUC18Tmini - Tn7T-Km	To integrate P_{S12} promoter 5' to *bcp-2*	Kan	(143)

Table 2.2 continued

pECG10	pUC18Tmini - Tn7T-Km	To deliver P_{S12}-*lacZ* to *att*Tn7 site	Amp, Kan	(130)
pUC*lacZ*	pUC18Tmini - Tn7T-Km	To deliver P_{neg}-*lacZ* (promoterless) to *att*Tn7 site	Amp, Kan	(130)
$P_{bcp\text{-}1}$-*lacZ*	pUC18Tmini - Tn7T-Km	To deliver $P_{bcpA\text{-}1}$-*lacZ* to *att*Tn7 site	Amp, Kan	(133)
$P_{bcp\text{-}2}$-*lacZ*	pUC18Tmini - Tn7T-Km	To deliver $P_{bcpA\text{-}2}$-*lacZ* to *att*Tn7 site	Amp, Kan	(133)
$P_{bcp\text{-}3}$-*lacZ*	pUC18Tmini - Tn7T-Km	To deliver $P_{bcpA\text{-}3}$-*lacZ* to *att*Tn7 site	Amp, Kan	(133)
pZKE20	pUC18Tmini - Tn7T-Km	To deliver $P_{bcpA\text{-}4}$-*lacZ* to *att*Tn7 site	Amp, Kan	This study
pZKE21	pUC18Tmini - Tn7T-Km	To deliver $P_{bcpB\text{-}4}$-*lacZ* to *att*Tn7 site	Amp, Kan	This study

Kan, Kanamycin; Amp, Ampicillin; Tet, Tetracycline

CHAPTER 3. Characterization of *B. dolosa* CDI system-1 BcpO protein

The Δ*bcpO* mutant strain was generated by Perault et al., 2018. Mass spectrometry analysis was performed by the Proteomics Core Facility of the University of Kentucky.

3.1 Introduction

Even though contact-dependent growth inhibition (CDI) systems are widespread among Proteobacteria, CDI systems are typically classified into two broad classes, the *E. coli*-type and *Burkholderia*-type CDI systems (130,132). The *Burkholderia*-type CDI systems are further divided into two phylogenetic groups, class I and class II. The subclassification was established based on the conserved amino acid sequences of the BcpB and BcpO proteins, as well as the conserved N-terminal domain (~2800 amino acids) of BcpA (130,132). In CDI systems the BcpA-CT and BcpI proteins function in an allele specific manner, as cognate immunity only provides protection against cognate BcpA-CTs but not heterologous BcpA-CTs. Interestingly, the *Burkholderia* class I BcpO proteins are conserved across alleles. The class I BcpO proteins are nearly identical at the amino acid level, after the cleavage of the signal sequence. However, the amino acid sequences of the *Burkholderia* class II BcpO proteins have no similarities among each other, to any characterized proteins, or protein domains (130,133).

Based on the presence of a lipobox located in the signal sequence, the class I *B. dolosa bcpO-1* gene is predicted to encode an outer membrane localized lipoprotein (133). Due to the level of homology among each other the

class I BcpO proteins are predicted to play a conserved, non-system specific function. To date no clear role has been identified for class I BcpO proteins, though *B. thailandensis* E264 and *B. dolosa bcp-1* mutants lacking the *bcpO* gene had a reduced CDI mediated killing of recipient cells (130,133). Previous work has not revealed a phenotype or function for the class II BcpO proteins (133,147). Based on the lack of similarities and known functions, the class II "BcpO" proteins should probably be renamed. Therefore, the reference of BcpO throughout this chapter corresponds to the class I BcpO proteins, more specifically the BcpO-1 encoded by the *B. dolosa* strain AU0158, unless otherwise noted.

Little is known about the function of lipoproteins in CDI systems. However, other protein secretion systems such as colicins, trimeric autotransporters, the β-barrel machine assembly BAM complex, and Type VI secretion systems (T6SS) encode lipoproteins that play important roles (168-173). Studies examining these essential lipoproteins demonstrate that proper lipoprotein localization is necessary for their role in machine assembly, toxin stability and secretion (170-172,174). Additionally, a lipoprotein in the Type Vc secretion system has been shown to directly enhance the stability and surface display of the SadA adhesin autotransporter (171).

Since BcpA interacts with the other CDI proteins, BcpI binds to BcpA-CT to prevent autotoxicity and BcpB binds BcpA to transport BcpA out of the cell; it is plausible that BcpO also interacts with BcpA or another CDI protein. Therefore, I hypothesize that *B. dolosa* BcpO-1 plays a role in BcpA secretion, by interacting

with BcpA in the periplasm before BcpA-CT secretion occurs. Moreover, I hypothesize that BcpO is acting with a chaperone, to prevent BcpA-CT degradation by periplasmic proteases.

BcpO is predicted to be an outer membrane localized lipoprotein based on bioinformatic analysis, however this has not been experimentally demonstrated. In this chapter I provide experimental evidence that BcpO is likely a lipoprotein that specifically functions with a cognate class I CDI system. Additionally, using pulldown assays and subsequent mass spectrometry analysis I identified potential BcpO binding partners. The findings highlighted here are steppingstones for future experiments to elucidate the role BcpO plays in *B. dolosa* BcpA-1 mediated CDI interbacterial competition.

3.2 Results

Δ*bcpO* phenotype is not due to a growth defect

To examine the function and localization of BcpO in subsequent experiments described in this chapter, I created a FLAG-tagged *bcpO* construct expressed constitutively in the previously generated Δ*bcpO* mutant strain (133). Growth curves were used to determine if the deletion of *bcpO* or the complementation of a Δ*bcpO* mutant strain with a constitutively expressed *bcpO*-$_{FLAG}$ is toxic to the donor cells. The Δ*bcpO* strain had a growth rate nearly identical to wild-type from lag phase to late stationary phase. The Δ*bcpO::bcpO*-$_{FLAG}$ complemented strain had a slight, but not statistically significant, decrease in

cell density compared to wild-type during stationary phase (**Fig. 3.1A**). This result suggests that the deletion or overexpression of *bcpO* does not significantly affect the growth rate of the donor cells in liquid medium.

I next aimed to test whether the FLAG epitope affects the function of BcpO. Consistent with previous findings (133), Δ*bcpO* donor cells competed against Δ*bcp-1* recipient cells resulted in a ~10-fold decrease in BcpA-1 mediated CDI killing compared to wild-type donor cells (**Fig. 3.1B**). When the Δ*bcpO* mutant was complemented with a single copy plasmid, constitutively expressing *bcpO*-FLAG (P_{S12}-*bcpO*-$_{FLAG}$) the CDI mediated killing was restored to levels similar to wild-type. This result suggests that the C-terminal FLAG epitope does not affect the function of BcpO.

Taken together these data indicate that the decrease in CDI activity caused by the deletion of *bcpO* is not due to a growth defect in the donor strain; instead implying that decrease CDI activity is specific to BcpA-1 toxin activity. Additionally, these results show that the presence of a C-terminal FLAG epitope does not affect the function of BcpO and therefore may not affect the localization of BcpO.

Class I BcpO functions specifically with cognate class I CDI systems

Even though *B. dolosa* encodes multiple CDI systems, only *bcp-1* is a class I system, which includes *bcpO* (130,133). Therefore, I sought to determine if the role BcpO plays in CDI activity is specific to class I CDI systems. To

investigate this, I competed wild-type and Δ*bcpO* donor cells against Δ*bcp-2* recipient cells to examine the class II BcpA-2 toxin activity. The competitive index for Δ*bcpO* was nearly identical to the competitive index of wild-type when competed against a Δ*bcp-2* recipient (**Fig. 3.2A**)**.** When the cognate immunity protein gene *bcpI-2* was provided in trans to the recipient cells, BcpA-2 CDI mediated activity was eliminated. These data suggest that BcpO-1 does not affect a *B. dolosa* class II BcpA-2 mediated CDI activity.

To confirm that BcpO does not function with class II CDI systems, I aimed to determine if BcpO can function with a non-class I CDI system produced in a different *B. cepacia* complex strain. To examine this, a single copy plasmid constitutively expressing *B. dolosa bcpO* was delivered to the *Burkholderia multivorans* CGD2M wild-type strain. *B. multivorans* encodes two functional class II CDI systems, though system-1 is not expressed under native laboratory conditions (134). *B. multivorans bcp-1* also encodes for a class II BcpO, whose function remains unknown. To examine *B. dolosa* BcpO activity, wild-type *B. multivorans* and *B. multivorans* strain expressing *B. dolosa bcpO* (*Bm*CG2DM+*Bd bcpO*) was competed against both Δ*bcp-1* and Δ*bcp-2* recipient cells to examine *B. multivorans* BcpA-1 and BcpA-2 activity, respectively. As expected, when a *B. multivorans* wild-type donor strain was competed against a Δ*bcp-1* recipient neither strain has a competitive advantage (**Fig. 3.2B**) (134). Expressing *B. dolosa bcpO* in *B. multivorans* did not induce BcpA-1 mediated CDI killing. Similarly, *B. dolosa bcpO* expression in *B. multivorans* did not significantly affect BcpA-2 meditated CDI activity. Therefore, these data suggest

that expressing *B. dolosa bcpO* does not affect the CDI activity of the *B. multivorans* class II CDI systems.

Taken together, these results demonstrate that the expression of *bcpO* did not affect the CDI activity of three distinct class II CDI systems. Therefore, suggesting that that the function of BcpO is likely specific for class I CDI systems.

BcpO is not necessary during low levels of CDI activity.

More recently some lipoproteins have been shown to act as sensors that function to influence the gene expression of phosphorelay systems (175-178). If BcpO is acting with a phosphorelay system, I would hypothesize that BcpO might affect the expression of the *bcpAIOB*-1 genes. I sought to determine if the Δ*bcpO* phenotype is due to changes in the expression of the other *bcp-1* genes. To investigate this, I compared the *bcpAIOB-1* gene expression in wild-type to the expression in the Δ*bcpO* strain using Reverse Transcriptase quantitative PCR (RT-qPCR). RNA was extracted from wild-type, Δ*bcpO,* and Δ*bcp-1* mono-strain colony spots. When normalized to wild-type, the *bcpA-1, bcpB-1,* and *bcpI-1* gene expression remained unchanged in the Δ*bcpO* strain (**Fig. 3.3A**). The *bcpO* gene expression was not detected the Δ*bcpO* strain, confirming that *bcpO* is deleted in this strain. As expected, there was no measurable detection of the *bcpAIOB-1* genes in the Δ*bcp-1* strain. These data indicate that the deletion of *bcpO* does not affect the expression of the other *bcp-1* genes.

Since the Δ*bcpO* phenotype is not due to changes in *bcp-1* gene expression, I next aimed to determine if overexpressing *bcpA-1* in the Δ*bcpO* mutant could overcome the CDI defect. I hypothesize that BcpO acts to assist in preventing the degradation of BcpA. Therefore, when BcpO is absent I would predict that the rate of BcpA degradation will increase. If the rate of BcpA production is higher than degradation, then I think the Δ*bcpO* CDI defect may be overcome by overexpressing *bcpA-1*. To investigate this, I competed wild-type and Δ*bcpO* donor cells, that has the *bcpA-1* promoter replaced with random plasmid DNA or with *B. thailandensis rpsL* (ribosomal S12 subunit) constitutive promoter, against Δ*bcp-1* recipient cells. When the *bcpA-1* promoter was replaced with random plasmid DNA there was low levels (~500-fold decrease compared to native promoter wild-type) of BcpA-1 mediated CDI activity that was similar for both the wild-type and Δ*bcpO* donor cells (**Fig. 3.3B**). Overexpression of *bcpA-1* increased CDI activity in the Δ*bcpO* mutant strain. There was a ~5-fold increase in the competitive index of both the wild-type and Δ*bcpO* strains when compared to the natively expressed wild-type and Δ*bcpO* strains, respectively. However, the competitive index of the constitutively expressed Δ*bcpO* strain was still less than a constitutively expressed wild-type strain. These data suggest that BcpO is not necessary when *bcpA-1* is lowly expressed.

Since the function of *bcpO* seems to be dependent on the level of CDI activity, I next wanted to determine if the density of the competition affects BcpO function. To examine this, cocultures of competition assays between wild-type or Δ*bcpO* donor cells and Δ*bcp-1* recipient cells were mixed at three cell densities

OD_{600}= 0.2, 2, and 4. The competitive index of the Δ*bcpO* mutant was less than wild-type at all tested densities (**Fig. 3.3C**). However, the differences between the wild-type and Δ*bcpO* competitive indices at OD_{600} = 0.2 was less than the differences at OD_{600} = 2 or 4. Interestingly, the level of BcpA-1 mediated CDI activity was different at all three densities, with OD_{600}= 2 resulting in the highest level of activity. These data suggest that increasing the competition density increases the level of CDI activity but in the absence of *bcpO* there is still a decrease in CDI activity compared to wild-type.

Taken together, these data suggest that when *bcp-1* is lowly expressed or at a low competition density, BcpO may not be necessary for sufficient BcpA-1 mediated CDI activity. Repeat experiments would be needed to determine if these differences are statistically significant.

bcpO likely encodes a lipoprotein

Bioinformatic analysis suggests that BcpO is a ~10 kDa lipoprotein localized to the outer membrane. This prediction is based on studies done on canonical *E. coli* lipoproteins which invariantly contain a cysteine residue at the +1 position in the lipobox (LAAC) (118). The presence of an aspartic acid residue at the +2 position typically leads to inner membrane localization, while any other residue leads to outer membrane localization (179,180). Since BcpO has a glutamic acid as the +2 residue BcpO is predicted to an outer membrane bound lipoprotein; although, this has not been experimentally demonstrated. Therefore,

I aimed to determine the localization of BcpO. To examine this, I performed subcellular fractionation using a selective detergent, Triton X-100, and ultracentrifugation on wild-type and a Δ*bcpO*::*bcpO*-$_{FLAG}$::*gltK*-$_{FLAG}$ strain. *B. multivorans* Gltk-$_{FLAG}$ is a ~21 kDa inner membrane protein (147), that will serve as an inner membrane control in these fractionation assays. In my initial fractionation assays a band corresponding to BcpO-$_{FLAG}$ was present only in the inner membrane (Triton X-100 soluble) fraction of the Δ*bcpO*::*bcpO*-$_{FLAG}$::*gltK*-$_{FLAG}$ strain (**Fig. 3.4A**). Given that both GltK and BcpO contained FLAG epitopes I also expressed the BcpO-$_{FLAG}$ construct in the Δ*bcpO* strain alone to confirm that there is no cross reactivity. Subcellular fractionation of the Δ*bcpO::bcpO*-$_{FLAG}$ also resulted in a band corresponding to BcpO-$_{FLAG}$ only in the inner membrane fraction. A band corresponding to BcpO-$_{FLAG}$ was not present in the whole cell lysate likely due to low amounts of BcpO-$_{FLAG}$. These data from this subcellular fractionation assay suggest that BcpO is an inner membrane localized lipoprotein.

Potential BcpO binding partners

Given that BcpA interacts with the other two proteins in the CDI system, BcpB and BcpI, I hypothesize that BcpO also interacts with the other CDI proteins. To determine if BcpO interacts with the CDI Bcp-1 proteins or other proteins, I attempted to isolate and identify potential BcpO binding partners. I performed pull down assays by incubating M2 FLAG magnetic beads with cleared cell lysate from Δ*bcpO* and Δ*bcpO*::*bcpO*-$_{FLAG}$ strains. Following

incubation, the beads were washed, and bound proteins were eluted by boiling beads in 4X SDS sample buffer. SYPRO Ruby staining of the SDS gel revealed unique banding patterns for each strain (**Fig. 3.5**). Five bands unique to the *bcpO*$_{-FLAG}$ sample were excised and sent to the University of Kentucky proteomics core facility for Mass Spectrometry (MS) analysis. As a negative control, the corresponding regions from the Δ*bcpO* samples were extracted and sent for mass spec analysis. Majority of the top proteins identified by MS were predicted to be cytoplasmic proteins that were also present in the Δ*bcpO* samples, indicating nonspecific binding. This pulldown assay did identify unique proteins, such as periplasmic proteases and chaperone proteins, that could be potential BcpO binding partners (**Table 3**). Interestingly, when Band E, which corresponds to the predicted size of BcpO$_{-FLAG,}$ was digested with trypsin BcpO was not identified in the Mass spec analysis. However, BcpO was identified when Band E was digested with chymotrypsin. Therefore, other potential BcpO binding partners may be identified if all the bands were digested with chymotrypsin. The other CDI proteins were not identified as potential binding partners in this pulldown assay. However, we cannot rule out the possibility of these interactions given that BcpO could interact indirectly or directly through transient interactions, which could have been missed under these tested conditions.

BcpO may need to be membrane bound to be functional.

To gain insight into the function of BcpO I aimed to determine whether proper localization is necessary for BcpO to be functional. To examine this, I

attempted to create BcpO point mutants that would change the invariant cysteine +1 residue ($BcpO_{C21S}$) and the +2 residue ($BcpO_{E22A}$), which typically determines the localization of some lipoproteins. I planned to constitutively express the *bcpO* point mutants in the Δ*bcpO* mutant strain to examine localization and measure BcpA-1 mediated CDI activity. However, I was unable to transform the P_{S12}-*bcpO*$_{C21S}$ plasmid into the RH03 *E. coli* cells. Therefore, I could not express the P_{S12}-*bcpO*$_{C21S}$ plasmid in *B. dolosa*. Given that the +1 cysteine is invariable in lipoproteins it is possible that overexpressing the *bcpO*$_{C21S}$ point mutant could have been toxic to the *E. coli* cells. It's been shown that the accumulation of mislocalized lipoproteins can lead to perturbed membrane integrity and therefore be toxic to the cell (181-183). Before determining the localization of the $BcpO_{E22A}$ point mutant I first examined its functionality. When competed against Δ*bcp-1* recipient cells the competitive index of a Δ*bcpO* donor strain complemented with *bcpO*$_{E22A}$ was ~3-fold higher than Δ*bcpO,* but ~2-fold less than wild-type donor cells (**Fig 3.6A**). This result suggests that the $BcpO_{E22A}$ point mutant is functional.

Given that my previous results suggest that BcpO is localized to the inner membrane I hypothesized that $BcpO_{E22A}$ would be trafficked to the outer membrane. When I fractionated the Δ*bcpO::bcpO*$_{E22A}$ strain as previously described, I got contradicting results. The first fractionation assay resulted in a band corresponding to $BcpO_{E22A\text{-}FLAG}$ in the inner membrane fraction; suggesting that the glutamic acid to alanine mutation at the +2 position does not affect the localization of BcpO **(Fig 3.6B).** However, when the fractionation assay was repeated there were no bands in any fraction that corresponded to $BcpO_{E22A\text{-}FLAG}$

(**Fig. 3.7**), although there was a BcpO-$_{FLAG}$ band present in the inner membrane fraction. This result would suggest that BcpO$_{E22A\text{-}FLAG}$ was degraded.

Taken together these data suggest that BcpO localization does not follow the *E. coli* LOL +2 rule; given that changing the negatively charged +2 glutamic acid to a non-polar alanine residue did not result in outer membrane localization. These results suggest that BcpO likely needs to be membrane bound to be functional. Additionally, the unsuccessful attempt to mutate the invariant +1 cysteine provides evidence that BcpO is likely a lipoprotein.

Inconsistent results when examining BcpO localization and functionality

While in the process of optimizing the selective detergent fractionations, I came across a study that demonstrated that lipoproteins can be solubilized by nonionic detergents like Triton X-100 (174). This would result in both inner and outer membrane bound lipoproteins appearing in the soluble (inner membrane) fraction. To validate the selective detergent subcellular fractionation assay, I attempted to examine the localization of BcpO using a sucrose density gradient. When a three density (20%, 53%, and 70%) sucrose gradient was used strong bands corresponding to BcpO-$_{3x\text{-}FLAG}$ were present in all the fractions except for the inner membrane (**Fig 3.8A**). Due to the low sample volume, I was unable determine the concentration of the samples so I could not confirm if proteins were present in the inner membrane fraction. However, faint bands corresponding to RpoB were present the inner membrane fractions, which would

suggest the presence of proteins in the sample. Repeated attempts to examine the localization of BcpO using a sucrose density gradient resulted in bands corresponding to BcpO-$_{FLAG}$ and the inner membrane control GltK-$_{FLAG}$ in all fractions (**Fig. 3.9**). These data suggest that the conditions used for the sucrose gradient was not sufficient for inner and outer membrane separation. Therefore, I cannot definitively determine the precise localization of BcpO. However, the results from the selective detergent fractionation would support the conclusion that BcpO is a lipoprotein.

Initial competitions assay comparing wild-type and Δ*bcpO* donor cells competed against Δ*bcp-1* recipient cells, resulted in a significant decrease in BcpA-1 mediated CDI activity for the Δ*bcpO* strain and activity was restored to wild-type levels when complemented with +*bcpO*-$_{FLAG}$, which was consistent with previously findings (133). However, subsequent competition assays, under the same conditions, resulted in a competitive index of Δ*bcpO* donor cells that was not significantly different from wild-type or the +*bcpO* complement strain (**Fig 3.8B**). These inconsistences led to difficulties in repeating the preliminary experiments described earlier in this chapter. Since the natural conditions in which CDI systems are active is not known, unintentional variation in experimental conditions could have occurred during competition assays that resulted in changes in the requirement of BcpO for CDI activity. However, when *bcpO* and *bcpB-1* were deleted together the decrease in BcpA-1 mediated CDI killing by the Δ*bcpOB* strain was consistent for all competition assays (**Fig. 3.8B**). Complementation of the Δ*bcpOB* strain with the +*bcpOB* construct resulted in

partial restoration of CDI activity. Additionally, data presented in chapter 4 demonstrate that the deletion of *bcpB-1* alone does not affect BcpA-1 mediated CDI activity (**Fig. 4.2A**). These results suggest that *bcpO* is responsible for the decrease in BcpA-1 mediated CDI activity in the Δ*bcpO and* Δ*bcpOB* mutants.

3.3 Discussion

When I began these studies, previous work suggested that *B. dolosa* BcpO-1 is an outer membrane localized lipoprotein, that is required for maximum BcpA-1 mediated CDI activity, through an unknown mechanism (133). In this chapter I provide experimental evidence that BcpO is a lipoprotein that specifically functions with a cognate class I CDI system. Additionally, I identified potential binding partners that may assist in the function of BcpO.

Due to the high similarity among class I BcpO amino acid sequences (~94% after signal sequence cleavage), class I BcpO proteins are predicted to function in a non-system specific manner (130,133). Given that expressing the *B. dolosa* class I *bcpO* in three different *B. cepacia* complex class II CDI systems did not provide a competitive advantage for these systems (**Fig. 3.2**), my data suggest that the class I BcpO proteins specifically function with class I CDI systems. Taken together with previous studies that show that class II BcpO proteins do not play a role in CDI activity (133,134), these results indicate that the class I and class II BcpO proteins are functionally distinct.

Little is known about the regulation of CDI system-encoding genes. In *B. thailandensis* only about 1 in 1,000 bacteria express *bcpAIOB* genes at a high

level under laboratory conditions (130). Moreover, the *B. dolosa bcp-3* system is only active when the native *bcpA* promoter is replaced with a constitutive promoter (133). My preliminary results suggest that a basal level of BcpA-1 mediated CDI activity occurs in the absence of the native *bcpA-1* promoter, and the presence or absence of *bcpO* made no difference in the low-level activity of BcpA-1 (**Fig. 3.3B**). Additionally, during low density competition assays there was a low level of BcpA-1 mediated CDI killing, that was not influenced by BcpO (**Fig. 3.3C**). Though it remains to be known the natural niche in which CDI systems are active or provide a fitness advantage for *B. dolosa.* This work sheds light on the conditions when CDI provides a competitive advantage and when BcpO is required to maximize this advantage.

The findings presented here also demonstrate that *bcpO* does not contribute to the regulation of the other *bcp-1* genes, suggesting that BcpO affects BcpA at the protein level. This is also supported by the fact that the level of BcpA-1 mediated CDI activity is decreased in the absence of BcpO, suggesting that the secreted toxin is less potent or the amount of secreted toxin is a reduced. More evidence supports the latter, given that toxin activators in donor cells as not been identified in other CDI systems. It is not known for CDI systems if the level of CDI activity is directly correlated to number of secreted toxins. Using antibodies that recognize the BcpA-CT domain, preliminary data (generated by Beth Oates) shows that the BcpA-CT protein level was not distinctly different when constitutively expressed in the Δ*bcpO* mutant strain compared to constitutively expressed wild-type. However, since the BcpA-CT

toxin domain would have likely been cleaved during this assay (due to direct contact with sister cells) generating antibodies against different BcpA domains could be helpful in determining whether the protein levels of the N-terminal portion of BcpA differ between the wild-type and Δ*bcpO* strains. Alternatively, I optimized a TpsA/BcpA secretion assay, discussed in detail in chapter 4, that could be used in subsequent studies to determine if less BcpA-1 protein is secreted when BcpO is not present. However, the decreased CDI activity from the competition assay provides evidence that there are less BcpA-1 molecules available to intoxicate recipient cells.

Bioinformatic analysis led to the original hypothesis that BcpO is an outer membrane localized lipoprotein (133). This prediction was based on the presence of a canonical lipobox (LAAC) in the amino acid sequence and a predicted signal peptidase II (SPase II) cleavage site, as SPase II exclusively cleaves lipoproteins (179,184). Much of what is known about bacterial lipoprotein biogenesis is based on work examining *E. coli*, *P. aeruginosa,* and *Borrelia burgdorferi* lipoproteins (185-187). Lipoprotein localization is typically based on the "+2 rule", where an aspartic acid at the +2 position predicts IM localization, but any other residue targets lipoproteins to the OM (185). Though this rule was first described for *E. coli* lipoproteins, subsequent studies revealed that the +2 rule applies to many other bacterial species (188). However, other studies have shown that when an asparagine residue is at the +3 position other residues such as phenylalanine, tryptophan, tyrosine, glycine, or proline can serves as a +2 IM retention signal (189). Additionally, in *P. aeruginosa* residues at positions 3 and 4

(Gly_{+2} $Lys_{+3}Ser_{+4}$) are responsible for the retention of lipoproteins in the IM (1). Based on the selective detergent subcellular fractionation assays BcpO appeared to be localized to the IM. Since BcpO contains a negatively charged residue, glutamic acid, at the +2 position it is possible that Glu+2 can still interact with the phosphatidylethanolamine to avoid the LolCDE sortase complex and therefore retain BcpO in the IM. However, when preliminary studies using sucrose density gradients for subcellular fractionations were conducted bands corresponding to BcpO appeared in the OM for one experiment but appeared in both the inner and outer membranes in repeat experiments. Therefore, I could not definitively determine the localization of BcpO. Further examination of BcpO localization could provide insight into how *Burkholderia* lipoprotein localization is determined.

Unexpectantly, a pulldown assay coupled with mass spectrometry resulted in major hits that are predicted cytoplasm factors. These cytoplasmic proteins were likely identified due to direct or indirect transient interactions that occurred after cell lysis. Alternatively, BcpO could remain in the cytoplasm, although lipoproteins are not known to attach to the cytoplasmic side of the inner membrane. One could speculate that BcpO interacts with a chaperone protein to indirectly assist in the stabilization of BcpA-1. This could explain why BcpA-1 is still secreted and functional in the absence of *bcpO*. Interestingly, BcpA-1 or any other Bcp-1 proteins, were not identified from this pulldown assay. However, due to the size difference between BcpO and the BcpA, it is possible that conditions used was not suitable to capture this interaction. Therefore, we cannot rule out

the possibility of a BcpA-BcpO interaction. Since the donor cells also express the compatible inner membrane receptor, it is not known if the BcpA-1 toxin can be transported back into the cytoplasm of the producing cell. Given that BcpO is membrane bound, BcpO could be acting to prevent BcpA-CT transport back into the cytoplasm of the donor cell, before secretion to the cell surface through BcpB. This would not be detrimental to the cell because BcpI would prevent self-intoxication. However, this could be an energy expensive process, especially if *bcpA* is always expressed. It is possible that in the absence of BcpO, the BcpA-CT pool is being wasted due to this transport back into the donor cell and therefore limiting the amount of available toxin that can be transported to the recipient cells. Before transport of BcpA-CT back into cytoplasm of the donor cell can occur, the toxin domain would need to be cleaved from the rest of the BcpA protein. For one *E. coli* CDI system, evidence suggests that an OMP, different from the CDI OM receptor, is responsible for cleaving the CT domain from the rest of the CdiA protein (135). However, this process has not been examined for *Burkholderia* CDI systems. Alternatively, given the location of the pre-toxin domain (PT), it could mediate auto-proteolysis to release the toxin domain from the rest of BcpA protein (190,191). For toxin transport across the inner membrane, it is hypothesized that the BcpA/CdiA toxins have autonomous membrane translocation activity, but inner membrane receptors are needed to facilitate the insertion of the toxin into the inner membrane (144,155). The process would be similar to the proposed model for the translocation of some

colicin nucleases (168,192-194). Therefore, I think that BcpO indirectly interacts with BcpA-CT, to help prevent BcpA-CT degradation and self-intoxication.

It remains to be understood how BcpO is enhancing BcpA-1 mediated CDI activity and why BcpO only plays a role in Bcp-1 CDI activity. Based on the results obtained in this study, I think BcpO is acting with a chaperone to prevent the degradation of BcpA in the producing cell. Along with subsequent studies, the work presented here will provide insight into not only the role BcpO plays in the *B. dolosa* AU0158 strain but also the role other class I BcpO proteins are play in their cognate CDI systems.

Figure 3.1 Validation of BcpO-FLAG construct functionality

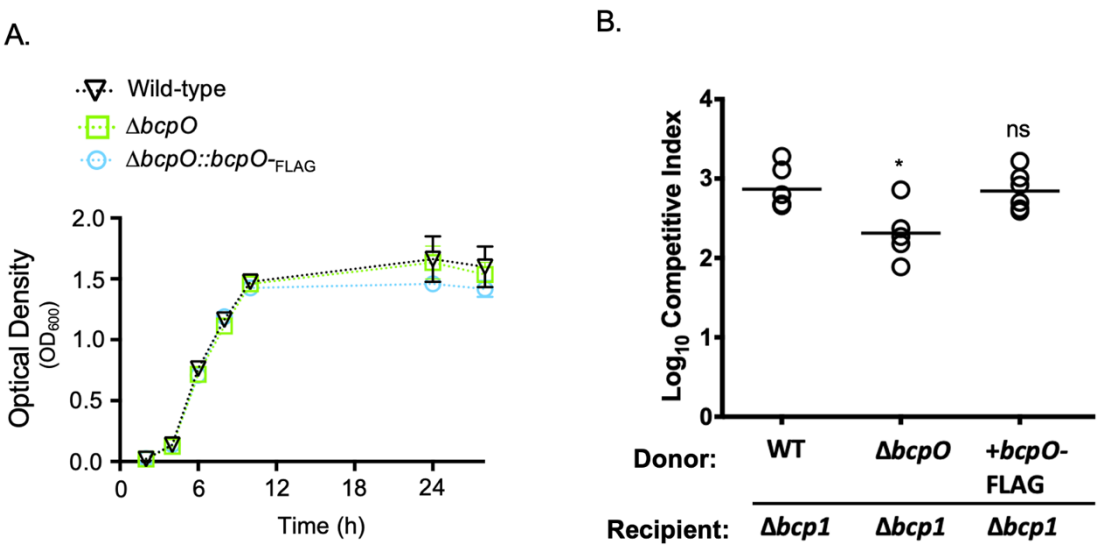

A) Growth curve experiments performed with wild-type, Δ*bcpO* mutant, and Δ*bcpO* constitutively expressing P_{S12}-*bcpO*-FLAG construct (Δ*bcpO::bcpO*-FLAG). Optical density for all strains were measured in triplicate through 0-28 h, symbols represent the mean with standard deviation. A one-way ANOVA was used to report significance from each time point, but no significant differences were found between the OD_{600} between any of the strains. **B)** Interbacterial competition assay between indicated donor cells: wild-type, ΔbcpO, or Δ*bcpO* constitutively expressing P_{S12}-*bcpO*-FLAG construct (Δ*bcpO::bcpO*-FLAG) and Δ*bcp*-1 recipient cell. Symbols represent $\log_{10}$ competitive index values (ratio of donor to recipient) from two independent experiments (n= 6). Dashed line shows $\log_{10}$ competitive index = 0; ns, not significant; *, $P < 0.05$.

Figure 3.2 BcpO functionality in non-class I CDI systems

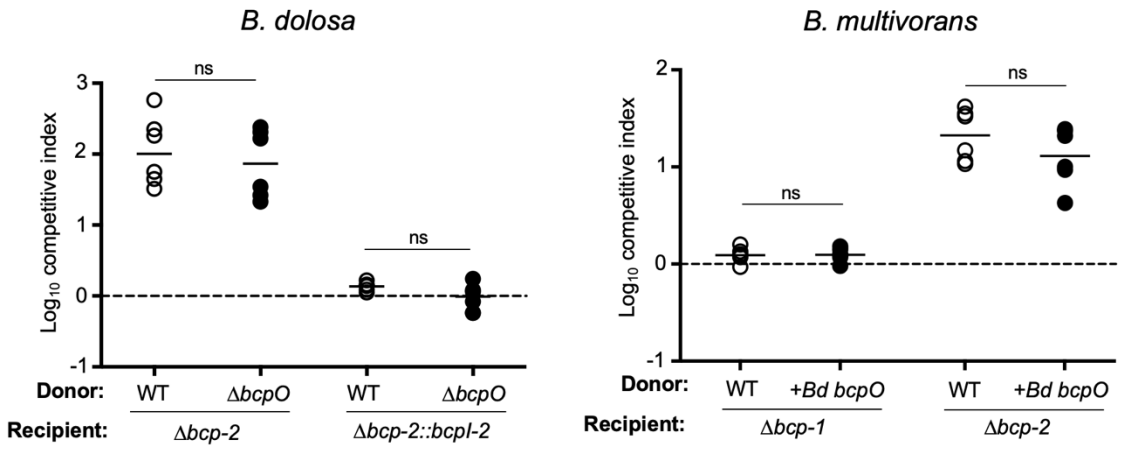

(A) Interbacterial competition assays between *B. dolosa* wild-type or Δ*bcpO* donor cells and Δ*bcp-2 or* Δ*bcp-2* complemented with cognate immunity (Δ*bcp-2::bcpI-2*) recipient cells. (**B)** Interbacterial competition assays between *B. multivorans* wild-type or *B. multivorans* wild-type complemented with a constitutively expressed copy of *B. dolosa bcpO* (+*Bd bcpO*) and *B. multivorans* Δ*bcp-1* or Δ*bcp-2* recipient cells. Symbols represent $\log_{10}$ competitive index values (ratio of donor to recipient) from two independent experiments (n= 6). Dashed line shows $\log_{10}$ competitive index = 0. A Student's *t* test was performed no significant differences were found, ns, not significant.

Figure 3.3 BcpO role in *bcp-1* expression

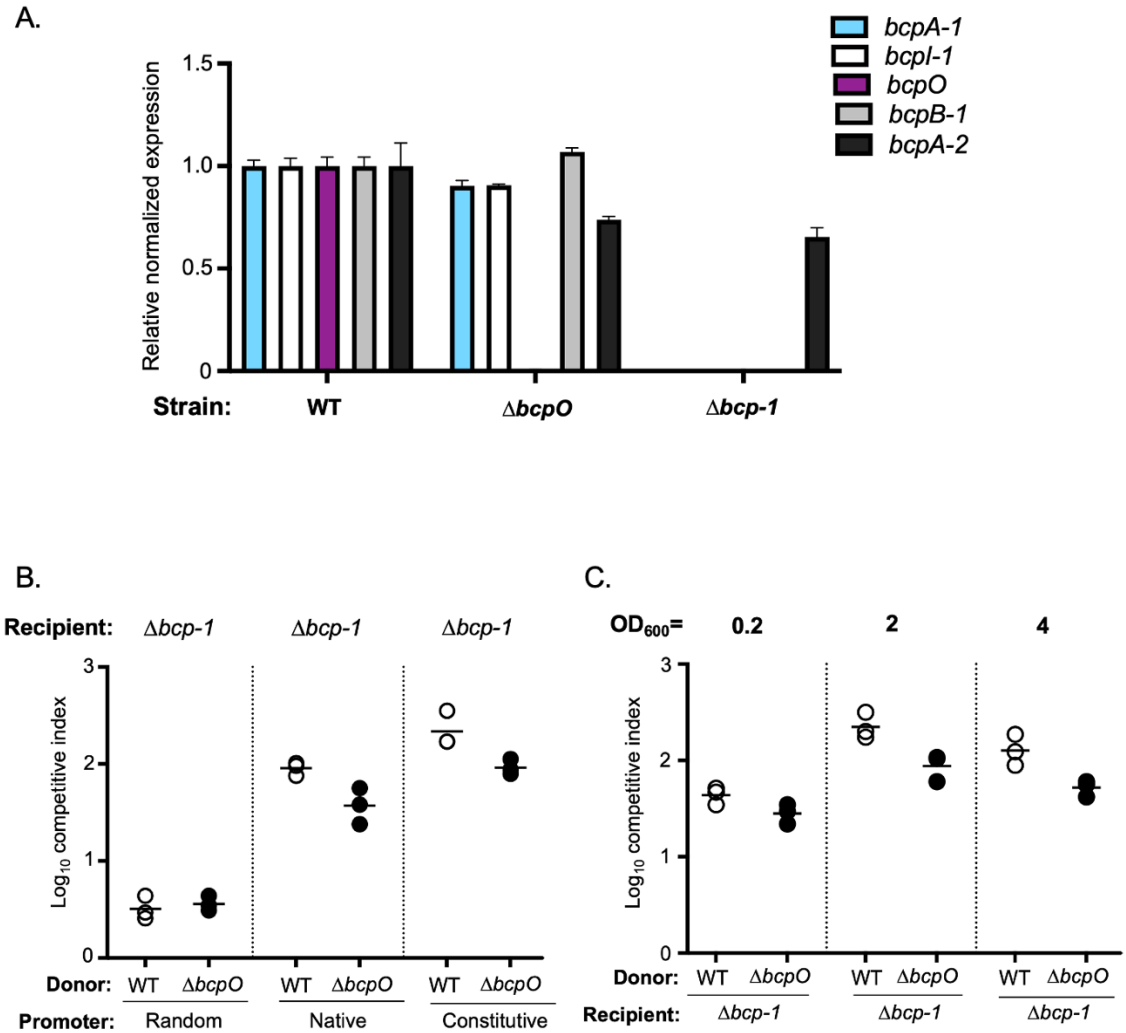

(A) Total RNA was extracted from *B. dolosa* wild-type, Δ*bcpO*, and Δ*bcp-1* monoculture colony spots. RNA samples were reverse transcribed into cDNA for qRT-PCR measurements of *bcpA-1*, *bcpI-1*, *bcpO-1, bcpB-1,* and *bcpA-2 genes*. All measurements were normalized to mean expression of the house-keeping gene *recA* and are relative to the wild-type sample. **(B)** Interbacterial competition assays between Δ*bcp-1* recipients cells and wild-type or Δ*bcpO* donor cells that has the region ~500 bp upstream of *bcpA-1* replaced with random plasmid DNA (Random), the native *bcpA-1* promoter (Native), or the *B. thailandensis rpsL* constitutive promoter (Constitutive). **C)** Interbacterial competition assays between wild-type or Δ*bcpO* donor cells and Δ*bcp-1* recipient cells, with donor and recipient cell densities standardized to OD_{600} = 0.2, 2, or 4. Symbols represent $\log_{10}$ competitive index values (ratio of donor to recipient) from one experiment (n= 3). Dashed line shows $\log_{10}$ competitive index = 0.

Figure 3.4 Examination of BcpO localization

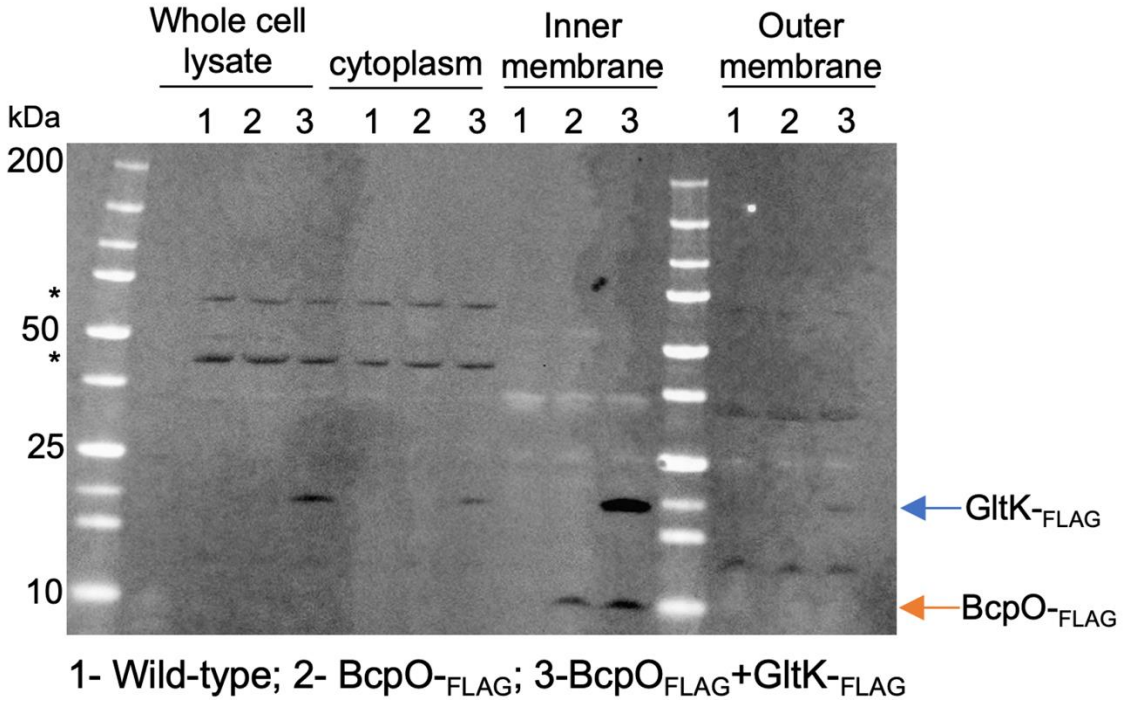

Western blot of selective detergent and ultracentrifugation subcellular fractionation of 1) wild-type, 2) Δ*bcpO* constitutively expressing P_{S12}-*bcpO*-FLAG construct (BcpO), and 3) Δ*bcpO* constitutively expressing P_{S12}-*bcpO*-FLAG and P_{S12}-*gltK*-FLAG (BcpO-GltK). Prior to cell lysis, cultures were standardized to the same OD_{600}. Membrane was probed with monoclonal anti-FLAG primary and fluorescent anti-mouse secondary antibodies. Blue and orange arrows represent GltK-FLAG and BcpO-FLAG bands, respectively. Asterisks indicate non-specific bands.

Figure 3.5 Potential BcpO binding partners

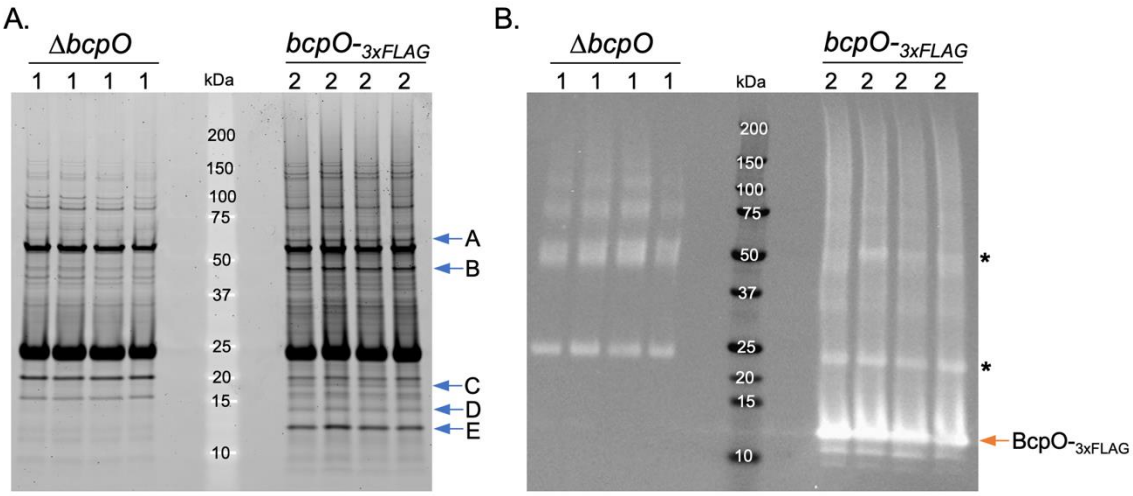

Pulldown assay of Δ*bcpO* and Δ*bcpO::bcpO-3XFLAG* (*bcpO-3xFLAG)* cell lysates incubated with magnetic M2 FLAG beads. Bound proteins were eluted from the beads via boiling in 4X SDS sample buffer. Prior to cell lysis, cultures were standardized to the same OD_{600}, and samples were loaded at equal volumes. Lanes labeled as 1 were loaded with Δ*bcpO* elution sample from the same experiment. Lanes labeled as 2 were loaded with *bcpO-3xFLAG* elution sample from the same experiment. **(A)** SDS-PAGE gels were stained with SYPRO Ruby for protein visualization. Bands labeled A-E from *bcpO-3XFLAG* lanes and corresponding regions in Δ*bcpO* lanes, were excised and sent to the Proteomics Core Facility at the University of Kentucky for Mass spectrometry analysis. **(B)** Western blot probed with monoclonal anti-FLAG primary and fluorescent anti-mouse secondary antibodies. Orange arrow shows BcpO-3XFLAG bands and asterisks indicate nonspecific bands.

Figure 3.6 Analysis of BcpO$_{E22A}$ point mutant

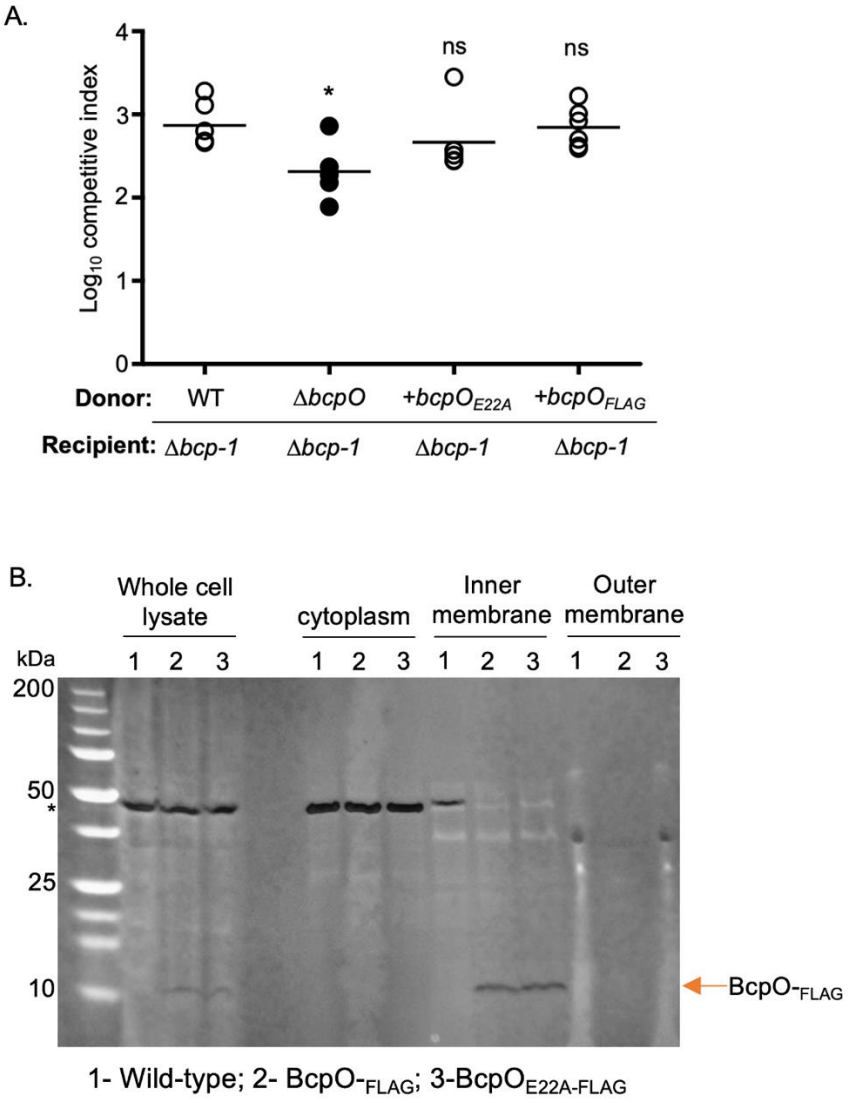

(A) Interbacterial competition assays between indicated donor cells: wild-type, Δ*bcpO*, Δ*bcpO* constitutively expressing P_{S12}-*bcpO*$_{E22A}$ point mutant construct (+*bcpO*-$_{E22A}$) or Δ*bcpO* constitutively expressing P_{S12}-*bcpO*-$_{FLAG}$ construct (+*bcpO*-$_{FLAG}$) and Δ*bcp*-1 recipient cells. Symbols represent $\log_{10}$ competitive index values (ratio of donor to recipient) from two independent experiments (n= 6). Dashed line shows $\log_{10}$ competitive index = 0. A one-way ANOVA was performed, ns, not significant; *, $P < 0.05$; compared to wild-type. **(B)** Western blot of selective detergent and ultracentrifugation subcellular fractionation of 1) wild-type, 2) Δ*bcpO* constitutively expressing P_{S12}-*bcpO*-$_{FLAG}$ construct (BcpO-$_{FLAG}$) and 3) Δ*bcpO* constitutively expressing P_{S12}-*bcpO*$_{E22A\text{-}FLAG}$ point mutant (BcpO$_{E22A\text{-}FLAG}$) strains. Prior to cell lysis, cultures were standardized to the same OD_{600}. Membrane blots were probed with monoclonal anti-FLAG primary and fluorescent anti-mouse secondary antibodies. Orange arrow shows BcpO-$_{FLAG}$ (or BcpO$_{E22A\text{-}FLAG}$) bands and asterisk indicates nonspecific bands.

Figure 3.7 Inconsistent BcpO fractionation

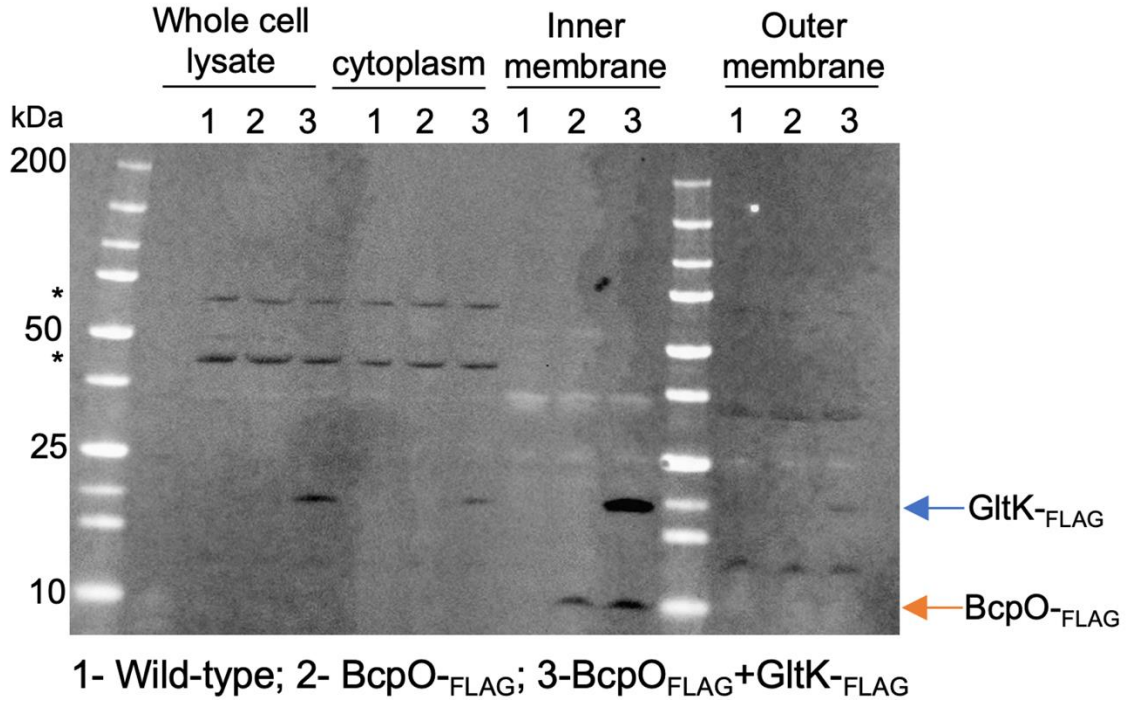

Selective detergent subcellular fractionation Western blot of 1) wild-type, 2) Δ*bcpO* constitutively expressing P_{S12}-*bcpO*-FLAG and 3) Δ*bcpO* constitutively expressing P_{S12}-*gltK*-FLAG and P_{S12}-*bcpO*-FLAG (BcpO-GltK). Prior to cell lysis, cultures were standardized to the same OD_{600}. Membrane blots were probed with monoclonal anti-FLAG primary and fluorescent anti-mouse secondary antibodies. Blue and orange arrows represent GltK-FLAG and BcpO-FLAG bands, respectively. Asterisks indicate non-specific bands.

Figure 3.8 Inconsistent BcpO results

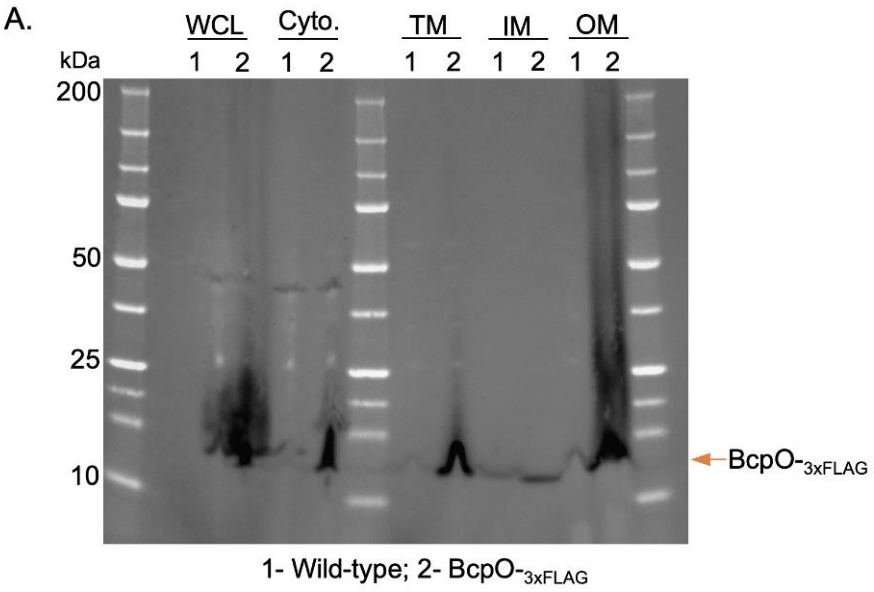

A) Sucrose density gradient subcellular fractionation Western blot of 1) wild-type and 2) Δ*bcpO* constitutively expressing P_{S12}-*bcpO*-3XFLAG. Whole cell lysate (WCL), cytoplasm (cyto.), total membrane (TM), inner membrane (IM) and outer membrane (OM) fractions were loaded at equal concentrations for each sample. Membrane blots were probed with monoclonal anti-FLAG primary and fluorescent anti-mouse secondary antibodies. Orange arrow shows BcpO-3xFLAG bands. **(B)** Interbacterial competition assay between indicated donor cells: wild-type, Δ*bcpOB*, Δ*bcpOB* constitutively expressing P_{S12}-*bcpOB* (+*bcpOB*), Δ*bcpO, or* Δ*bcpO* constitutively expressing P_{S12}-*bcpO* (+*bcpO*) and Δ*bcp-1* recipient cells. Symbols represent $\log_{10}$ competitive index values (ratio of donor to recipient) from two independent experiments (n= 6). Dashed line shows $\log_{10}$ competitive index = 0. A one-way ANOVA was performed, ns, not significant; *, $P < 0.05$; compared to wild-type, unless noted by brackets.

Figure 3.9 Inconsistent BcpO-$_{3XFLAG}$ fractionation

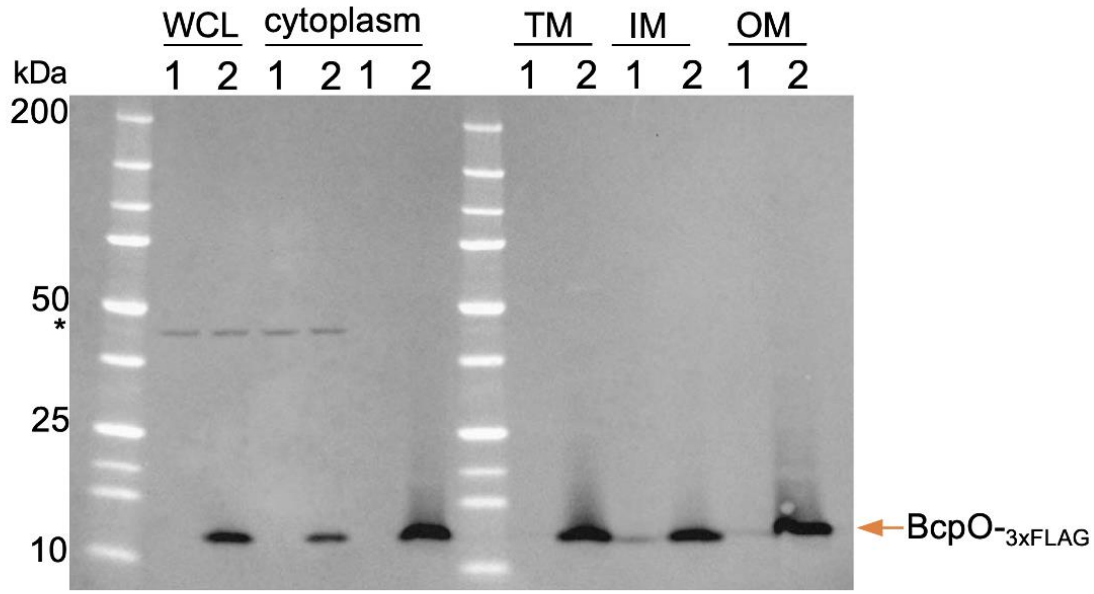

1- Wild-type; 2- BcpO-$_{3xFLAG}$

Sucrose density gradient subcellular fractionation western blot of 1) wild-type and 2) Δ*bcpO* constitutively expressing P$_{S12}$-*bcpO*-$_{3XFLAG}$. Whole cell lysate (WCL), cytoplasm, total membrane (TM), inner membrane (IM) and outer membrane (OM) fractions were loaded at equal concentrations for each sample. Membrane blots were probed with monoclonal anti-FLAG primary and fluorescent anti-mouse secondary antibodies. Orange arrow shows BcpO-$_{3xFLAG}$ bands and asterisk indicates nonspecific bands.

Table 3.1 Unique protein hits identified by LC-MS/MS

Description	Score[a]	Coverage[b]	MW[c]	Band[d]
Major facilitator superfamily (MFS_1) transporter	98.62	6.61	49.2	A
Periplasmic protease	86.52	15.89	56.4	A
ATP-dependent Clp protease, ATP-binding subunit ClpX	392.28	54.61	46.4	B
phenylacetic acid degradation protein paaN	294.48	23.94	60.4	B
IspG protein	196.01	17.12	46.9	B
methyl-accepting chemotaxis (MCP) signaling domain protein	192.24	18.30	54.6	B
potassium uptake protein	156.06	14.44	69.2	B
lysE type translocator family protein	107.12	15.09	22.5	C
hypothetical membrane protein AK34_2385	90.97	9.69	24.9	C
Hypothetical membrane protein BDAG_02405	90.97	10.00	24.1	C
type VI secretion system effector, Hcp1 family protein	74.80	15.57	18.4	C
hypothetical protein AK34_1701	93.77	36.23	14.6	D
hypothetical protein BDAG_01797	93.77	33.33	16.0	D
disulfide bond formation DsbB family protein	66.96	5.29	18.7	D
type II secretion system protein G	62.58	25.33	16.7	D
bcpO	646.33	45.00	11.3	E
type IV pilus biogenesis family protein	84.56	19.85	14.1	E
hypothetical protein BDAG_02706	61.49	8.23	17.8	E
doxX-like family protein	55.13	7.30	14.4	E

[a] The protein score, which is the sum of the scores of the individual peptides

[b] The percentage of the protein sequence covered by identified peptides

[c] The molecular weight, in kilodaltons, of the predicted protein

[d] The gel band from which the protein was isolated from

CHAPTER 4. Interplay between CDI systems produced in *Burkholderia cepacia* complex species

This work was a submitted publication: **“**Relaxed specificity of BcpB transporters mediates interactions between *Burkholderia cepacia* complex contact-dependent growth inhibition systems.” Elery ZK., Myers-Morales T., Phillips ED., and Garcia EC. mSphere 2023.

4.1 Introduction

Some organisms encode multiple CDI systems that each contain a distinct toxin-immunity pair. In *Escherichia coli*, *Acinetobacter baumannii*, *Pseudomonas aeruginosa,* and several *Burkholderia cepacia* complex species, these systems have been shown to independently mediate interbacterial competition, often displaying differences in gene expression or toxin potency (133,134,157,195,196). Whether cross talk may occur among CDI systems produced by the same strain has not been examined.

Research on representative TPS systems has defined a model for the secretion pathway of these proteins. After transport into the periplasm via the Sec machinery, TpsA remains in an unfolded state until the TpsB transporter incorporates TpsA into the outer membrane and it is progressively folded at the cell surface (75,197,198). The TpsA proteins are large filamentous exoproteins with typical hemagglutinin repeats and a conserved N-terminal TPS domain required for recognition by a TpsB transporter (75). The TpsB transporters are Omp85 superfamily members that consist of an outer membrane-embedded β-

barrel channel, an N-terminal α-helix (H1) plug that inserts into the barrel pore, a short periplasmic polypeptide linker, and two periplasmic polypeptide transport associated (POTRA) domains (113,199,200). The POTRA domains interact with the TPS domain on the TpsA protein and are necessary for substrate recognition and secretion (110,111). However, the precise role each POTRA domain plays in substrate secretion remains unknown and may vary between systems.

The specificity of a TpsB transporter for its cognate TpsA partner also varies between systems. Many TpsB transporters can secrete only their cognate partner, while other transporters can secrete more than one TpsA effector (104). The CdiB transporters from *A. baumannii* ACICU and *E. coli* EC93, which share ~23% amino acid sequence identity, are not interchangeable and specifically secrete their cognate CdiA proteins (114). However, little is known about the specificity of more closely related BcpB or CdiB transporters, such as those that would be produced by an organism with multiple CDI systems.

Here we use *B. cepacia* complex species that each produce multiple distinct CDI systems to examine the specificity of BcpB transporters for BcpA toxin secretion. The results show that even though each complete CDI system includes an associated BcpB, the transporters display a high degree of promiscuity and generally secrete both cognate and non-cognate BcpA proteins efficiently. While three BcpB proteins in *Burkholderia dolosa* each secreted multiple BcpA toxins, differences in gene expression appeared to limit which transporters were available. We also report that the relaxed specificity of BcpB proteins extends to *Burkholderia multivorans,* suggesting that interaction of non-

cognate BcpB-BcpA pairs may be a common characteristic of bacterial species that produce multiple CDI systems.

4.2 Results

B. dolosa AU0158 contains an additional putative CDI system.

B. dolosa strain AU0158 (*Bd*AU0158) was shown to produce three unique CDI systems capable of mediating interbacterial competition, but only system-1 and system-2 were expressed in laboratory conditions (133). Each of the three CDI systems encodes a distinct BcpB transporter, sharing ~80% amino acid identity. Additionally, we identified a fourth *bcpB* gene downstream of a cryptic *bcp* locus (referred to as *bcp-4)* located on *Bd*AU0158 chromosome 3 (**Fig. 4.1A**). The *bcp-4* region resembles other loci that encode *Burkholderia*-type CDI systems, with the gene order *bcpAI(O)B*. However, the distance between the *bcpI* and *bcpB* genes is ~8,000 bp, a gap larger than what is typically found for *Burkholderia*-type CDI loci. The *bcp-4* locus has multiple open reading frames (ORFs) between the *bcpI* and *bcpB genes,* although none of these ORFs are predicted to encode a BcpO lipoprotein. Instead, many of the ORFs are predicted to encode transposases, integrases, or genes that produce uncharacterized hypothetical proteins. Interestingly, immediately downstream of *bcpAI-4* are additional *bcp*-like genes: an ORF annotated to encode an immunity 45 family protein and truncated *bcpB* and *bcpA* genes. Despite the chromosomal distance

between the *bcpAI-4* and *bcpB-4* genes, the *bcp-4* region contains the genetic components necessary to produce a CDI system.

Putative *Bd*AU0158 *bcpA-4* promoter is active under *in vitro* competition conditions.

To examine the expression of the *bcp-4* genes, ~500 bp 5' to the *bcpA-4* and *bcpB-4* translational start sites were fused to promoterless *lacZ* genes and delivered to *att*Tn7 sites of *Bd*AU0158. The resulting reporter strains were compared to similar reporter strains generated for the other three *Bd*AU0158 *bcpA* genes (133). When grown in monoculture under the same conditions as those used for competition experiments, the *bcpA-1* and bcpA-2 reporters showed low levels of β-galactosidase activity (**Fig. 4.1B**). By contrast, P_{bcpA-3}-*lacZ* showed no detectable activity (**Fig. 4.1B**), as previously demonstrated (133). The P_{bcpA-4}-*lacZ* reporter also showed low levels of β-galactosidase activity, while the P_{bcpB-4}-*lacZ* activity levels did not significantly differ from the promoterless control. These data suggest that *bcpA-4* is expressed and therefore may produce a functional CDI system protein, while *bcpB-4* is likely not expressed under the conditions tested.

***Bd*AU0158 *bcp-4* encodes a functional CDI system.**

To determine the functionality of the *Bd*AU0158 *bcp-4* CDI system, a mutant strain containing an unmarked, in-frame deletion of *bcpA-4* through *bcpB-*

4 was generated (Δ*bcp-4*). When wild-type donor cells were competed against the Δ*bcp-4* recipient cells at a 1:1 or 10:1 ratio, there was no difference in the competitive index between non-immune recipient cells or those producing cognate immunity protein BcpI-4 (**Fig. 4.1C**). These data suggest that the *Bd*AU0158 BcpAIB-4 CDI system does not mediate interbacterial competition under conditions of native expression *in vitro*.

We hypothesized that native expression of *bcpA-4* is not sufficient for CDI-mediated competition and constructed a strain in which the putative *bcpA-4* promoter was replaced with the strong, constitutively active *Burkholderia thailandensis rpsL* (ribosomal S12 subunit) promoter, resulting in strain *bcp-4*^{C}. Following co-culture, the *Bd*AU0158 *bcp-4*^{C} donor bacteria outcompeted the Δ*bcp-4* mutant by ~10-fold when inoculated at a 1:1 ratio and by ~100-fold when inoculated at a 10:1 ratio (**Fig. 4.1C**). Introduction of the cognate *bcpI-4* immunity gene protected recipient cells from *bcpA-4* mediated killing. As expected, complementation with a gene encoding a heterologous immunity protein from *B. multivorans* (*Bm*CGD2M *bcpI-2*) did not provide protection against CDI, indicating that *bcpI-4* protection was allele-specific. These results indicate that the *bcp-4* locus encodes a functional CDI system that can mediate interbacterial competition when expressed at a high level.

Cognate BcpB transporters are not required for *B. dolosa* CDI-mediated competition.

Many bacterial species encode multiple CDI systems within the same strain. Since *B. dolosa* AU0158 contains four unique CDI systems, this strain provides a useful model for investigating potential interplay between distinct CDI systems. To examine the specificity of *Bd*AU0158 BcpB transporters, strains containing unmarked, in-frame deletion mutations of each of the *bcpB* genes were generated, resulting in Δ*bcpB-1*, Δ*bcpB-2,* Δ*bcpB-3,* and Δ*bcpB-4* mutants. Interbacterial competition assays between these *bcpB* mutants and the corresponding immunity-deficient (Δ*bcpAIOB*) recipient cells were used to determine if each BcpB protein is required for the secretion of its cognate BcpA toxin. Surprisingly, the Δ*bcpB-1* mutant inhibited the Δ*bcp-1* recipient strain similarly to wild-type donors, implying that wild-type levels of BcpA-1 were still secreted and delivered to recipient bacteria in the absence of BcpB-1 (**Fig. 4.2A**). The Δ*bcpB-2* mutant was also able to outcompete susceptible recipient cells, but showed a ~10-fold defect in competitive index as compared to wild-type donor bacteria (**Fig. 4.2B**). Interbacterial killing was restored to wild-type levels when donor cells were complemented with *bcpB-2* at a neutral chromosomal site. Thus, BcpB-2 is also unnecessary for secretion of its cognate BcpA protein but does appear to participate in BcpA-2 secretion.

Because *bcpA-3* is not expressed under laboratory conditions, competitions investigating this toxin were conducted in strains that constitutively expressed *bcpA-3* due to replacement of the native *bcpA-3* promoter with P_{S12}

(*bcp-3*^{C}), as previously described (133). The *bcp-3*^{C} Δ*bcpB-3* mutant outcompeted Δ*bcp-3* recipient cells, although the CDI activity was ~100-fold less than for the *bcp-3*^{C} parent strain (**Fig. 4.2C**). These results show that BcpB-3 contributes to but is not required for cognate BcpA-3 secretion.

The *bcp-4* overexpression strain (*bcp-4*^{C}, **Fig. 4.1C**) was also used here to test the contribution of *bcpB-4*. Similar to *bcpB-1*, there was no defect in growth inhibition of Δ*bcp-4* recipient bacteria by donor cells lacking *bcpB-4* (**Fig. 4.2D**), indicating that BcpB-4 is not required for BcpA-4 secretion. However, complementation of the Δ*bcpB-4* mutant with overexpressed *bcpB-4* resulted in a high level of BcpA-4-mediated CDI, representing a ~1000-fold increase in competitive index as compared to the *bcp-4*^{C} parent or Δ*bcpB-4* mutant strains. This high level of CDI activity was eliminated when the complemented donor strain (*bcp-4*^{C} Δ*bcpB-4*+*bcpB-4*) was competed against recipient cells supplemented with cognate *bcpI-4* immunity. These data show that BcpB-4 is not necessary for BcpA-4 secretion, but suggest that the transporter can secrete the toxin when it is overproduced.

Altogether, these data indicate that the four BcpA toxins still mediate CDI in the absence of their cognate BcpB transporters. Because the percent identity among the *Bd*AU0158 BcpB polypeptide transport associated (POTRA) domains, POTRA-1 and POTRA-2 are 74% and 93%, respectively (**Fig. 4.2E, 4.3**), we hypothesized that BcpA proteins could be secreted by non-cognate BcpB transporters.

Specificity of BcpB transporters for BcpA TPS domains.

It has been previously shown for other TPS systems that a truncated TpsA protein consisting of the signal peptide and the TPS domain is efficiently secreted into the culture supernatant in a TpsB-dependent manner (104,111,201,202). To directly examine the secretion of the BcpA proteins, similar TpsA constructs were created for the two proteins that mediate CDI under laboratory conditions, BcpA-1 and BcpA-2. These genetic constructs encoded C-terminally truncated BcpAs encompassing the signal peptide, predicted TPS domain, a portion of the FHA β helical repeat domains, and a FLAG epitope tag (**Fig. 4.4A**). To determine the role each BcpB transporter plays in BcpA secretion, a quadruple Δ*bcpB* mutant lacking all four transporters *(*Δ*bcpB1-4*) and a series of triple Δ*bcpB* deletion mutants that each contained only one natively expressed transporter were constructed. The two constructs encoding truncated BcpA-1 and BcpA-2 proteins, termed *tpsA-1* and *tpsA-2*, were each delivered in single copy to a neutral chromosome site in these mutant strains.

TpsA-FLAG proteins of the expected size (~50 kDa) were only detected in culture supernatants (**Fig. 4.4B, 4.4C, 4.5**). As expected, TpsA-1 and TpsA-2 were not detected in the Δ*bcpB1-4* mutant or in the wild-type strain lacking *tpsA* constructs. Both TpsA-1 (**Fig. 4.4B**) and TpsA-2 (**Fig. 4.4C**) were detected in supernatants when they were produced in wild-type bacteria or the triple *bcpB* mutants containing *bcpB-2* or *bcpB-3* alone. Low levels of TpsA-1 were sometimes observed above the limit of detection in the culture supernatant of the strains containing *bcpB-1* or *bcpB-4* (**Fig. 4.4B, 4.5D**). The non-secreted TpsA-1

and TpsA-2 did not accumulate in the cytoplasm or insoluble (membrane) fractions, but appeared to be degraded (**Fig. 4.5A**).

Overall, these results indicate that truncated BcpA polypeptides are produced and secreted into the culture medium in a BcpB-dependent manner, primarily by BcpB-2 and BcpB-3. This indicates that the domains contained on these proteins are sufficient for BcpA secretion, which is consistent with observations in other TPS and CDI systems (104,110,114). Furthermore, these results support our previous findings that secretion of BcpA-1 and BcpA-2 is not dependent upon the cognate BcpB transporter.

BcpB-2 and BcpB-3 transporters can secrete all four BcpA toxins.

Our findings suggest that both cognate and non-cognate BcpB transporters participate in BcpA secretion in *B. dolosa*. To determine the role each BcpB transporter plays in BcpA toxin secretion and delivery, we used the triple Δ*bcpB* mutants to individually examine the activity of one natively expressed transporter at a time. These *bcpB* deletion mutants were competed against a series of recipient cells that each lack one CDI system (thus lacking immunity to only one BcpA protein). As expected, the quadruple Δ*bcpB1-4* mutant did not outcompete any recipient strain, as it lacks all BcpB transporters (**Fig. 4.6**).

Only the donor strains containing *bcpB-2* or *bcpB-3* outcompeted a Δ*bcp-1* recipient, indicating that BcpB-2 and BcpB-3 each secreted BcpA-1 toxin that

was capable of mediating CDI (**Fig. 4.6A**). However, these competitive indices were significantly less than those of wild-type donors, suggesting that production of only one BcpB transporter is not sufficient for maximum BcpA-1-mediated killing. The donor strains containing only *bcpB-1* or *bcpB-4* did not outcompete Δ*bcp-1* recipient cells, suggesting that BcpA-1 was not secreted by natively produced BcpB-1 or BcpB-4, or that BcpA-1 secreted by these transporters was unable to mediate CDI. While Figure 1A indicated that BcpB-1 is not required for BcpA-1 secretion, these results further suggest that BcpB-1 does not participate in the secretion of its cognate BcpA protein under these conditions.

Similar results supporting the importance of BcpB-2 and BcpB-3 were also found for the remaining BcpA proteins. CDI activity against Δ*bcp-2* or Δ*bcp-3* mutant recipients was only observed for donor strains producing BcpB-2 or BcpB-3 (**Fig. 4.6B-C**). In each case, donor strains producing the cognate BcpB transporter outcompeted recipient bacteria at levels similar to wild-type donors. Donor bacteria producing the non-cognate transporter (either BcpB-2 or BcpB-3) also outcompeted recipient cells, but at levels less than wild-type. These data suggest that BcpA-2 and BcpA-3 can be secreted by multiple BcpB transporters but may prefer their cognate transporters.

BcpA-4 also appeared to utilize BcpB-2 and BcpB-3, but the competitive indices for these mutant co-cultures were significantly less than for the parent strain (**Fig. 4.6D**). This result suggests that production of either BcpB-2 or BcpB-3 is not sufficient for maximum BcpA-4 mediated killing. BcpA-4 activity was not observed when secretion depended on BcpB-4, likely due to poor *bcpB-4*

expression under these conditions **(Fig. 4.1B).** Moreover, previous data showed that *bcpB-4* overexpression led to increased CDI by BcpA-4 (**Fig. 4.2D**), implying that BcpA-4 can be efficiently secreted by its cognate transporter. By contrast, overexpression of *bcpB-1* did not affect BcpA-1 mediated CDI (**Fig. 4.2A**), suggesting that low *bcpB-1* expression may not explain the lack of CDI activity by donor bacteria that only contain *bcpB-1.*

Together these findings indicate that *B. dolosa* BcpA toxins mediate CDI activity when secreted from both cognate and non-cognate BcpB, but the toxins vary in their specificity for the transporters. All four BcpA proteins were secreted from strains containing either *bcpB-2* or *bcpB-3*, but none of the toxins mediated CDI when only *bcpB-1* or *bcpB-4* was present. An implication of this result is that BcpB-3 must be produced and active even though the *bcpA-3* promoter is inactive under these conditions (133). Thus, the activities of this cognate BcpA/BcpB pair are uncoupled in *B. dolosa*.

These results are also generally consistent with the TpsA-1 and TpsA-2 secretion assays, which showed secretion primarily by BcpB-2 and BcpB-3 (**Fig. 4.4**). While we cannot rule out differences in the secretion of truncated BcpA polypeptides (‘TpsA-1’ and ‘TpsA-2’) as compared to full-length BcpAs, it is likely that the occasional low level of TpsA secretion detected for BcpB-1 and/or BcpB-4 (**Fig. 4.4, 4.5**) was insufficient to cause measurable CDI.

Competition between BcpA-1 and BcpA-2 for secretion by BcpB-3

Since our data indicate that multiple BcpA toxins are secreted by BcpB-2 and BcpB-3, we next sought to determine whether competition occurs for secretion by the available BcpB transporters. To do this, we compared the CDI activities of donor strains that utilized only BcpB-3, but had varying levels of potentially competing BcpA-1 and BcpA-2 proteins. This allowed us to ask whether secretion through a single transporter, BcpB-3, was impacted by levels of substate BcpA proteins. When examining BcpA-1 activity, we asked whether interbacterial killing was impacted by BcpA-2 levels, and vice versa.

These experiments utilized a Δ*bcpB-1* Δ*bcpB-2* double mutant that depends on BcpB-3 for secretion of BcpA-1 and BcpA-2. Since this double mutant lacks BcpB-2, it outcompeted both Δ*bcp-1* (**Fig. 4.7A**) and Δ*bcp-2* (**Fig. 4.7B**) recipient cells to a lesser extent than wild-type donors (**Fig. 4.7A-B, panels 1 and 2**). Elimination of BcpB-3 from this mutant (by testing a triple Δ*bcpB-1* Δ*bcpB-2* Δ*bcpB-3* mutant) abolished interbacterial killing of both recipient strains, indicating that the double mutant indeed depended on BcpB-3 for secretion of BcpA-1 and BcpA-2 (**Fig, 4.7A-B, panel 3**). Interestingly, when *bcpA-2* was overexpressed, the BcpA-1 mediated CDI activity of the donor cells was eliminated completely (**Fig. 4.7A, panel 4**). Similarly, overexpression of *bcpA-1* prevented BcpA-2 mediated CDI activity (**Fig. 4.7B, panel 4**). These results indicate that high levels of one BcpA protein can negatively impact the activity of other BcpA proteins when BcpB transporters are limited, likely by competing for secretion by BcpB.

Consistent with this hypothesis, a donor strain lacking *bcpA-2* (Δ*bcp-2* Δ*bcpB-1*) showed significantly higher levels of BcpA-1 mediated CDI (**Fig. 4.7A, panel 5**). However, the reciprocal was not true. Loss of *bcpA-1* did not alter interbacterial killing by BcpA-2 (**Fig. 4.7B, panel 5**). These data suggest that BcpA-2 secretion is less sensitive to the presence of BcpA-1 when both BcpA proteins are utilizing a single BcpB transporter, implying that the BcpB-3 transporter may have a higher affinity for BcpA-2 toxin. Altogether, these data indicate that there can be competition among BcpA proteins for secretion by limited BcpB transporters and the transporters likely a have higher affinity for specific BcpA toxins.

Replacing the BcpB-1 POTRA domains changes the functionality of BcpB-1.

Previous data showed that natively expressed *bcpB-1* does not allow donor cells to inhibit recipient cell growth even with cognate BcpA-1. To determine whether insufficient *bcpB-1* gene expression contributes to this defect, we overexpressed *bcpB-1* in the quadruple Δ*bcpB1-4* mutant that does not contain any native *bcpB* genes. While bacteria that overproduced BcpB-2 secreted BcpA-1 (**Fig. 4.8B**) and BcpA-2 (**Fig. 4.8C**), donor bacteria overexpressing wild-type *bcpB-1* did not show any interbacterial toxicity. Thus, even overproduced BcpB-1 is defective for some step of BcpA secretion or delivery to recipient cells.

To further investigate the apparent lack of BcpB-1 functionality, we utilized chimeric BcpB proteins. For TPS systems in some *Neisseria* species, swapping the POTRA domains can change TpsB specificity (110). To test whether differences in the BcpB-1 and BcpB-2 POTRA domains account for the proteins' functional differences, we generated chimeric *bcpB-1* genes that had the regions encoding the POTRA-1 (residues 95-165) or POTRA-1 and POTRA-2 (residues 95-165 and 167-219) domains replaced with the corresponding regions from *bcpB-2* (**Fig. 4.8A**). To examine the activity of the BcpB-1 chimeric proteins, they were produced in the Δ*bcpB1-4* mutant strain and competed against Δ*bcp-1* and Δ*bcp-2* recipient bacteria. The chimeric proteins BcpB-1^{Chim1} and BcpB-1^{Chim2} were able to induce a low level of BcpA-1- and BcpA-2-mediated CDI (**Fig. 4.8B, 4.8C**). Therefore, replacement of the POTRA-1 or POTRA-1 and POTRA-2 domains of BcpB-1 likely allows for increased secretion of BcpA-1 and BcpA-2, although not to the levels observed for full-length BcpB-2.

TpsB family proteins like BcpB contain an H1 plug that blocks the barrel pore in the resting conformation; this plug needs to be removed for secretion to occur (199,200). The plug is connected to the first POTRA domain by a short periplasmic polypeptide, referred to as the linker (**Fig. 4.9C, 4.10**). It has been shown in other TPS systems that the linker is also necessary for substrate secretion (92,113,114,199). To examine the function of the plug-linker, a third BcpB-1 chimera (BcpB-1^{Chim3}) that has the plug and linker regions of BcpB-1 replaced with the regions from BcpB-2 was generated. Donor bacteria producing BcpB-1^{Chim3} were not able to intoxicate either Δ*bcp-1* (**Fig. 4.8B**) or Δ*bcp-2* (**Fig.**

4.8C) recipient cells, suggesting that alterations to the plug-linker regions do not explain the low secretion activity for BcpB-1. Lastly, a fourth BcpB-1 chimera (BcpB-1^{Chim4}) was generated to replace the plug-linker, POTRA-1, and POTRA-2 domains from BcpB-1 with the corresponding regions from BcpB-2. Similar to BcpB-1^{Chim1} and BcpB-1^{Chim2}, donor bacteria producing BcpB-1^{Chim4} showed a ~5-fold and ~10-fold increase in CDI activity as compared to the non-secreting Δ*bcpB1-4* mutant.

The three chimeras that contained the BcpB-2 POTRA-1 domain were the only BcpB-1 proteins to show CDI activity. These data suggest that the specificity of the POTRA-1 domain may contribute to the low secretion activity of native BcpB-1. Although we have not ruled out contributions of POTRA-2, only two amino acids differ between the proteins in this region. None of the chimeric BcpB-1 proteins functioned similarly to BcpB-2, indicating that additional differences elsewhere in the protein contribute to the functional differences between BcpB-1 and BcpB-2. Considerable sequence variability between BcpB-1 and BcpB-2 exists C-terminal to the POTRA-2 domain, which is predicted to form the β-barrel (**Fig. 4.9C, 4.10**).

BcpB^{E264}, a close *B. dolosa* BcpB-1 homolog, can secrete BcpA-1 and BcpA-2

Interestingly, it has been previously reported that the *Burkholderia thailandensis* E264 *bcp* and *B. dolosa* AU0158 *bcp-1* toxin and immunity alleles

are functionally interchangeable. The *Bd*AU0158 BcpI-1 and *Bt*E264 BcpI immunity proteins provided cross-protection against both the *Bd*AU0158 BcpA-1 and *Bt*E264 BcpA toxins (133). Even though the *Bd*AU0158 BcpB-1 and *Bt*E264 BcpB proteins are ~95% identical at the amino acid level (**Fig. 4.10**), based on our data we hypothesize that they are not functionally identical. Unlike *Bd*AU0158, *Bt*E264 produces only one CDI system with one *bcpB* gene, so we expect the BcpB$^{Bt\text{E264}}$ protein to be functional. To examine the functionality of the *Bt*E264 BcpB protein for secretion of *Bd*AU0158 BcpA proteins, we expressed *Bt*E264 *bcpB* gene in the *Bd*AU0158 Δ*bcpB1-4* mutant. Unlike *Bd*AU0158 BcpB-1, *Bt*E264 BcpB was able to mediate CDI against Δ*bcp-1* (**Fig. 4.9A**) or Δ*bcp-2* (**Fig. 4.9B**) recipient cells at levels not significantly different from wild-type donor cells. These data indicate that the few amino acid differences between the two closely related BcpB proteins are responsible for a large difference in functionality (**Fig. 4.10**).

Sequence comparison between *Bd*AU0158 BcpB-1, which appears defective for one or more steps in BcpA secretion or delivery, and the CDI-competent *Bd*AU0158 BcpB-2 and *Bt*E264 BcpB shows a limited number of amino acid differences. Only 20 residues differ in BcpB-1$^{Bd\text{AU0158}}$ as compared to BcpB-2$^{Bd\text{AU0158}}$ or BcpB$^{Bt\text{E264}}$ (**Fig. 4.10**). Nine of these residues map to the predicted beta-barrel of BcpB-1, including three each in β-strands β7 and β16 (**Fig. 4.9C**). Six residues are predicted to be found in or immediately adjacent to (β15) extracellular loops. Three residues are predicted in the POTRA-1 domain,

and one residue is located in each of the plug-linker region and the region N-terminal to H1.

Overproduction of BcpB reveals differences in transporter specificity.

Overexpression of *bcpB-1* did not allow donor bacteria to outcompete Δ*bcp-1* or Δ*bcp-2* recipient cells (**Fig. 4.8**). To examine whether differences in gene expression could account for other interbacterial toxicity differences observed for the *bcpB* mutant donor cells, we overexpressed the remaining *bcpB* genes in Δ*bcpB1-4* donor bacteria. Interestingly, overexpression of *bcpB-2*, *bcpB-3*, or *bcpB-4* allowed intoxication by BcpA-1 (**Fig. 4.11A**) or BcpA-2 (**Fig. 4.11B**). These data indicate that BcpB-4 can secrete non-cognate toxin when overproduced and suggest that the low activity of natively-expressed *bcpB-4* (**Fig. 4.6**) is likely due to insufficient gene expression under the conditions used here. These experiments also showed differences in BcpB-3 function. Consistent with the finding that natively expressed *bcpB-3* facilitates reduced BcpA-1-mediated CDI (**Fig. 4.6A**), activity of BcpA-1 also appeared diminished here when secretion was dependent on overproduced BcpB-3 (**Fig. 4.11A**). By contrast, overproduced BcpB-3 allowed wild-type levels of BcpA-2 toxicity here (**Fig. 4.11B**), while competition by donor cells producing native BcpB-3 was reduced (**Fig. 4.6B**). These results suggest that BcpB-3 is less competent for BcpA-1 secretion or delivery, while these processes occur more efficiently for BcpA-2.

BcpB transporter specificity in other *B. cepacia* complex species.

Since the *B. dolosa* BcpB transporters appear to have relaxed specificity, we hypothesized that BcpB proteins found in other *Burkholderia* strains may also secrete non-cognate BcpA proteins. *Burkholderia multivorans* CGD2M encodes two CDI systems that can mediate interbacterial toxicity (134) and the associated BcpB proteins are 78-86% identical to the *Bd*AU0158 transporters (**Fig. 4.3**). To assess whether BcpA toxins can be secreted by cross-species BcpB transporters, *Bm*CGD2M BcpB proteins were overproduced in *Bd*AU0158 Δ*bcpB1-4* donor bacteria. *Bm*CGD2M BcpB-2 showed wild-type levels of BcpA-1 (**Fig. 4.11A**) and-BcpA-2 (**Fig. 4.11B**) mediated toxicity, while donors producing *Bm*CGD2M BcpB-1 showed only a low level of BcpA-1 activity. These data suggest that both *Bm*CGD2M BcpB-1 and BcpB-2 can secrete and deliver non-cognate BcpA substrates, although to different extents.

To test whether these *Bm*CGD2M BcpB proteins mediate secretion of non-cognate BcpA proteins in their native organism, we performed interbacterial competition assays with *B. multivorans*. Because previous work from our lab indicated that *Bm*CGD2M CDI system-1 (*bcpAIOB-1*) mediates interbacterial competition only when overexpressed (134), we measured the activity of BcpA-2$^{Bm\text{CGD2M}}$. Reflecting the inactivity of CDI system-1, Δ*bcp-1* donor cells outcompeted Δ*bcp-1* Δ*bcp-2* recipient bacteria at a level similar to wild-type donors (**Fig. 4.11C**), indicating that the interbacterial toxicity is due to the BcpA-2 toxin. *Bm*CGD2M donor cells lacking *bcpB-2* outcompeted recipient cells ~5-fold,

but these competitive indices were not significantly different from those of the *bcpB*-deficient Δ*bcp-1* Δ*bcpB-2* mutant donor cells, likely reflecting low native expression of *bcpB-1* (**Fig. 4.11C, 4.11D**). Complementation of the Δ*bcp-1* Δ*bcpB-2* mutant with overexpressed *Bm*CGD2M *bcpB-1* or *bcpB-2* resulted in interbacterial toxicity, indicating that both transporters can secrete BcpA-2. Only complementation with *bcpB-2* restored interbacterial toxicity to wild-type levels, though, suggesting that BcpA-2 may show preference for its cognate transporter. Together these data indicate that both *B. multivorans* BcpB-1 and BcpB-2 transporters can secrete BcpA-2, but cognate BcpB-2 is necessary for maximum secretion or delivery.

B. dolosa BcpB transporters were also capable of secreting *B. multivorans* BcpA-2. Overexpression of *B. dolosa bcpB-3* or *bcpB-4* in the *Bm*CGD2M Δ*bcp-1* Δ*bcpB-2* donor strain resulted in wild-type levels of CDI (**Fig. 4.11D**). *B. multivorans* donor cells producing *B. dolosa* BcpB-2 also inhibited the growth of recipient cells, but to a lesser extent than cells producing the native transporter. Consistent with our previous observations, *Bd*AU0158 BcpB-1 did not allow CDI activity in *B. multivorans*.

Together, these findings indicate that the relaxed specificity of the BcpB transporters occurs in several Bcc species that produce multiple CDI systems. By comparing donor cells that overproduced BcpB proteins (**Fig. 4.11**), the relative secretion/delivery efficiencies of each BcpA substrate by each transporter could be determined. BcpB-4$^{Bd\text{AU0158}}$ and BcpB-2$^{Bm\text{CGD2M}}$ appeared the most promiscuous, mediating wild-type levels of CDI from all three distinct BcpA

substrates (**Fig. 4.11A, 4.11B, 4.11D**). BcpB-1$^{Bm\text{CGD2M}}$ also secreted all three substrates, but cells producing this transporter displayed diminished interbacterial inhibition (**Fig. 4.11A-C**). Interestingly, BcpB-2$^{Bd\text{AU0158}}$ and BcpB-3$^{Bd\text{AU0158}}$ showed variable transporter function. Both proteins mediated wild-type levels of growth inhibition by BcpA-2$^{Bd\text{AU0158}}$, but differed in their abilities to cause CDI by BcpA-1$^{Bd\text{AU0158}}$ and BcpA-2$^{Bm\text{CGD2M}}$ (**Fig. 4.11**). Overall, the six distinct BcpB proteins examined here showed variable specificity that depended on the particular BcpA substrate.

4.3 Discussion

In this study, we investigated the impact of interactions between distinct contact-dependent growth inhibition (CDI) systems on interbacterial antagonism. Surprisingly, we found that BcpB transporters were dispensable for the secretion of their cognate BcpA toxin. BcpB transporters in multiple *Burkholderia* species showed relaxed specificity and secreted both cognate and non-cognate full-length BcpA toxins. One toxin (*Bd*AU0158 BcpA-1) was secreted exclusively by non-cognate transporters, as its cognate BcpB protein appeared non-functional under the conditions tested here. The promiscuity of the BcpB transporters led to the observation that competition between CDI systems for substrate secretion can occur when transporters are limited. These findings suggest a model in which distinct CDI systems produced by the same organism may not function independently, but instead interact to secrete the available pool of toxins (**Fig. 4.12A**).

Activity of cognate BcpB/BcpA pairs in *B. dolosa* was sometimes uncoupled, likely due to differences in gene expression. The *bcpA-3* promoter was inactive under laboratory conditions and detection of BcpA-3-mediated CDI required introduction of a strong, constitutive promoter. However, BcpB-3 was highly active under these same conditions and contributed to the secretion of both BcpA-1 and BcpA-2. Expression of *bcpB-3* may be due, in part, to an active promoter upstream of *bcpI-3* that was previously identified (133). Similarly, *bcpA-4* and *bcpB-4* also showed differences in promoter activity. This differential gene expression may produce distinct BcpA/BcpB repertoires in different conditions

and, combined with the secretion flexibility we observed, could tune optimal toxin secretion for different environmental niches.

Surprisingly, *B. dolosa* BcpB-1 was not able to secrete or deliver sufficient toxin, either cognate or non-cognate, to mediate interbacterial competition. Changes to the BcpB-1 POTRA-1 domain by replacement with BcpB-2 sequences increased its activity slightly, suggesting that one or more of the 13 amino acid differences in this region contribute to BcpA recognition and/or secretion. In addition, although *Bd*AU0158 BcpB-1 and *Bt*E264 BcpB are ~95% identical, only BcpB^{BtE264} appeared functional for BcpA secretion. Comparison of all three transporters (BcpB-1^{BdAU0158}, BcpB-2^{BdAU0158}, and BcpB^{BtE264}) identified 20 residues that are unique to BcpB-1^{BdAU0158} (**Fig. 4.9C** and **4.10**). While additional work will be needed to elucidate their potential contributions, three unique residues are located in β-barrel strand β16, which is part of an interface (β1-β16) implicated to undergo rearrangements during CdiB secretion (114). It is possible that these sequence differences allow for BcpB-1^{BdAU0158} activity under particular environmental conditions. Alternatively, these differences may represent an accumulation of mutations that decreased BcpB-1 function. Unlike *Bt*E264, which produces a single BcpB transporter, detrimental mutations might be tolerated in *B. dolosa* because it produces compensatory BcpB proteins.

The secretion specificity of TpsA-TpsB pairs has been shown to be dependent on recognition of the exoprotein TPS domain (201,202). Although the BcpA proteins are highly variable, the N-terminus which includes the TPS domain, is well-conserved (**Fig. 4.5** and **4.13**). *B. dolosa* BcpA-1 and BcpA-2

share only ~37% identity overall, but their TPS domains are 76% identical. By contrast, the TPS domains of *E. coli* and *A. baumannii* CdiA proteins, which are not secreted by each other's CdiB transporters, share only 46% sequence identity (114). Thus, similarity of the TPS domains among BcpA proteins likely accounts for much of the relaxed specificity observed for the BcpB transporters. However, among the relatively similar *B. cepacia* complex BcpA proteins tested here, there does not appear to be a strong correlation between TPS domain similarity and substrate secretion. For example, the *B. dolosa* BcpA-1 and *B. multivorans* BcpA-2 TPS domains are ~95% identical (**Fig. 4.13**), but these substrates utilize BcpB transporters with differing efficiencies (**Fig. 4.11A** and **4.11D**). The amino acid variations between these two TPS domains do not appear to map to a particular region (**Fig. 4.13**). However, these results suggest that the closely related BcpA and BcpB proteins examined here may provide a useful framework for investigating additional mechanistic details of CDI system protein secretion and toxin release. Moreover, given the precisely controlled release of partially-secreted CdiA/BcpA that has been proposed to occur upon recipient cell engagement (135), it is likely that additional interactions between the substrate protein and BcpB transporter are critical to achieve optimal toxin delivery.

While specificity of a 'TpsB' transporter for its partner 'TpsA' exoprotein is a hallmark of Two-Partner Secretion systems, substrate flexibility has been observed for other systems. Some organisms encode 'orphan' TpsA proteins that do not occur with a partner transporter. *Bordetella bronchiseptica* produces a

single transporter, FhaC, which secretes three distinct substrates – FhaB, FhaL, and FhaS (203,204). Similarly, *Neisseria meningitidis* TpsB2 secretes five TpsA proteins, including cognate, non-cognate, and orphan TpsA proteins, while TpsB1 secretes only two of these (104).

Our results indicate that the relaxed specificity of BcpB transporters leads to interactions between distinct CDI systems produced within the same *B. cepacia* complex strain. Many bacterial species encode two or more complete CDI systems, raising the possibility that similar interactions also occur in these organisms. An examination of >450 clinical and environmental *Burkholderia pseudomallei* isolates showed that 57% harbored two or three distinct *bcpA* (termed '*fhaB3'*) gene clusters (205). *Acinetobacter baumannii*, *A. baylyi*, and 81% of *Pseudomonas aeruginosa* strains carry two *cdi* loci, several of which have been shown to mediate interbacterial competition (154,155,157,195,206,207). Comparisons of the CdiB/BcpB proteins that co-occur in these species indicate similarities **(Fig. 4.12B)**, suggesting that CDI system interactions may not only occur in other *Burkholderia* species, such as *B. pseudomallei*, but also in other Gram-negative bacteria that produce multiple CDI systems.

B. cepacia complex bacteria can occupy various environmental niches and cause opportunistic infections in immunocompromised individuals. The natural niches in which CDI systems are active or provide a fitness advantage are not known, but it may be advantageous for *Burkholderia* species to produce multiple CDI systems within the same strain. In addition to providing increased

toxin diversity and broader immunity, encoding multiple CDI systems may increase secretion efficiency or flexibility by providing additional BcpB transporters.

Figure 4.1 Activity of putative *B. dolosa* CDI system-4

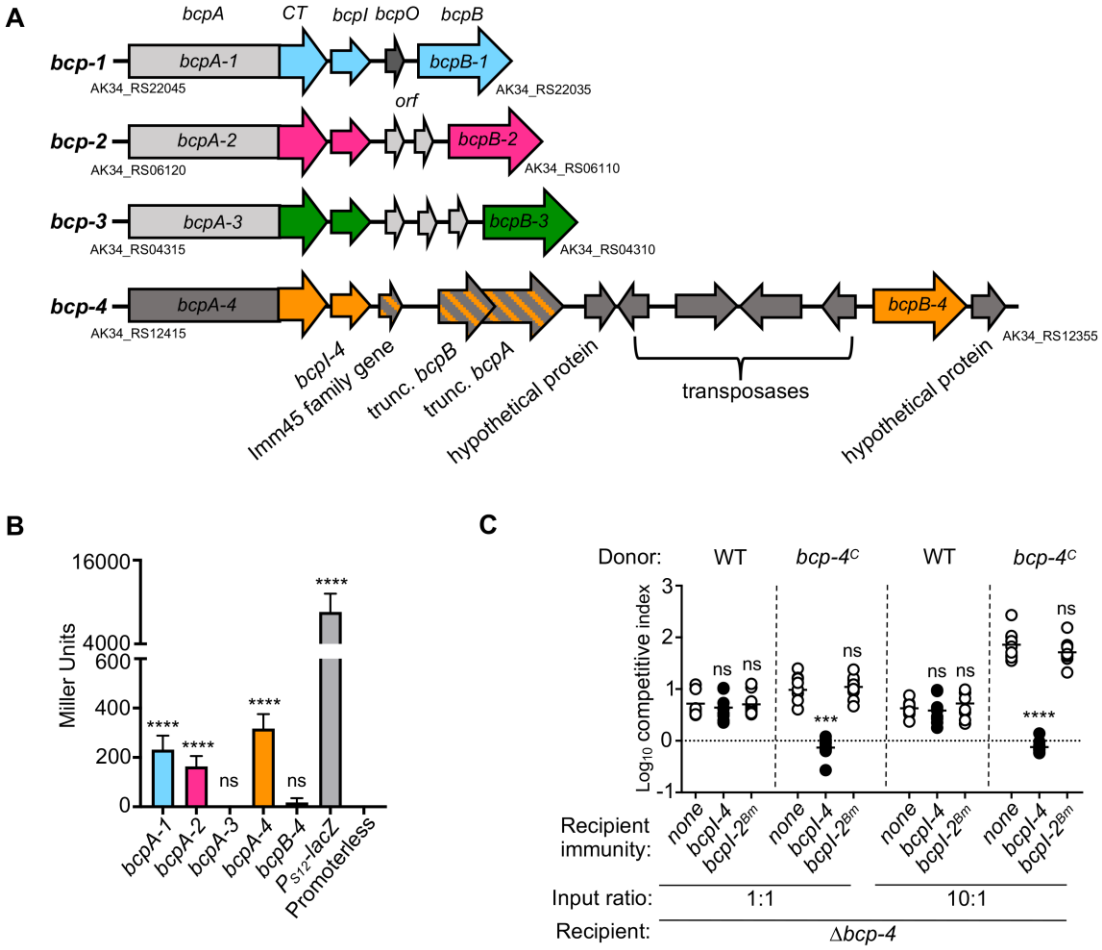

(A) Diagram of the *Bd*AU0158 *bcp-1*, *bcp-2*, *bcp-3,* and *bcp-4* loci. Truncated *bcp* genes are located 3' to *bcpI-4* and are indicated by slashes. Non-*bcp* genes associated with *bcp-4* (dark gray) encode hypothetical proteins and putative transposases. **(B)** Beta-galactosidase assay of *lacZ* reporters for putative promoters of the *Bd*AU0158 *bcpA-1*, *bcpA-2*, *bcpA-3, bcpA-4*, or *bcpB-4* genes and control reporters P_{S12}-*lacZ* (constitutive) and promoterless *lacZ*. Bars show the mean of miller units from three independent experiments, each with three replicates. **(C)** Interbacterial competition assays between *Bd*AU0158 WT or constitutively expressed *bcpA-4* (*bcp-4*^{C}) donor bacteria and Δ*bcp-4* recipient bacteria that were complemented with the cognate *bcpI-4, bcpI-2* from *B. multivorans* CGD2M (*bcpI-2*^{Bm}*),* or no *bcpI* (none). Symbols represent $\log_{10}$ competitive index values (ratio of donor to recipient) from three independent experiments and bars show the means (*n*=9). Competition assays were performed at a 1:1 or 10:1 (donor to recipient) ratio as indicated. Dashed line shows $\log_{10}$ competitive index = 0 (no competition). ns, not significant; ***, *p*<0.001; and ****p<0.0001; compared to WT donor cells competed against no immunity (none) recipient cells in each panel for competition assays or promoterless reporter for the beta-galactosidase assay.

Figure 4.2 Role of cognate BcpB transporters in BcpA-mediated interbacterial antagonism

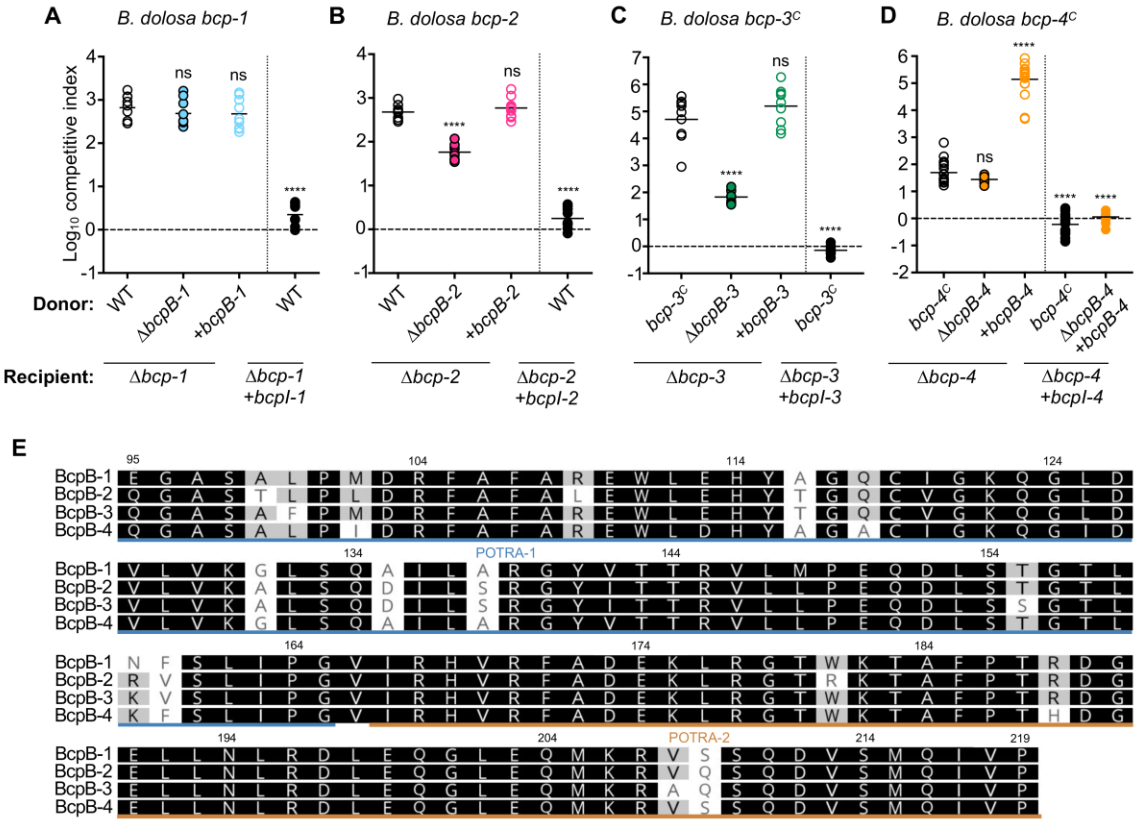

(A) Interbacterial competition assays between the indicated donor cells: *Bd*AU0158 wild-type (WT; open circles), Δ*bcpB-1* (closed blue circles), or Δ*bcpB-1* complemented with P_{S12}-*bcpB-1* at an *att*Tn7 site (+*bcpB-1*; open blue circles) and recipient cells: Δ*bcp-1* or Δ*bcp-1* complemented with cognate *bcpI-1.* **(B)** Interbacterial competition assays between the indicated donor cells: *Bd*AU0158 wild-type (WT) (open circles), Δ*bcpB-2* (closed pink circles), or Δ*bcpB-2* complemented with P_{S12}-*bcpB-2* at an *att*Tn7 site (+*bcpB-2*; open pink circles) and recipient cells: Δ*bcp-2* or Δ*bcp-2* complemented with cognate *bcpI-2.* **(C)** Interbacterial competition assays between donor bacteria constitutively expressing: *Bd*AU0158 *bcpAIOB-3* (*bcpA-3*^{C}) (parent; open circles), *bcpA-3*^{C} Δ*bcpB-3* (closed green circles), or *bcpA-3*^{C} Δ*bcpB-3* complemented with P_{S12}-*bcpB-3* at an *att*Tn7 site (+*bcpB-3*; open green circles) and recipient cells: Δ*bcp-3* or Δ*bcp-3* complemented with cognate *bcpI-3.* **(D)** Interbacterial competition assays between the donor cells that constitutively express: *Bd*AU0158 *bcpA-4* (*bcpA-4*^{C}) (parent; open circles), *bcpA-4*^{C} Δ*bcpB-4* (closed orange circles), or *bcpA-4*^{C} Δ*bcpB-4* complemented with P_{S12}-*bcpB-4* at an *att*Tn7 site (+*bcpB-4*; open orange circles) and the indicated recipient cells: Δ*bcp-4* or Δ*bcp-4* complemented with cognate *bcpI-4* immunity. Competitive Index (CI) for competition assays were calculated as (output donor CFU/recipient CFU) / (Input donor CFU/recipient CFU). Symbols represent $\log_{10}$ CI values from three independent experiments and horizontal bar shows means (*n*=9-18). Competition assays in panel D were performed at a 10:1 ratio. Dashed line shows $\log_{10}$ competitive index = 0 (no competition). ns, not significant and ****p<0.0001;

compared to WT donor cells competed against no immunity recipient cells. **(E)** Amino acid alignments of *Bd*AU0158 BcpB-1, BcpB-2, BcpB-3, and BcpB-4 polypeptide transport associated (POTRA) domains. Similarity is denoted by grayscale; residues similar in all sequences are highlighted in black and residues similar in 50% of sequences are highlighted in gray. Regions underlined in blue or orange, represent POTRA-1 or POTRA-2 domains, respectively.

Figure 4.3 Alignment of *B. dolosa* and *B. multivorans* BcpB proteins.

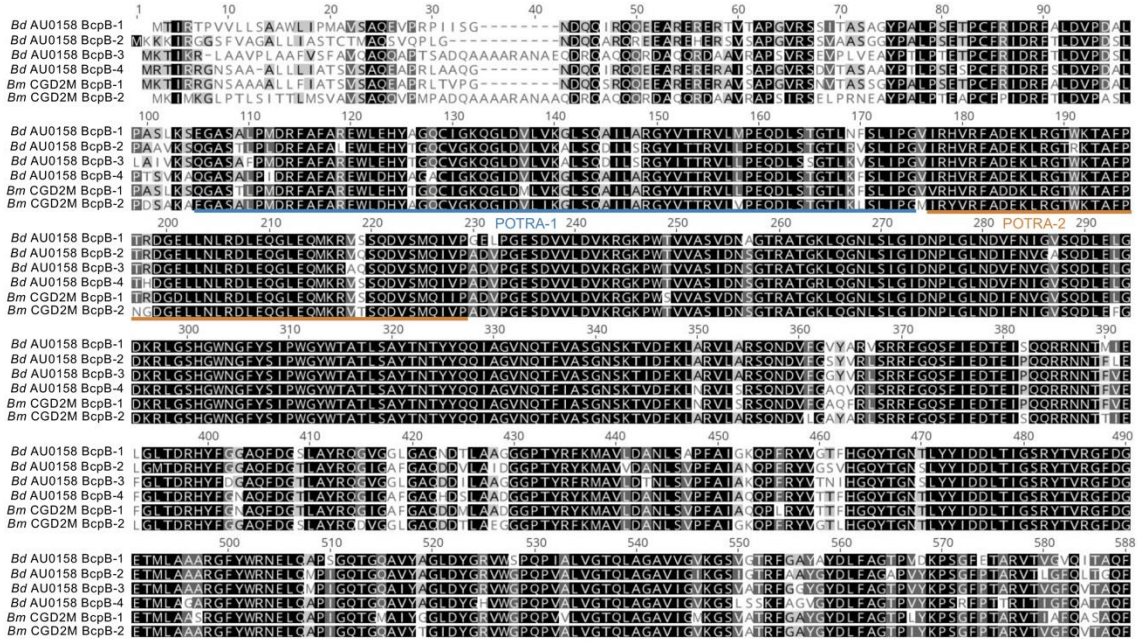

Amino acid alignment of *B. dolosa* and *B. multivorans* BcpB proteins. Similarity is denoted by grayscale; residues similar in all sequences are highlighted in black and residues similar in 50% of sequences are highlighted in gray. Regions underlined in blue or orange, represent POTRA-1 or POTRA-2 domains, respectively.

Figure 4.4 Secretion of truncated BcpA polypeptides by BcpB transporters

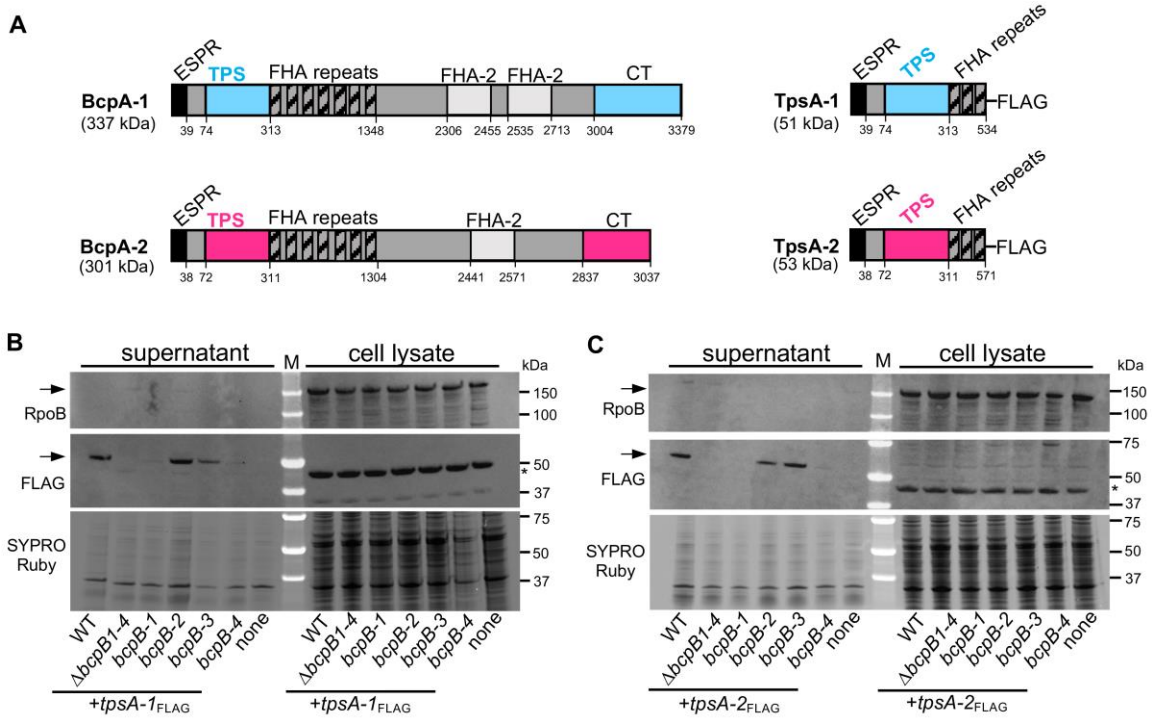

(A) Graphic representation of the BcpA-1 and BcpA-2 proteins (left) and corresponding TpsA-1 and TpsA-2 polypeptides (right). FHA repeats identified as FHA β helical repeats, ESPR classified as extended signal peptide of Type V secretion systems, and FHA-2 identified as Fil_Haemagg_2 by NCBI Conserved Domain Database. **(B, C)** Western blots of concentrated culture supernatants and whole cell lysate of wild-type (WT), quadruple Δ*bcpB-1* Δ*bcpB-2* Δ*bcpB-3* Δ*bcpB-4* mutant *(*Δ*B1-4*), triple mutants containing one natively expressed *bcpB* gene: Δ*bcpB-2* Δ*bcpB-3* Δ*bcpB-4* (*bcpB-1*), Δ*bcpB-1* Δ*bcpB-3* Δ*bcpB-4* (*bcpB-2*), Δ*bcpB-1* Δ*bcpB-2* Δ*bcpB-4* (*bcpB-3*), and Δ*bcpB-1* Δ*bcpB-2* Δ*bcpB-3* (*bcpB-4*) complemented with either **(B)** FLAG-tagged BcpA-1 TPS (*tpsA-1)* or **(C)** FLAG-tagged BcpA-2 TPS (*tpsA-2*). Wild-type bacteria that lack a *tpsA* construct (none) were used as a negative FLAG control. Equal protein amounts for each fraction (supernatant and cell lysate) were resolved on SDS-PAGE gels. Panels shown blotting with anti-*E. coli* RNA Polymerase β subunit (RpoB, top) or anti-FLAG peptide (middle) antibodies and total protein visualization by SYPRO Ruby stained gels (bottom). Expected masses for TpsA-1, TpsA-2, and RpoB are ~53, ~56, and 150 kDa, respectively. Arrows show TpsA-FLAG or RpoB bands and asterisks indicate nonspecific bands.

Figure 4.5 Secretion of truncated BcpA polypeptides by BcpB transporters

replicates

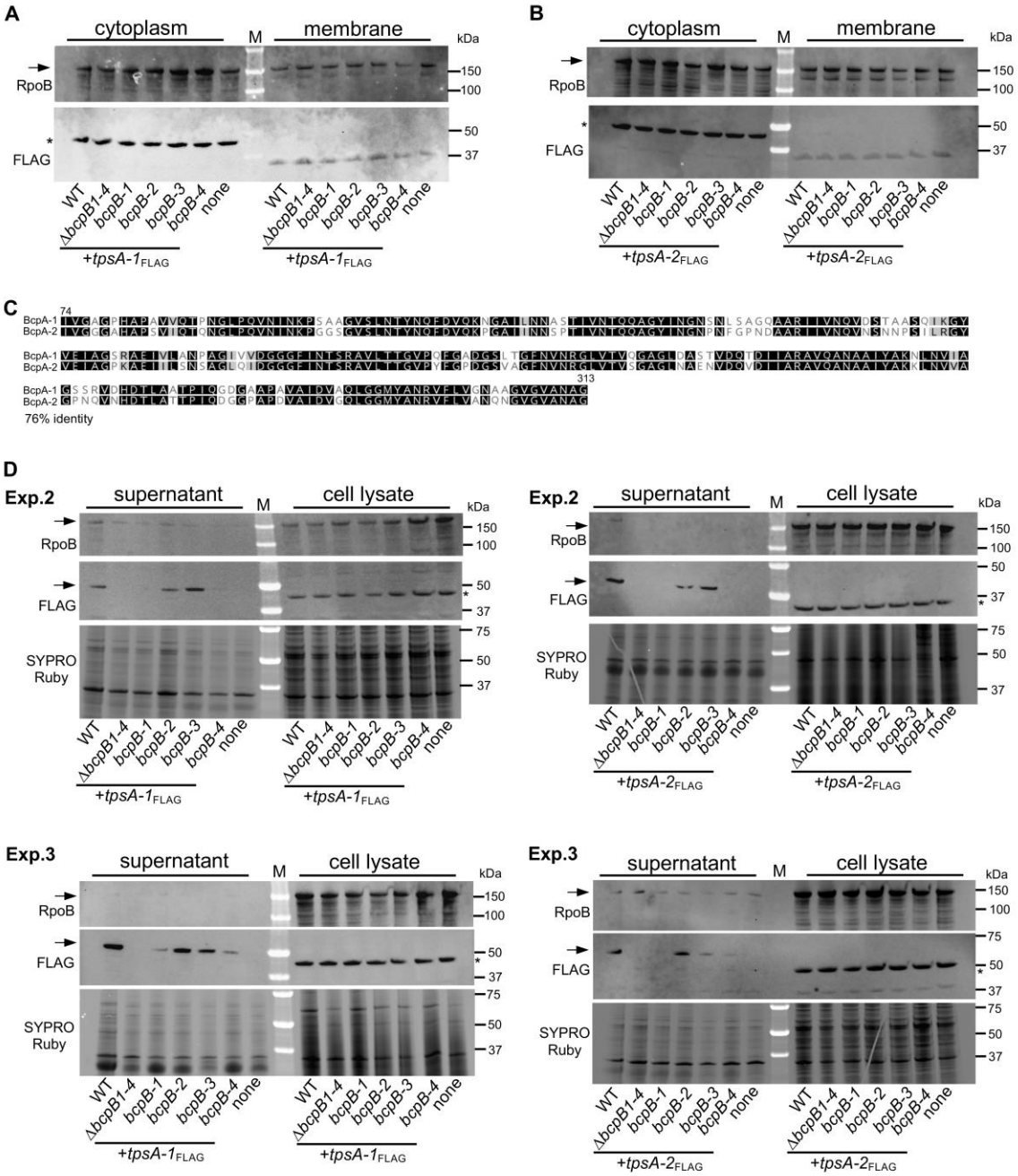

(A) Western blots of concentrated culture supernatants and subcellular fractionations of wild-type (WT), Δ*bcpB-1* Δ*bcpB-2* Δ*bcpB-3* Δ*bcpB-4 (*Δ*B1-4*), Δ*bcpB-2* Δ*bcpB-3* Δ*bcpB-4* (*bcpB-1*), Δ*bcpB-1* Δ*bcpB-3* Δ*bcpB-4* (*bcpB-2*), Δ*bcpB-1* Δ*bcpB-2* Δ*bcpB-4* (*bcpB-3*), and Δ*bcpB-1* Δ*bcpB-2* Δ*bcpB-3* (*bcpB-4*) bacteria complemented with either FLAG-tagged BcpA-1 TPS (*tpsA-1)* or **(B)** the FLAG-tagged BcpA-2 TPS (*tpsA-2*). A wild-type (none) strain that lacks a *tpsA* construct was used as a negative FLAG control. Equal protein amounts for each fraction (cytoplasm and total membrane) were resolved on SDS-PAGE gels and blots were probed with anti-FLAG peptide or anti-*E. coli* RNA Polymerase β subunit (RpoB) antibodies. Expected masses for TpsA-1, TpsA-2, and RpoB are ~53, ~56, and 150 kDa, respectively. Arrows show RpoB bands and asterisk indicate nonspecific bands. **(C)** Amino acid alignment of *B. dolosa* BcpA-1 and BcpA-2 TPS domains. Similarity is denoted by grayscale; residues similar in all sequences are highlighted in black and residues similar in 50% of sequences are highlighted in gray. **(D)** Replicates of TPS secretion assays. Western blots of concentrated culture supernatants and whole cell lysate of wild-type (WT), Δ*bcpB-1* Δ*bcpB-2* Δ*bcpB-3* Δ*bcpB-4 (*Δ*B1-4*), Δ*bcpB-2* Δ*bcpB-3* Δ*bcpB-4* (*bcpB-1*), Δ*bcpB-1* Δ*bcpB-3* Δ*bcpB-4* (*bcpB-2*), Δ*bcpB-1* Δ*bcpB-2* Δ*bcpB-4* (*bcpB-3*), and Δ*bcpB-1* Δ*bcpB-2* Δ*bcpB-3* (*bcpB-4*) bacteria complemented with either FLAG-tagged BcpA-1 TPS (*tpsA-1)* or the FLAG-tagged BcpA-2 TPS (*tpsA-2*). A wild-type (none) strain that lacks a *tpsA* construct was used as a negative FLAG control. Equal protein amounts for each fraction (supernatant and cell lysate) were resolved on SDS-PAGE gels. Gels were visualized by SYPRO Ruby

staining and blots were probed with anti-FLAG peptide or anti-*E. coli* RNA Polymerase β subunit (RpoB) antibodies. Expected masses for TpsA-1, TpsA-2, and RpoB are ~53, ~56, and 150 kDa, respectively. Arrows show TpsA-FLAG or RpoB bands and asterisks indicate nonspecific bands.

Figure 4.6 Contribution of natively expressed BcpB transporters during *Bd*AU0158 CDI-mediated competition

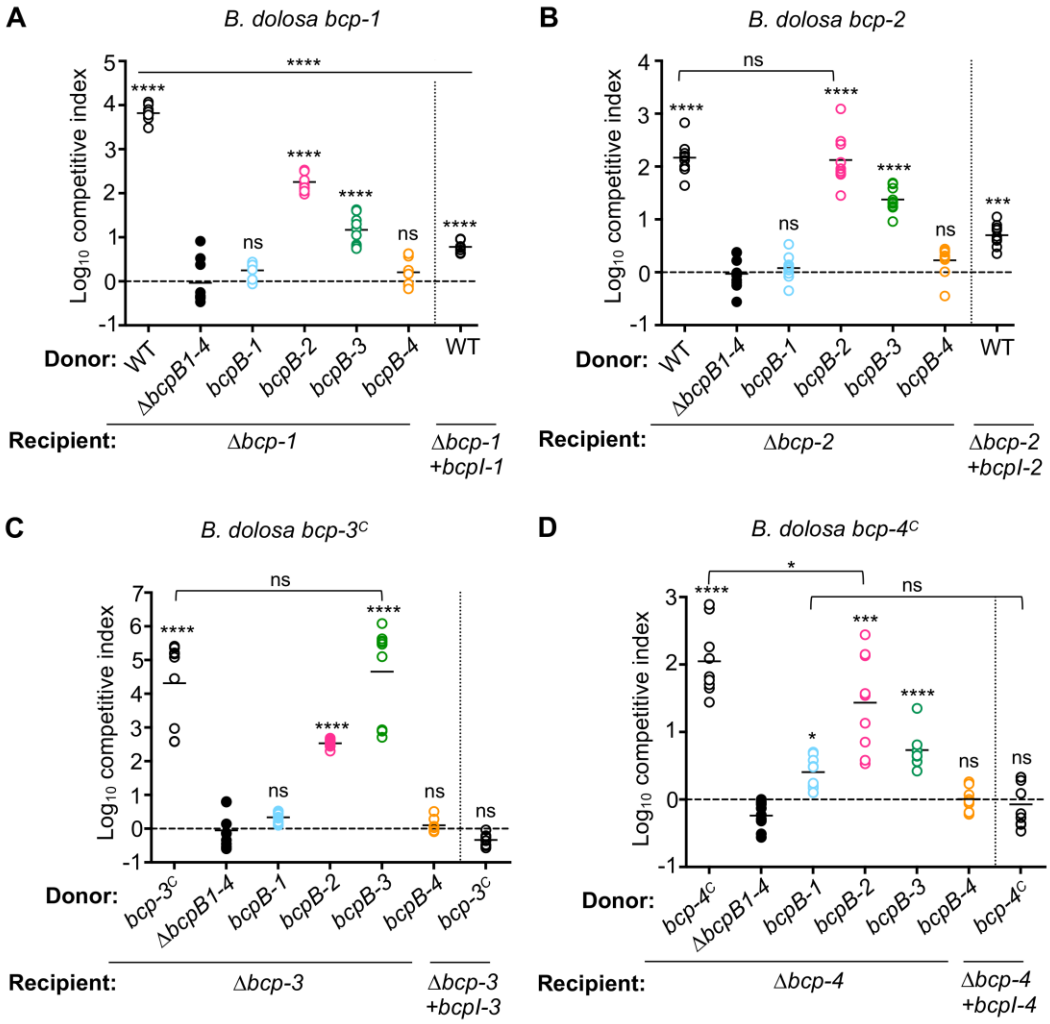

Interbacterial competition assays between the indicated donor cells: *Bd*AU0158 wild-type (WT; open circles), Δ*bcpB-1* Δ*bcpB-2* Δ*bcpB-3* Δ*bcpB-4 (*Δ*bcpB1-4;* closed circles), Δ*bcpB-2* Δ*bcpB-3* Δ*bcpB-4* (*bcpB-1*; blue circles), Δ*bcpB-1* Δ*bcpB-3* Δ*bcpB-4* (*bcpB-2*; pink circles), Δ*bcpB-1* Δ*bcpB-2* Δ*bcpB-4* (*bcpB-3*; green circles), Δ*bcpB-1* Δ*bcpB-2* Δ*bcpB-3* (*bcpB-4*; orange circles), and the indicated recipient cells: **(A)** Δ*bcp-1* or Δ*bcp-1* complemented with cognate *bcpI-1,* **(B)** Δ*bcp-2* or Δ*bcp-2* complemented with cognate *bcpI-2,* **(C)** Δ*bcp-3* or Δ*bcp-3* complemented with cognate *bcpI-3,* and **(D)** Δ*bcp-4* or Δ*bcp-4* complemented with cognate *bcpI-4.* For the donor cells in panels **(C)** and **(D)**, the *bcpA-3* and *bcpA-4* promoters were replaced with the P_{S12} constitutive promoter to generate *bcpA-3*^{C} and *bcpA-4*^{C} parent strains, respectively. Symbols represent $\log_{10}$ competitive index values (ratio of donor to recipient) from three independent experiments and bars show the mean (n=9). Experiments in **(D)** were performed at a 10:1 (donor to recipient) ratio. Dashed line shows $\log_{10}$ competitive index = 0 (no competition). ns, not significant; *, p<0.05; ***, p<0.001; and ****, p<0.0001 compared to Δ*bcpB1-4* donor cells, unless indicated by line or brackets.

Figure 4.7 Competition among BcpA toxins for secretion by the BcpB-3 transporter

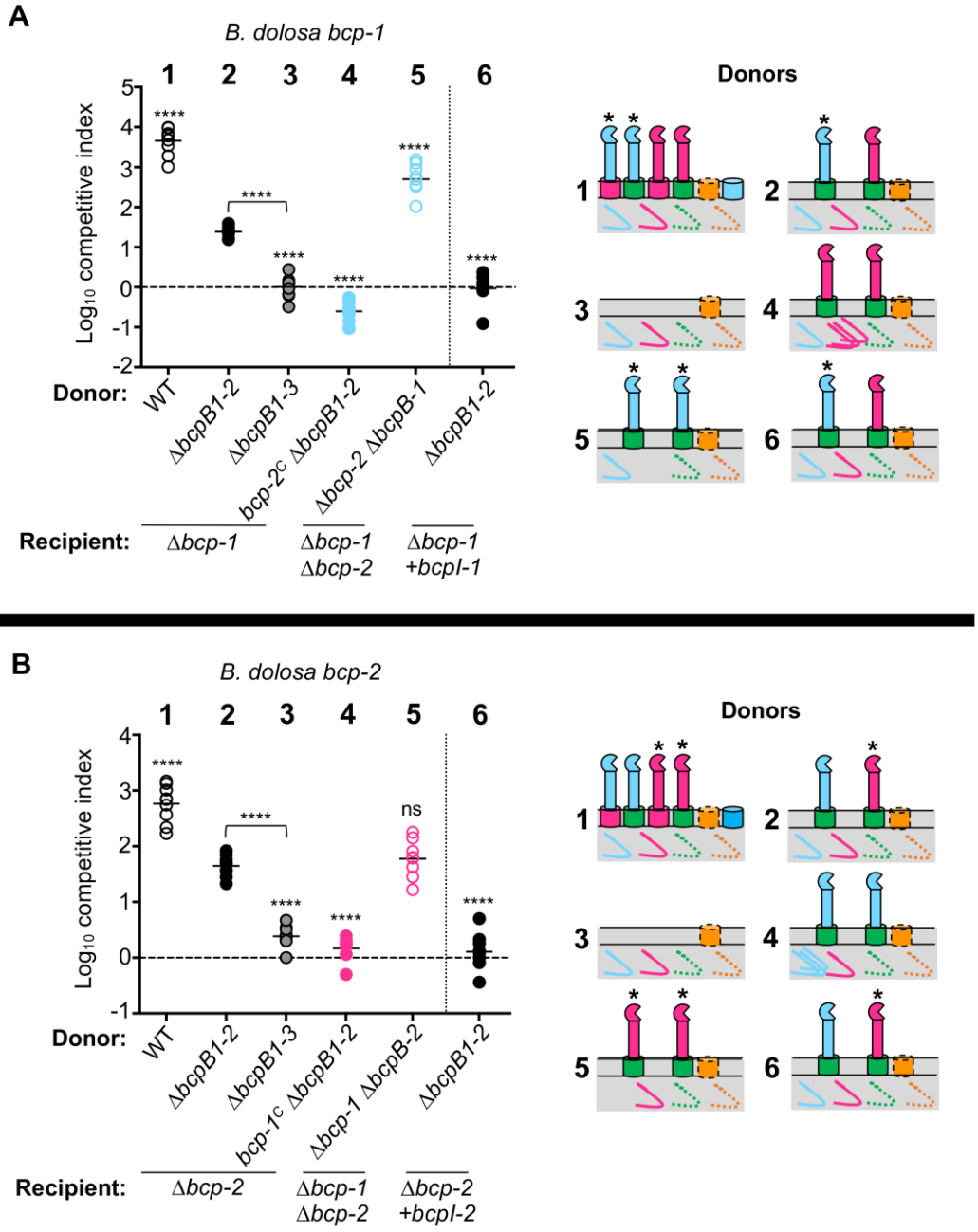

(A) Interbacterial competition assays (left) between the indicated donor cells: *Bd*AU0158 wild-type (WT; closed black circles), Δ*bcpB-1* Δ*bcpB-2* (Δ*bcpB1-2*; closed black circles), Δ*bcpB-1* Δ*bcpB-2* Δ*bcpB-3 (*Δ*bcpB1-3;* closed gray circles), Δ*bcpB1-2* mutant that overexpresses *bcpAIOB-2* (*bcp-2*^{C} Δ*bcpB-1-2*; closed blue circles), and Δ*bcp-2* Δ*bcpB-1* (open blue circles) and the indicated recipient cells: Δ*bcp-1,* Δ*bcp-1* Δ*bcp-2,* or Δ*bcp1* complemented with cognate *bcpI-1.* (Right) Simplified cartoon model to illustrate donor cells used in the assay (numbers correspond to co-cultures numbered above graph). Barrels represent OM BcpB proteins. Curved lines represent periplasmic BcpA that is secreted by the indicated BcpB proteins to the cell surface ('stick-pacman' shapes are secreted BcpA). Blue, BcpAB-1; pink, BcpAB-2; green, BcpAB-3; orange, BcpAB-4. Asterisks highlight that BcpA-1 activity is measured in this assay. **(B)** Interbacterial competition assays (left) between the indicated donor cells *Bd*AU0158 wild-type (WT; open black circles), Δ*bcpB-1* Δ*bcpB-2* (Δ*bcpB1-2*; closed black circles), Δ*bcpB-1* Δ*bcpB-2* Δ*bcpB-3 (*Δ*bcpB1-3;* closed gray circles), Δ*bcpB1-2* mutant that overexpresses *bcpAIOB-1* (*bcp-1*^{C} Δ*bcpB-2*; closed pink circles), and Δ*bcp-1* Δ*bcpB-2* (open pink circles) and the indicated recipient cells: Δ*bcp-2,* Δ*bcp-1* Δ*bcp-2,* or Δ*bcp2* complemented with cognate *bcpI-2.* Symbols represent $\log_{10}$ competitive index values (ratio of donor to recipient) from three independent experiments and bars show the mean (*n*=9). Dashed line shows $\log_{10}$ competitive index = 0 (no competition). ns, not significant; and ****, *p*<0.0001 compared Δ*bcpB1-2* donor cells vs Δ*bcp-1* or Δ*bcp-2* recipient cells,

unless indicated by brackets. (Right) Simplified cartoon model to illustrate donor cells used in the assay, as in **(A)**.

Figure 4.8 Contribution of BcpB-1 POTRA domains to the secretion of BcpA toxins

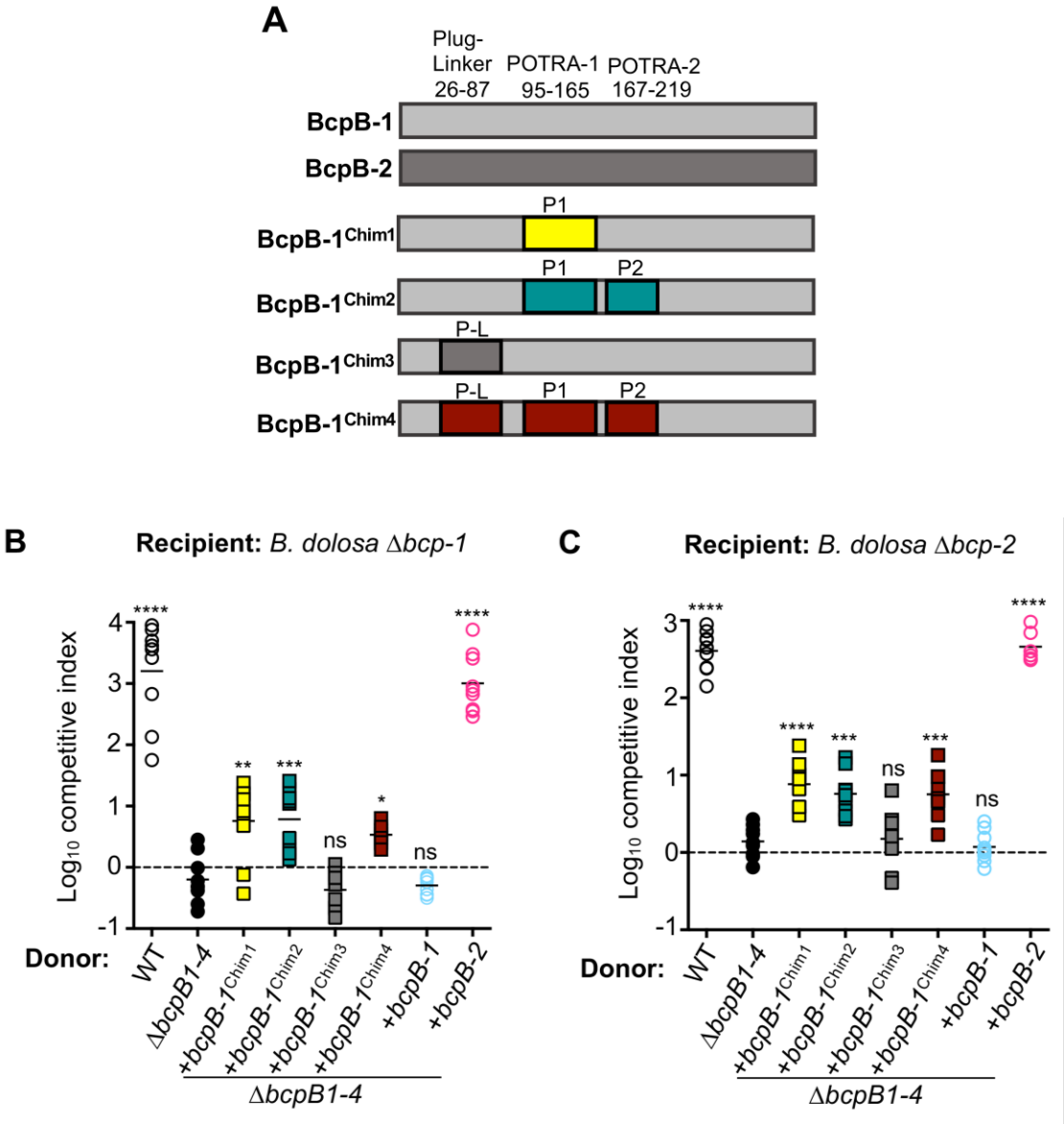

(A) Graphical representation of the BcpB-1 and BcpB-2 proteins from *B. dolosa* and the four BcpB-1 chimeras. Residue numbers refers to Plug-linker, POTRA-1, or POTRA-2 domains used to construct the chimeras. **(B, C)** Interbacterial competition assays between the indicated donor cells: *Bd*AU0158 wild-type (WT; open black circles), Δ*bcpB-1* Δ*bcpB-2* Δ*bcpB-3* Δ*bcpB-4* (Δ*bcpB1-4*; closed black circles), and Δ*bcpB1-4* complemented with overexpressed *bcpB-1* (+*bcpB-1*^{Bd}; open blue circles), *bcpB-2* (+*bcpB-2*^{Bd}; open pink circles), or genes to produce BcpB-1 chimeras Chim1 (+*bcpB-1*^{Chim1}; closed yellow squares), Chim2 (+*bcpB-1*^{Chim2}; closed teal squares), Chim3 (+*bcpB-1*^{Chim3}; closed gray squares), or Chim4 (+*bcpB-1*^{Chim4}; closed red squares), and *Bd*AU0158 **(B)** Δ*bcp-1* recipient cells or **(C)** Δ*bcp-2* recipient cells. Symbols represent $\log_{10}$ CI values from three independent experiments and horizontal bars show the mean (n=6 or 9). Dashed line shows $\log_{10}$ competitive index = 0 (no competition). ns, not significant; *, p<0.05; **, p<0.005; ***, p<0.001; and ****, p<0.0001; compared to Δ*bcpB1-4* mutant donor cells.

Figure 4.9 Comparison of *B. thailandensis* BcpB and *B. dolosa* BcpB-1 transporters

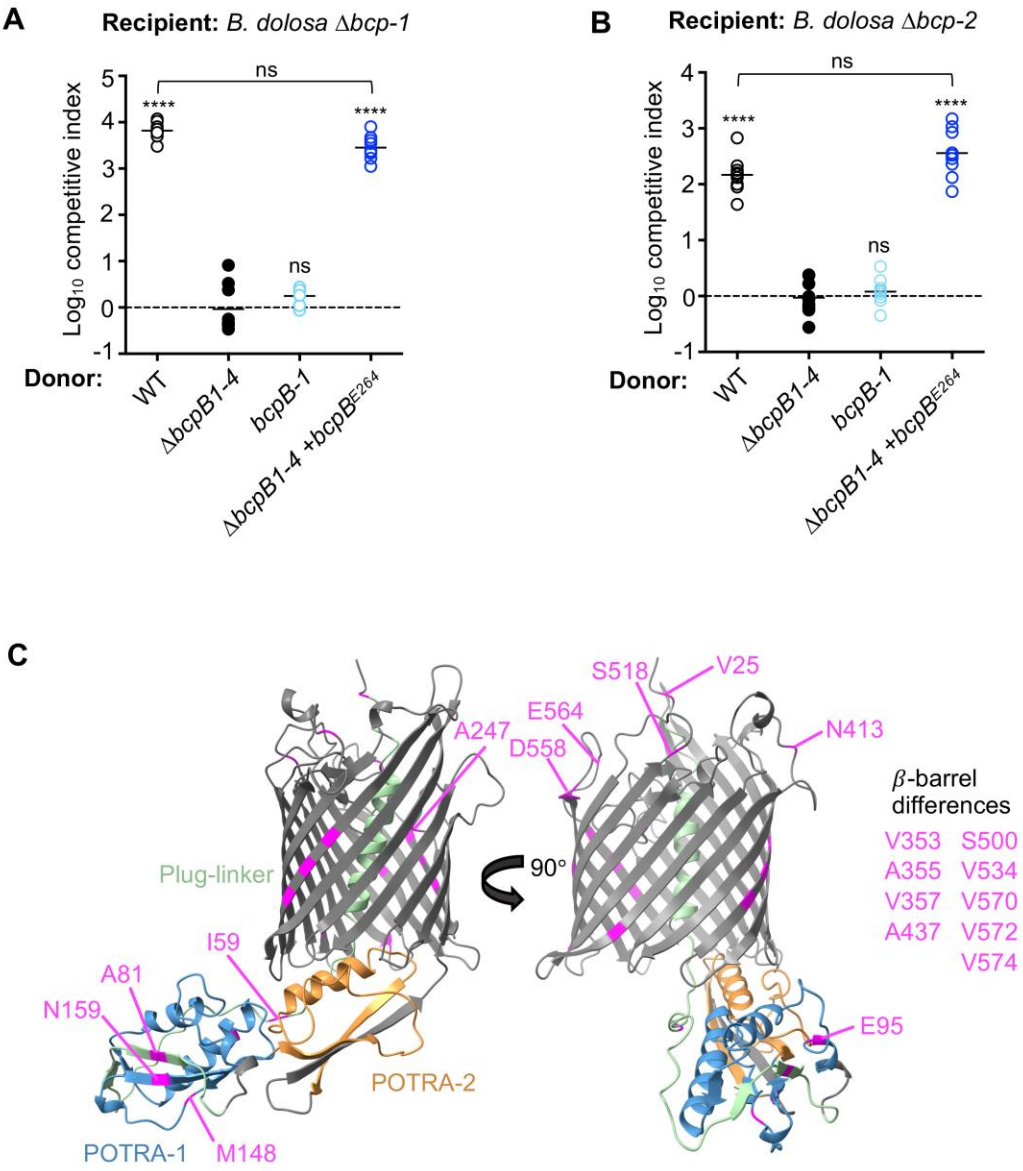

Interbacterial competition assays between the indicated donor cells: *Bd*AU0158 wild-type (WT; open circles), Δ*bcpB-1* Δ*bcpB-2* Δ*bcpB-3* Δ*bcpB-4 (*Δ*bcpB1-4;* closed circles), Δ*bcpB-2* Δ*bcpB-3* Δ*bcpB-4* (*bcpB-1*; light blue circles), Δ*bcpB1-4* complemented with overexpressed *Bt*E264 *bcpB* (Δ*bcpB1-4* +*bcpB*^{E264}; dark blue circles), and *Bd*AU0158 **(A)** Δ*bcp-1* recipient cells or **(B)** Δ*bcp-2* recipient cells Symbols represent $\log_{10}$ CI values from three independent experiments and horizontal bars show the mean (*n*= 9). Dashed line shows $\log_{10}$ competitive index = 0 (no competition). ns, not significant; and ****p<0.0001; compared to Δ*bcpB1-4* donor cells. **(C)** Predicted structure of *B. dolosa* BcpB-1 (without signal sequence) generated by AlphaFold. Plug-linker (green), POTRA-1 (blue), and POTRA-2 (orange) domains are shown. Amino acid residues labeled in pink (numbered according to full-length BcpB-1) represent unique residues that differ in *B. dolosa* BcpB-1 compared to *B. dolosa* BcpB-2 or *B. thailandensis* E264 BcpB protein sequences.

Figure 4.10 Examination of *B. thailandensis* BcpB transporter

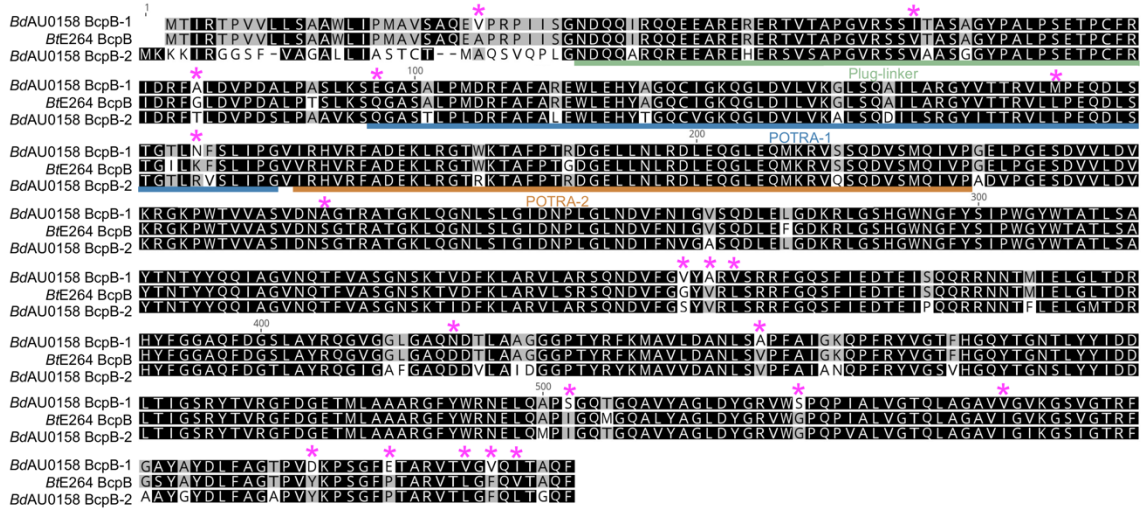

Amino acid alignment of *Burkholderia dolosa* BcpB-1, BcpB-2 and *Burkholderia thailandensis* BcpB proteins. Similarity is denoted by grayscale; residues similar in all sequences are highlighted in black and residues similar in 50% of sequences are highlighted in gray. Regions underlined in green, blue, or orange, represent the Plug-linker, POTRA-1, or POTRA-2 domains, respectively. Pink asterisks represent unique amino acid residues that differ in BcpB-1 sequence compared to the other two protein sequences.

Figure 4.11 Specificity of *B. dolosa* and *B. multivorans* BcpB transporters for non-cognate BcpA toxins

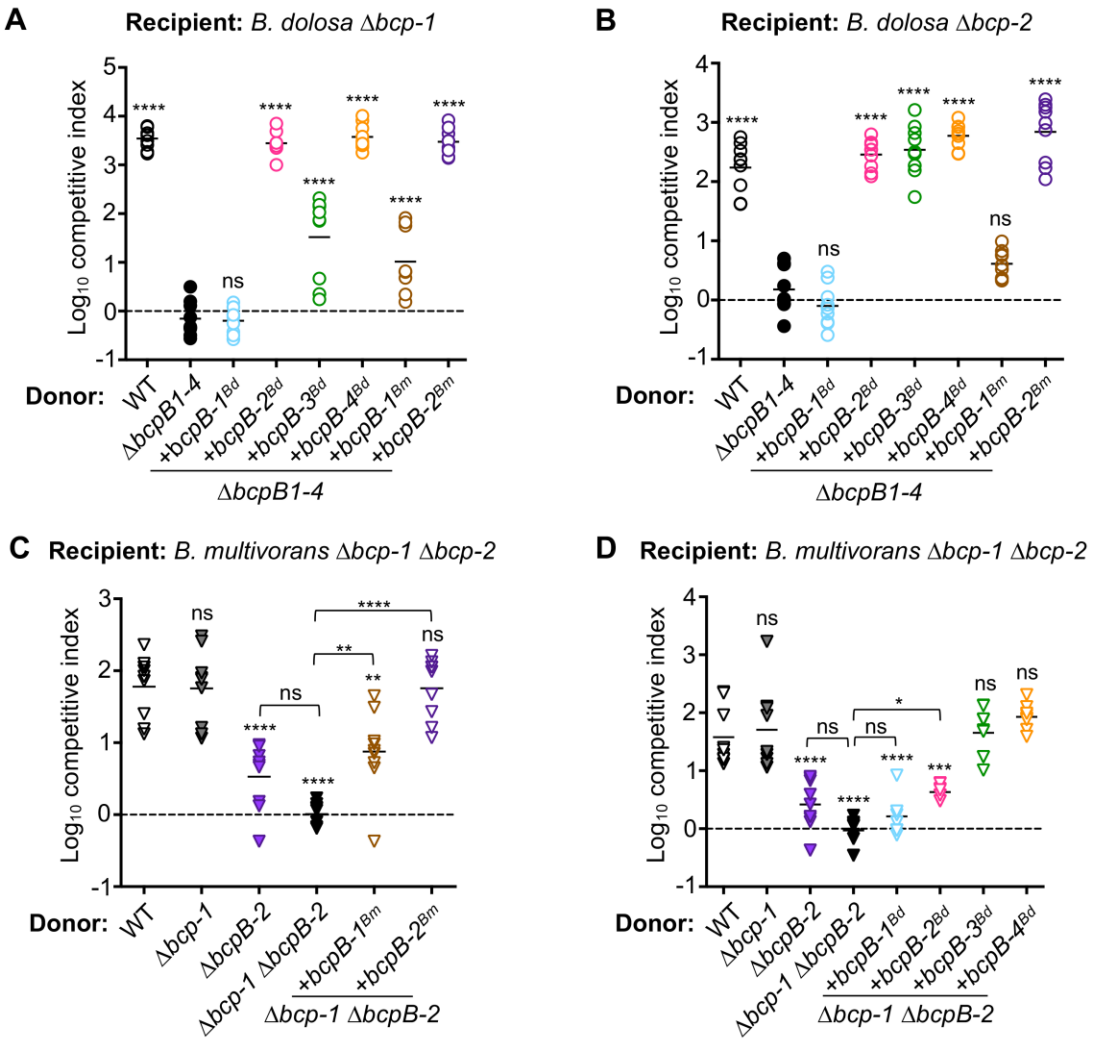

(A, B) Interbacterial competition assays between the indicted donor cells: *Bd*AU0158 wild-type (WT; open black circles), Δ*bcpB-1* Δ*bcpB-2* Δ*bcpB-3* Δ*bcpB-4* (Δ*bcpB1-4*; closed black circles), or Δ*bcpB1-4* complemented with overexpressed *Bd*AU0158 *bcpB-1* (+*bcpB-1*^{Bd}; open blue circles), *bcpB-2* (+*bcpB-2*^{Bd}; open pink circles), *bcpB-3* (+*bcpB-3*^{Bd}; open green circles), *bcpB-4* (+*bcpB-4*^{Bd}; open orange circles), or *Bm*CGD2M *bcpB-1* (+*bcpB-1*^{Bm}; open brown circles), *bcpB-2* (+*bcpB-2*^{Bm}; open purple circles) and **(A)** *Bd*AU0158 Δ*bcp-1* recipient cells or **(B)** *Bd*AU0158 Δ*bcp-2* recipient cells. **(C, D)** Interbacterial competition assays between *Bm*CGD2M Δ*bcp-1* Δ*bcp-2* recipient bacteria and the indicated donor cells: *Bm*CGD2M wild-type (WT; open black triangles), Δ*bcp-1* (closed gray triangles), Δ*bcp-2* (closed purple triangles), Δ*bcp1* Δ*bcpB-2* (closed black triangles), and Δ*bcp1* Δ*bcpB-2* complemented with overexpressed **(C)** *Bm*CGD2M *bcpB-1* (+*bcpB-1*^{Bm}; open brown triangles) or *bcpB-2* (+*bcpB-2*^{Bm}; open purple triangles) or **(D)** Δ*bcp1* Δ*bcpB-2* complemented with overexpressed *Bd*AU0158 *bcpB-1* (+*bcpB-1*^{Bd}; open blue triangles), *bcpB-2* (+*bcpB-2*^{Bd}; open pink triangles), *bcpB-3* (+*bcpB-3*^{Bd}; open green triangles), or *bcpB-4* (+*bcpB-4*^{Bd}; open orange triangles). Symbols represent $\log_{10}$ CI values from three independent experiments and horizontal bars show the mean (*n*=8 or 9). Dashed line shows $\log_{10}$ competitive index = 0 (no competition). ns, not significant; *, $p<0.05$; ** $p < 0.01$; and **** $p<0.0001$; compared to WT donor cells, unless indicated by brackets.

Figure 4.12 Model for relaxed substrate specificity of BcpB transporters

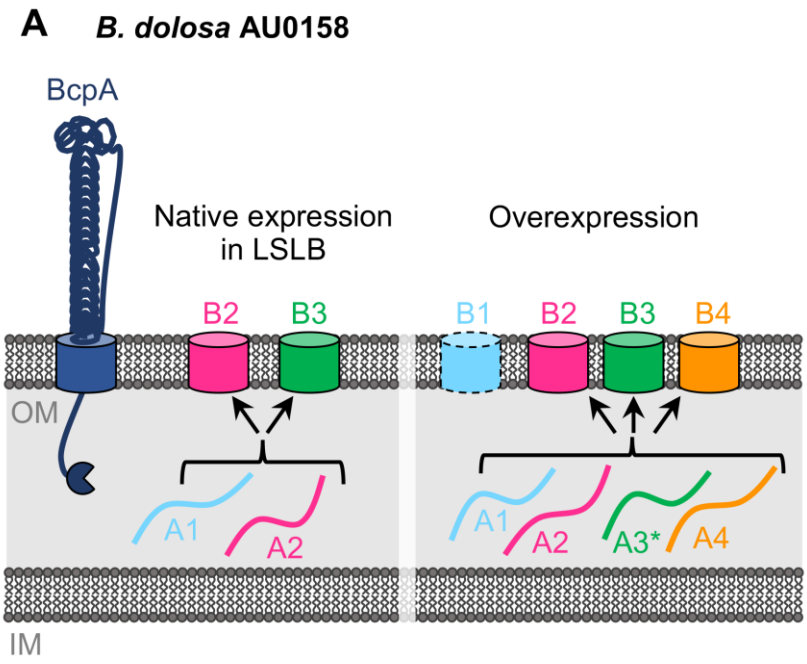

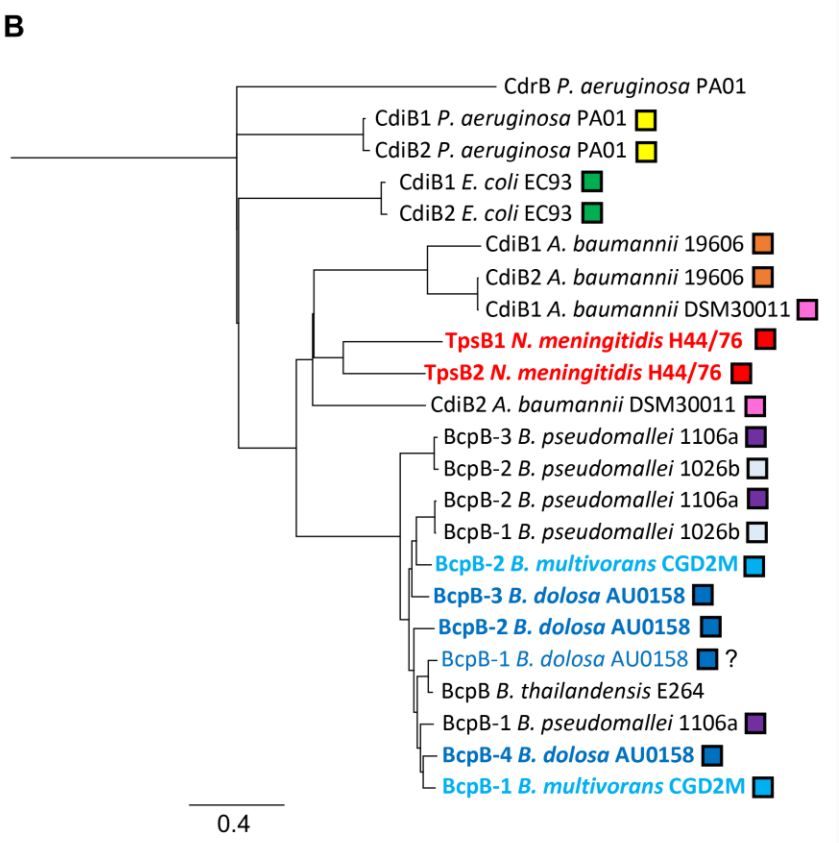

(A) Simplified model of *B. dolosa* BcpA secretion by BcpB transporters. Barrels on cell surface represent BcpB proteins (blue BcpB-1, pink BcpB-2, green BcpB-3, orange BcpB-4) and lines indicate corresponding BcpA proteins (blue BcpA-1, pink BcpA-2, green BcpA-3, orange BcpA-4). Under conditions of native gene expression (left), BcpA-1 and BcpA-2 can be secreted by BcpB-2 or BcpB-3. When *bcpA*/*bcpB* genes are overexpressed (right), all four BcpA toxins can be secreted by BcpB-2, BcpB-3, or BcpB-4. BcpB-1 does not appear to secrete any BcpA protein under the tested conditions. Asterisk denotes that BcpA-3 secretion by BcpB-4 has not been tested. **(B)** Phylogenetic tree based on alignment of CdiB/BcpB proteins and non-CdiB/BcpB TPS protein *P. aeruginosa* CdrB (root). Colored boxes indicate proteins produced within the same strain and bold colored text indicates transporters for which there is evidence of secretion of cognate and non-cognate substrates. Scale bar represents 0.4 amino acid substitutions per site.

Figure 4.13 Comparison of *B. dolosa* and *B. multivorans* BcpA TPS domains

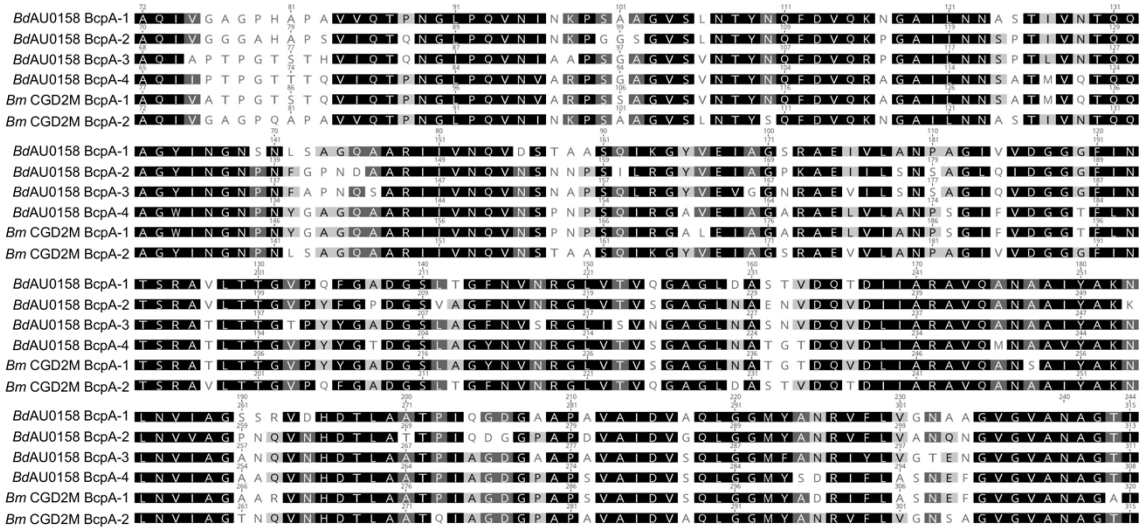

Amino acid alignment of *B. dolosa* and *B. multivorans* BcpA TPS domains. Similarity is denoted by grayscale; residues similar in all sequences are highlighted in black and residues similar in 50% of sequences are highlighted.

CHAPTER 5. Conclusion and future directions

Summary of research accomplishments

Contact dependent growth inhibition (CDI) systems are a type of TPS system that mediates interbacterial competition through the delivery of a toxin from one bacterium to another. CDI systems were first discovered in *E. coli,* but further investigations led to the discovery of CDI systems in many pathogenic Gram-negative bacteria, including CF pathogens such as *P. aeruginosa* and *Burkholderia cepacia* complex (Bcc) bacteria. Majority of the work done to characterize CDI systems has examined *E. coli*-type CDI systems or used *E. coli* as a model organism. However, examining the mechanisms of *Burkholderia*-type CDI in pathogenic *Burkholderia* species provides an opportunity to examine how CDI may play a role in pathogenesis. The goals of this dissertation project were to: 1) Investigate the role the accessory BcpO proteins plays in *Burkholderia*-type CDI and 2) Determine whether cross talk occurs between CDI systems produced with in the same bacterium.

From this work, we demonstrated that *B. dolosa* BcpO-1 specifically functions with class I CDI systems and identified potential binding partners that may aid in the function of BcpO. Moreover, based on the results obtained in Chapter 3, we predict that BcpO is functioning with a chaperone to enhance the stability of BcpA-1 prior to secretion out of the donor cell. Unexpectantly, work done to characterize the role of BcpO led to the discovery of a relaxed specificity

among BcpB transporters. The promiscuity of the BcpB transporters led to the observation that competition between CDI systems for substrate secretion can occur when transporters are limited. Furthermore, we demonstrated that BcpB transporters in multiple *Burkholderia* species exhibit relaxed specificity. Since our studies use pathogenic *Burkholderia* spp., which often encode for multiple CDI systems, we were afforded the opportunity to observe the interplay that occurs between CDI systems.

Future Directions

Based on the results obtained from chapter 3 it appears that other proteins are necessary for efficient CDI activity. In other T5SSs chaperones and proteases have been described to interact with the passenger domain or proteins. Specific chaperones have not been identified to interact with CDI systems. The mass spec data obtained in chapter 3 identified a variety of potential proteins that may bind to BcpO. Majority of the predicted proteins were hypothetical membrane proteins and periplasmic proteases. Future work examining the function of the proteins identified by mass spec could help determine the role BcpO plays in *B. dolosa* AU0158 CDI activity.

As previously shown when *B. dolosa bcpO-1* is deleted, BcpA-1 mediated CDI activity is reduced (133). It has not been experimentally determined if BcpA and BcpO directly interact. Therefore, additional pulldown assays or immunoprecipitation assays are necessary to determine if BcpO and BcpA bind

directly or indirectly. Once it has been determined if the two proteins interact, additional experiments could be aimed at determining which domain of BcpA, BcpO binds. Understanding how BcpO interacts with BcpA could give insight into the specificity of class I BcpO proteins. We demonstrated that the *B. dolosa* class I BcpO protein does not function with class II CDI systems. It is not known whether the class I BcpO proteins are specific for their cognate BcpA protein or can they enhance the CDI activity of all class I CDI BcpA toxins. It also remains to be known why the class II BcpA proteins do not require a BcpO protein for maximum CDI activity. Further examination of the domain differences between the class I and class II BcpA proteins will aid in understanding the role the class II "BcpO" proteins play in CDI systems. Pulldown assays comparing class I and class II BcpA proteins could be done to determine if there are similarities in potential binding partners. Additional experiments using chimeric CDI systems, may aid in determining the function and specificity of the class I BcpO accessory proteins.

Interplay between CDI systems

We demonstrated that when the production of BcpB transporters is limited competition can occur between the BcpA proteins for secretion. We showed that the BcpB transporters likely have different levels of affinity for the BcpA proteins. Even though there was a high level of homology among BcpB proteins at the amino acid level there were differences in their substrate secretion specificity. Future experiments aimed at understanding the structural differences between

the BcpB transporters, including the inactive BcpB-1 protein, will provide insight into which regions are important for substrate recognition and secretion.

Furthermore, studies should also be focused on determining the regions in BcpA that allows for secretion through various BcpB transporters. Generating chimeric BcpA constructs that have the TPS domains changed could be used to determine if the TPS domain alone is responsible for transporter specificity. Additional experimentation with the chimeric CDI proteins could also give insight into to the rate of secretion and potency of the BcpA toxins. We observed higher levels of BcpA-1 mediated CDI activity compared to BcpA-2. This difference in CDI activity could be due to differences in toxin potencies or due to differences in the rate of toxin secretion under the tested conditions.

In chapter 4 we demonstrated that the relaxed specificity of BcpB transporters leads to interplay between distinct CDI systems produced within the same strain of *Burkholderia cepacia* complex bacteria. We also showed that this phenomenon does not appear to be species specific. Therefore, we hypothesize that the interplay between CDI systems may not only occur in other *Burkholderia* species but may occur in other Gram-negative bacteria that produce multiple CDI system. Specifically, *Pseudomonas* and *Acinetobacter* species which often harbor multiple systems within the same strain (155,195,208). The *Pseudomonas aeruginosa* strains PABL017 and PAO1, encode for CDI systems that mediates competition among closely related bacteria and are also virulence factors against a mammalian host (157,209). Therefore, future studies should be aimed at examining the interactions between CDI systems produced in other pathogenic

bacteria. Based on the results presented in this study, when examining CDI activity in bacteria that encode for multiple CDI systems it is important to consider the possibility of interplay between CDI systems. Research enhancing our understanding of interplay between *B. cepacia* complex CDI systems in their natural niches, will provide insight into why encoding multiple CDI systems may increase CDI efficiency in pathogenic bacteria.

Regulation of CDI system-encoding genes

Despite almost 20 years of research on CDI mechanisms, many questions still remain for the field to answer. Though some work has shed light on the regulation of CDI genes, it remains to be known when and where bacteria express the genes encoding CDI system proteins. In liquid cultures, *Bt*E264 *bcpAIOB* gene expression is high in only ~0.2% of bacteria (130). However, on solid surfaces the *bcpAIOB* genes are likely expressed in majority of the bacteria for a significantly level of competition to occur. There seems to be a high level of complexity regarding the regulation of CDI encoding genes. In *B. dolosa* two out of the four *bcpA* genes are expressed under standard laboratory conditions. Even though *bcpA-3* and *bcpA-4* genes need to be expressed under a constitutive promoter to mediate CDI activity, they appear to be regulated differently. The *bcp-3* locus has an internal promoter that drives *bcpI-3* expression (133). Additionally, our data suggest that *bcpB-3* is also driven by an internal promoter, likely the same promoter that drives *bcpI-3* expression, and is natively expressed under standard laboratory conditions (**Fig. 4.6**). In the near

future, studies should be aimed at identifying and characterizing the regulators that control *bcp* gene expression. Furthermore, how control of *bcp* expression by regulators contributes to interbacterial competition should also be determined. We observed that when *bcpA-4* and *bcpB-4* are both overexpressed the level of BcpA-4 mediated CDI activity increases ~1500-fold (**Fig. 4.2D**). This provides further evidence that in some CDI systems each gene in the locus may be controlled by a different regulator. RNA-seq could be used to determine the range of genes controlled by each regulator. We hypothesize that expression of the *bcpAIOB* genes is controlled by a complex regulatory circuit and that each regulator controls a distinct pattern of gene expression in response to specific environmental conditions.

Bioengineered applications

CDI systems exhibit potent antibacterial toxicity and high levels of variability. Therefore, they have a unique potential to be exploited to eliminate undesirable bacteria from various environmental niches. Anderson et al., 2012, showed that CDI systems can mediate competitive exclusion by not allowing non-self bacteria into a pre-establish biofilm community in vitro (129). Therefore, the next area of CDI research may be aimed at determining whether bacteria producing CDI system proteins can eliminate bacteria from pre-established niches in vivo. It is possible that an engineered strain expressing multiple CDI system-encoding loci could be developed for use as a mechanism to remove pathogenic bacteria from biofilms. If bacteria expressing CDI system-encoding

loci can cause clearance of pathogen *Burkholderia* spp. in vitro and in vivo, it would suggest that these systems may be able to be developed for use as a therapeutic. CDI systems could also be manipulated to treat bacterial infections. Specific CDI toxin-immunity pairs (or whole loci) could be constitutively expressed in a nonpathogenic *Burkholderia* species. The nonpathogenic *B. thailandensis* E264 strain has been shown to outcompete a pathogenic Bcc strain (134). However, until the OM and IM receptors and possibly permissive factors, promoting BcpA-CT toxicity are identified and characterized the range of susceptible target cells will remain unknown.

In some pathogenic bacteria, CDI systems have been described as virulence factors or major mechanisms for competition among other bacteria within a host environment (155,195). Therefore, an antibacterial drug could be developed to neutralize CDI activity or eliminate the producing pathogenic bacteria. Due to the high level of variability among the BcpA-CT toxin domain creating an antibacterial to neutralize the toxic activity would not be feasible. An alternative approach to neutralize CDI activity could be to eliminate the transporter activity of the BcpB proteins. In chapter 4, we demonstrated that when a compatible BcpB transporter is not available the BcpA toxin is unable to mediate CDI activity and therefore the donor cells do not have a competitive advantage over the recipient cells. Due to the high level of homology among the BcpB transporters, antibiotics could be developed to target one of the extracellular loops of BcpB. Studies examining other Omp85 superfamily members, CdiA^{Ec93} and CdiA^{AbACICU}, have demonstrated that the L6 loop is

required for substrate secretion (114). The extracellular L6 loop is conserved among Omp85 superfamily members (113,210). Consequently, the development of an antibiotic that targets the L6 loop may lead to unwanted effects against commensal bacteria. Therefore, further work examining the function of the BcpB extracellular loops is necessary to determine which portion of BcpB would be most effective for the development of an antibacterial target.

There are many follow-up questions that need to be addressed to better understand interspecies CDI: 1) What are the receptors and permissive factors on target bacteria required for susceptibility to CDI and how wide-spread or conserved are the proteins? 2) What is the variability range of species-specificity in BcpA-CT toxin activity? 3) What are the environmental conditions that would initiate interactions between bacteria of different species, and what is the consequence of competition to the bacterial community structure? Answering these questions will provide considerable insight as to the biological role of CDI mediated competition in nature or in a host environment.

APPENDIX

aa	Amino acid
ABC	ATP-binding cassette
AT	Autotransporter
ATPase	Adenosine triphosphatase
BamA	β-barrel assembly machinery protein A
Bcc	*Burkholderia cepacia* complex
bcpAIOB	*Burkholderia* CDI protein genes
*Bd*AU0158	*Burkholderia dolosa* strain AU0158
*Bm*CGD2M	*Burkholderia multivorans* CGD2M
*Bt*E264	*Burkholderia thailandensis* E264
bp	base pair
CDI	Contact-dependent growth inhibition
cdiBAI	CDI protein genes
CF	Cystic fibrosis
CFU	Colony forming units
CGD	Chronic granulomatous disease
C.I.	Competitive index
CT	C terminus
DAP	Diaminopimelic acid
DNA	Deoxyribonucleic acid
DNase	Deoxyribonuclase

(e)DNA	Extracellular deoxyribonucleic acid
ESPR	Extended signal peptide region
FHA	Filamentous hemagglutinin
IM	Inner membrane
IMR	Inner membrane receptor
Kan	Kanamycin
kDa	Kilodalton
LOL	Localization of lipoprotein
LPS	Lipopolysaccharide
LSLB	Low Salt Luria-Bertani
MS	Mass spectrometry
ns	Not significant
NT	N terminus
OD_{420}	Optical density, 420 nm
OD_{600}	Optical density, 600 nm
OM	Outer membrane
OMP	Outer membrane protein
ORF	Open reading frame
PBS	Phosphate-buffered saline
PCR	Polymerase chain reaction
POTRA	Polypeptide-associated transport
QS	Quorum sensing

RNA	Ribonucleic acid
RT-qPCR	Reverse transcriptase qualitative polymerase chain reaction
SDS-PAGE	Sodium dodecyl sulfate-polyacrylamide gel electrophoresis
TAT	Trimeric autotransporter
Tet	Tetracycline
TPS	Two partner secretion
TBS	Tris-buffered saline
T5SS	Type V secretion system
T6SS	Type VI secretion system
V	Volts
WT	Wild-type

REFERENCES

1.Mahenthiralingam E, Urban TA, Goldberg JB. 2005. The multifarious, multireplicon *Burkholderia cepacia* complex. Nature Reviews Microbiology 3:144-156. 10.1038/nrmicro1085.

2.Dance DAB. 2000. Ecology of *Burkholderia pseudomallei* and the interactions between environmental *Burkholderia* spp. and human–animal hosts. Acta Tropica 74:159-168. 10.1016/S0001-706X(99)00066-2.

3.Coenye T, Gillis M, Vandamme P. 2000. *Pseudomonas antimicrobica* Attafuah and Bradbury 1990 is a junior synonym of *Burkholderia gladioli* (Severini 1913) Yabuuchi et al. 1993. International Journal of Systematic and Evolutionary Microbiology 50:2135-2139. 10.1099/00207713-50-6-2135.

4.Coenye T, Vandamme P. 2003. Diversity and significance of *Burkholderia* species occupying diverse ecological niches. Environmental Microbiology 5:719-729. 10.1046/j.1462-2920.2003.00471.x.

5.Parke JL, Gurian-Sherman D. 2001. Diversity of the *Burkholderia cepacia* complex and implications for risk assessment of biological control strains. Annual Review of Phytopathology 39:225-258. 10.1146/annurev.phyto.39.1.225.

6.Burkholder WH. 1950. Sour skin, a bacterial rot of onion bulbs. Phytophathology 40:115-117.

7.Wiersinga WJ, van der Poll T, White NJ, Day NP, Peacock SJ. 2006. Melioidosis: insights into the pathogenicity of *Burkholderia pseudomallei*. Nature Reviews Microbiology 4:272-282. 10.1038/nrmicro1385.

8.Coenye T, Vandamme P, Govan JRW, LiPuma JJ. 2001. Taxonomy and identification of the *Burkholderia cepacia* complex. Journal of Clinical Microbiology 39:3427-3436. 10.1128/JCM.39.10.3427-3436.2001.

9.Yabuuchi E, Kosako Y, Oyaizu H, Yano I, Hotta H, Hashimoto Y, Ezaki T, Arakawa M. 1992. Proposal of *Burkholderia* gen. nov. and transfer of seven species of the genus *Pseudomonas* homology group II to the new genus, with the type species *Burkholderia cepacia* (Palleroni and Holmes 1981) comb. nov. Microbiology and Immunology 36:1251-1275. https://doi.org/10.1111/j.1348-0421.1992.tb02129.x.

10.Johnston RB. 2001. Clinical aspects of chronic granulomatous disease. Current Opinion in Hematology 8:17-22. 10.1097/00062752-200101000-00004.

11.Ratjen F, Döring G. 2003. Cystic fibrosis. The Lancet 361:681-689. 10.1016/S0140-6736(03)12567-6.

12.Carla Patrícia C, Sandra Costa Dos S, Andreia E, Nuno Pereira M, Ana Sílvia M, Isabel E-C. 2011. Long-term colonization of the cystic fibrosis lung by *Burkholderia cepacia* complex bacteria: epidemiology, clonal variation and genome-wide expression alterations. Frontiers in cellular and infection microbiology 1:12-12. 10.3389/fcimb.2011.00012.

13.Isles A, Maclusky I, Corey M, Gold R, Prober C, Fleming P, Levison H. 1984. *Pseudomonas cepacia* infection in cystic fibrosis: An emerging problem. The Journal of Pediatrics 104:206-210. 10.1016/S0022-3476(84)80993-2.
14.LiPuma JJ. 2010. The changing microbial epidemiology in cystic fibrosis. Clinical Microbiology Reviews 23:299-323. 10.1128/CMR.00068-09.
15.Branstetter JW, Yarbrough A, Poole C. 2020. Management of cepacia syndrome with a combination of intravenous and inhaled antimicrobials in a non-cystic Fibrosis pediatric patient. The Journal of Pediatric Pharmacology and Therapeutics 25:730-734. 10.5863/1551-6776-25.8.730.
16.Govan JRW, Doherty CJ, Nelson JW, Brown PH, Greening AP, Maddison J, Dodd M, Webb AK. 1993. Evidence for transmission of *Pseudomonas cepacia* by social contact in cystic fibrosis. The Lancet 342:15-19. 10.1016/0140-6736(93)91881-L.
17.Chen JS, Witzmann KA, Spilker T, Fink RJ, LiPuma JJ. 2001. Endemicity and inter-city spread of *Burkholderia cepacia* genomovar III in cystic fibrosis. The Journal of Pediatrics 139:643-649. 10.1067/mpd.2001.118430.
18.Jones AM, Dodd ME, Govan JRW, Barcus V, Doherty CJ, Morris J, Webb AK. 2004. *Burkholderia cenocepacia* and *Burkholderia multivorans*: influence on survival in cystic fibrosis. Thorax 59:948-951. 10.1136/thx.2003.017210.
19.Coenye T, LiPuma John J. 2002. Multilocus restriction typing: A novel tool for studying global epidemiology of *Burkholderia cepacia* complex infection in cystic fibrosis. The Journal of Infectious Diseases 185:1454-1462. 10.1086/340279.
20.Drevinek P, Mahenthiralingam E. 2010. *Burkholderia cenocepacia* in cystic fibrosis: epidemiology and molecular mechanisms of virulence. Clinical Microbiology and Infection 16:821-830. 10.1111/j.1469-0691.2010.03237.x.
21.Schwab U, Abdullah LH, Perlmutt OS, Albert D, Davis CW, Arnold RR, Yankaskas JR, Gilligan P, Neubauer H, Randell SH, Boucher RC. 2014. Localization of *Burkholderia cepacia* Complex Bacteria in Cystic Fibrosis Lungs and Interactions with *Pseudomonas aeruginosa* in Hypoxic Mucus. Infection and Immunity 82:4729-4745. 10.1128/IAI.01876-14.
22.Anonymous. 2019. Cystic Fibrosis Foundation Patient Registry 2018 Annual Data Report.
23.Zhou J, Chen Y, Tabibi S, Alba L, Garber E, Saiman L. 2007. Antimicrobial susceptibility and synergy studies of *Burkholderia cepacia* complex isolated from patients with cystic fibrosis. Antimicrobial Agents and Chemotherapy 51:1085-1088. 10.1128/AAC.00954-06.
24.Burns JL, Wadsworth CD, Barry JJ, Goodall CP. 1996. Nucleotide sequence analysis of a gene from *Burkholderia* (*Pseudomonas*) *cepacia* encoding an outer membrane lipoprotein involved in multiple antibiotic resistance. Antimicrobial Agents and Chemotherapy 40:307-313. 10.1128/AAC.40.2.307.
25.Podnecky NL, Rhodes KA, Schweizer HP. 2015. Efflux pump-mediated drug resistance in *Burkholderia*. Frontiers in Microbiology 06 10.3389/fmicb.2015.00305.
26.Rhodes KA, Schweizer HP. 2016. Antibiotic resistance in *Burkholderia* species. Drug Resistance Updates 28:82-90. 10.1016/j.drup.2016.07.003.

27.Beckman W, Lessie TG. 1979. Response of *Pseudomonas cepacia* to β-Lactam antibiotics: utilization of penicillin G as the carbon source. Journal of Bacteriology 140:1126-1128. 10.1128/jb.140.3.1126-1128.1979.
28.Cox AD, Wilkinson SG. 1991. Ionizing groups in lipopolysaccharides of *Pseudomonas cepacia* in relation to antibiotic resistance. Molecular Microbiology 5:641-646. 10.1111/j.1365-2958.1991.tb00735.x.
29.Shimomura H, Matsuura M, Saito S, Hirai Y, Isshiki Y, Kawahara K. 2003. Unusual Interaction of a Lipopolysaccharide Isolated from *Burkholderia cepacia* with Polymyxin B. Infection and Immunity 71:5225-5230. 10.1128/IAI.71.9.5225-5230.2003.
30.Shaw D, Poxton IR, Govan JRW. 1995. Biological activity of *Burkholderia* (*Pseudomonas*) *cepacia* lipopolysaccharide. FEMS Immunology & Medical Microbiology 11:99-106. 10.1111/j.1574-695X.1995.tb00095.x.
31.Vinion-Dubiel AD, Goldberg JB. 2003. Lipopolysaccharide of *Burkholderia cepacia* complex. Journal of Endotoxin Research 9:201-213. 10.1179/096805103225001404.
32.Tomich M, Herfst CA, Golden JW, Mohr CD. 2002. Role of flagella in host cell invasion by *Burkholderia cepacia*. Infection and Immunity 70:1799-1806. 10.1128/IAI.70.4.1799-1806.2002.
33.Urban TA, Griffith A, Torok AM, Smolkin ME, Burns JL, Goldberg JB. 2004. Contribution of *Burkholderia cenocepacia* flagella to infectivity and inflammation. Infection and Immunity 72:5126-5134. 10.1128/IAI.72.9.5126-5134.2004.
34.Carmody LA, Zhao J, Kalikin LM, LeBar W, Simon RH, Venkataraman A, Schmidt TM, Abdo Z, Schloss PD, LiPuma JJ. 2015. The daily dynamics of cystic fibrosis airway microbiota during clinical stability and at exacerbation. Microbiome 3:12-12. 10.1186/s40168-015-0074-9.
35.Bernier SP, Workentine ML, Li X, Magarvey NA, O'Toole GA, Surette MG. 2016. Cyanide toxicity to *Burkholderia cenocepacia* is modulated by polymicrobial communities and environmental factors. Frontiers in Microbiology 7 10.3389/fmicb.2016.00725.
36.Perault AI, Chandler CE, Rasko DA, Ernst RK, Wolfgang MC, Cotter PA. 2020. Host adaptation predisposes *Pseudomonas aeruginosa* to Type VI secretion system-mediated predation by the *Burkholderia cepacia* complex. Cell Host & Microbe 10.1016/j.chom.2020.06.019.
37.Hall-Stoodley L, Costerton JW, Stoodley P. 2004. Bacterial biofilms: from the natural environment to infectious diseases. Nature Reviews Microbiology 2:95-108. 10.1038/nrmicro821.
38.Hobley L, Harkins C, MacPhee CE, Stanley-Wall NR. 2015. Giving structure to the biofilm matrix: an overview of individual strategies and emerging common themes. FEMS Microbiology Reviews 39:649-669. 10.1093/femsre/fuv015.
39.Peters BM, Jabra-Rizk MA, O'May GA, Costerton JW, Shirtliff ME. 2012. Polymicrobial interactions: impact on pathogenesis and human disease. Clinical microbiology reviews 25:193-213. 10.1128/CMR.00013-11.

40.Flemming H-C, Wingender J, Szewzyk U, Steinberg P, Rice SA, Kjelleberg S. 2016. Biofilms: an emergent form of bacterial life. Nature Reviews Microbiology 14:563-575. 10.1038/nrmicro.2016.94.
41.Konopka A. 2009. What is microbial community ecology? The ISME Journal 3:1223-1230. 10.1038/ismej.2009.88.
42.Sekirov I, Russell SL, Antunes LCM, Finlay BB. 2010. Gut microbiota in health and disease. Physiological Reviews 90:859-904. 10.1152/physrev.00045.2009.
43.Ma B, Forney LJ, Ravel J. 2012. Vaginal microbiome: rethinking health and disease. Annual Review of Microbiology 66:371-389. 10.1146/annurev-micro-092611-150157.
44.Byrd AL, Belkaid Y, Segre JA. 2018. The human skin microbiome. Nature Reviews Microbiology 16:143-155. 10.1038/nrmicro.2017.157.
45.Lamont RJ, Koo H, Hajishengallis G. 2018. The oral microbiota: dynamic communities and host interactions. Nature Reviews Microbiology 16:745-759. 10.1038/s41579-018-0089-x.
46.Socransky SS, Haffajee AD. 1992. The bacterial etiology of destructive periodontal disease: current concepts. Journal of Periodontology 63:322-331. 10.1902/jop.1992.63.4s.322.
47.Muzny CA, Schwebke JR. 2016. Pathogenesis of bacterial vaginosis: discussion of current hypotheses. Journal of Infectious Diseases 214:S1-S5. 10.1093/infdis/jiw121.
48.Percival SL, Suleman L, Vuotto C, Donelli G. 2015. Healthcare-associated infections, medical devices and biofilms: risk, tolerance and control. Journal of Medical Microbiology 64:323-334. 10.1099/jmm.0.000032.
49.Siddiqui AR, Bernstein JM. 2010. Chronic wound infection: Facts and controversies. Clinics in Dermatology 28:519-526. 10.1016/j.clindermatol.2010.03.009.
50.Høiby N, Bjarnsholt T, Givskov M, Molin S, Ciofu O. 2010. Antibiotic resistance of bacterial biofilms. International Journal of Antimicrobial Agents 35:322-332. 10.1016/j.ijantimicag.2009.12.011.
51.Hibbing ME, Fuqua C, Parsek MR, Peterson SB. 2010. Bacterial competition: surviving and thriving in the microbial jungle. Nature Reviews Microbiology 8:15-25. 10.1038/nrmicro2259.
52.Nealson KH, Platt T, Hastings JW. 1970. Cellular control of the synthesis and activity of the bacterial luminescent system. Journal of Bacteriology 104:313-322. 10.1128/jb.104.1.313-322.1970.
53.Miller MB, Bassler BL. 2001. Quorum Sensing in Bacteria. Annual Review of Microbiology 55:165-199. 10.1146/annurev.micro.55.1.165.
54.Bassler BL. 2002. Small Talk. Cell 109:421-424. 10.1016/S0092-8674(02)00749-3.
55.Li Y-H, Tian X. 2012. Quorum sensing and bacterial social interactions in biofilms. Sensors 12:2519-2538. 10.3390/s120302519.
56.Papenfort K, Bassler BL. 2016. Quorum sensing signal–response systems in Gram-negative bacteria. Nature Reviews Microbiology 14:576-588. 10.1038/nrmicro.2016.89.

57.Griffin AS, West SA, Buckling A. 2004. Cooperation and competition in pathogenic bacteria. Nature 430:1024-1027. 10.1038/nature02744.
58.Diggle SP, Griffin AS, Campbell GS, West SA. 2007. Cooperation and conflict in quorum-sensing bacterial populations. Nature 450:411-414. 10.1038/nature06279.
59.Mukherjee S, Bassler BL. 2019. Bacterial quorum sensing in complex and dynamically changing environments. Nature Reviews Microbiology 17:371-382. 10.1038/s41579-019-0186-5.
60.Foster Kevin R, Bell T. 2012. Competition, not cooperation, dominates interactions among culturable microbial species. Current Biology 22:1845-1850. 10.1016/j.cub.2012.08.005.
61.Riley MA, Wertz JE. 2002. Bacteriocins: Evolution, Ecology, and Application. Annual Review of Microbiology 56:117-137. 10.1146/annurev.micro.56.012302.161024.
62.Cotter PD, Ross RP, Hill C. 2013. Bacteriocins — a viable alternative to antibiotics? Nature Reviews Microbiology 11:95-105. 10.1038/nrmicro2937.
63.Gradisteanu Pircalabioru G, Popa LI, Marutescu L, Gheorghe I, Popa M, Czobor Barbu I, Cristescu R, Chifiriuc M-C. 2021. Bacteriocins in the era of antibiotic resistance: rising to the challenge. Pharmaceutics 13:196-196. 10.3390/pharmaceutics13020196.
64.Jakes KS, Cramer WA. 2012. Border Crossings: Colicins and Transporters. Annual Review of Genetics 46:209-231. 10.1146/annurev-genet-110711-155427.
65.Green ER, Mecsas J. 2016. Bacterial Secretion Systems: An Overview. Microbiology Spectrum 4 10.1128/microbiolspec.VMBF-0012-2015.
66.Granato ET, Meiller-Legrand TA, Foster KR. 2019. The evolution and ecology of bacterial warfare. Current Biology 29:R521-R537. 10.1016/j.cub.2019.04.024.
67.Whitney JC, Peterson SB, Kim J, Pazos M, Verster AJ, Radey MC, Kulasekara HD, Ching MQ, Bullen NP, Bryant D, Goo YA, Surette MG, Borenstein E, Vollmer W, Mougous JD. 2017. A broadly distributed toxin family mediates contact-dependent antagonism between gram-positive bacteria. eLife 6 10.7554/eLife.26938.
68.Pena RT, Blasco L, Ambroa A, González-Pedrajo B, Fernández-García L, López M, Bleriot I, Bou G, García-Contreras R, Wood TK, Tomás M. 2019. Relationship between quorum sensing and secretion systems. Frontiers in Microbiology 10 10.3389/fmicb.2019.01100.
69.Schell MA, Ulrich RL, Ribot WJ, Brueggemann EE, Hines HB, Chen D, Lipscomb L, Kim HS, Mrázek J, Nierman WC, DeShazer D. 2007. Type VI secretion is a major virulence determinant in *Burkholderia mallei*. Molecular Microbiology 64:1466-1485. 10.1111/j.1365-2958.2007.05734.x.
70.Burtnick MN, Brett PJ, Harding SV, Ngugi SA, Ribot WJ, Chantratita N, Scorpio A, Milne TS, Dean RE, Fritz DL, Peacock SJ, Prior JL, Atkins TP, DeShazer D. 2011. The Cluster 1 type VI secretion system is a major virulence determinant in *Burkholderia pseudomallei*. Infection and Immunity 79:1512-1525. 10.1128/IAI.01218-10.

71.Spiewak HL, Shastri S, Zhang L, Schwager S, Eberl L, Vergunst AC, Thomas MS. 2019. *Burkholderia cenocepacia* utilizes a type VI secretion system for bacterial competition. MicrobiologyOpen 8 10.1002/mbo3.774.
72.St Geme JW. 1994. The HMW1 adhesin of nontypeable *Haemophilus influenzae* recognizes sialylated glycoprotein receptors on cultured human epithelial cells. Infection and Immunity 62:3881-3889. 10.1128/iai.62.9.3881-3889.1994.
73.Cope LD, Thomas SE, Hrkal Z, Hansen EJ. 1998. Binding of heme-hemopexin complexes by soluble HxuA protein allows utilization of this complexed heme by *Haemophilus influenzae*. Infection and Immunity 66:4511-4516. 10.1128/IAI.66.9.4511-4516.1998.
74.Cotter PA, Yuk MH, Mattoo S, Akerley BJ, Boschwitz J, Relman DA, Miller JF. 1998. Filamentous hemagglutinin of *Bordetella bronchiseptica* Is required for efficient establishment of tracheal colonization. Infection and Immunity 66:5921-5929. 10.1128/IAI.66.12.5921-5929.1998.
75.Jacob-Dubuisson F, Fernandez R, Coutte L. 2004. Protein secretion through autotransporter and two-partner pathways. Biochimica et Biophysica Acta (BBA) - Molecular Cell Research 1694:235-257. 10.1016/j.bbamcr.2004.03.008.
76.Aoki SK, Pamma R, Hernday AD, Bickham JE, Braaten BA, Low DA. 2005. Contact-dependent inhibition of growth in *Escherichia coli*. Science (New York, NY) 309:1245-1248. 10.1126/science.1115109.
77.Henderson IR, Navarro-Garcia F, Desvaux Ml, Fernandez RC, Ala'Aldeen D. 2004. Type V Protein secretion pathway: the autotransporter story. Microbiology and Molecular Biology Reviews 68:692-744. 10.1128/MMBR.68.4.692-744.2004.
78.Leo JC, Grin I, Linke D. 2012. Type V secretion: mechanism(s) of autotransport through the bacterial outer membrane. Philosophical Transactions of the Royal Society B: Biological Sciences 367:1088-1101. 10.1098/rstb.2011.0208.
79.Locht C, Berlin P, Menozzi FD, Renauld† G. 1993. The filamentous haemagglutinin, a multifaceted adhesin produced by virulent Bordetella spp. Molecular Microbiology 9:653-660. 10.1111/j.1365-2958.1993.tb01725.x.
80.Kajava AV, Cheng N, Cleaver R, Kessel M, Simon MN, Willery E, Jacob-Dubuisson F, Locht C, Steven AC. 2001. Beta-helix model for the filamentous haemagglutinin adhesin of *Bordetella pertussis* and related bacterial secretory proteins. Molecular Microbiology 42:279-292. 10.1046/j.1365-2958.2001.02598.x.
81.Clantin B, Hodak H, Willery E, Locht C, Jacob-Dubuisson F, Villeret V. 2004. The crystal structure of filamentous hemagglutinin secretion domain and its implications for the two-partner secretion pathway. Proceedings of the National Academy of Sciences 101:6194-6199. 10.1073/pnas.0400291101.
82.Kajava AV, Steven AC. 2006. The turn of the screw: Variations of the abundant β-solenoid motif in passenger domains of Type V secretory proteins. Journal of Structural Biology 155:306-315. 10.1016/j.jsb.2006.01.015.

83.Jacob-Dubuisson F, El-Hamel C, Saint N, Guédin S, Willery E, Molle G, Locht C. 1999. Channel formation by FhaC, the outer membrane protein involved in the secretion of the *Bordetella pertussis* filamentous hemagglutinin. Journal of Biological Chemistry 274:37731-37735. 10.1074/jbc.274.53.37731.
84.Guédin S, Willery E, Tommassen J, Fort E, Drobecq H, Locht C, Jacob-Dubuisson F. 2000. Novel topological Features of FhaC, the outer membrane transporter involved in the secretion of the *Bordetella pertussis* filamentous hemagglutinin. Journal of Biological Chemistry 275:30202-30210. 10.1074/jbc.M005515200.
85.Thanassi DG, Stathopoulos C, Karkal A, Li H. 2005. Protein secretion in the absence of ATP: the autotransporter, two-partner secretion and chaperone/usher pathways of Gram-negative bacteria (Review). Molecular Membrane Biology 22:63-72. https://doi.org/10.1080/09687860500063290.
86.Roman-Hernandez G, Peterson JH, Bernstein HD. 2014. Reconstitution of bacterial autotransporter assembly using purified components. eLife 3 10.7554/eLife.04234.
87.Klauser T, Pohlner J, Meyer TF. 1993. The secretion pathway of IgA protease-type proteins in gram-negative bacteria. BioEssays 15:799-805. 10.1002/bies.950151205.
88.Leyton DL, Rossiter AE, Henderson IR. 2012. From self sufficiency to dependence: mechanisms and factors important for autotransporter biogenesis. Nature Reviews Microbiology 10:213-225. 10.1038/nrmicro2733.
89.Jacob-Dubuisson F, Guérin J, Baelen S, Clantin B. 2013. Two-partner secretion: as simple as it sounds? Research in Microbiology 164:583-595. 10.1016/j.resmic.2013.03.009.
90.Jacob-Dubuisson F, Locht C, Antoine R. 2001. Two-partner secretion in Gram-negative bacteria: a thrifty, specific pathway for large virulence proteins. Molecular Microbiology 40:306-313. 10.1046/j.1365-2958.2001.02278.x.
91.Meuskens I, Saragliadis A, Leo JC, Linke D. 2019. Type V Secretion Systems: An overview of passenger domain functions. Frontiers in Microbiology 10 10.3389/fmicb.2019.01163.
92.Delattre AS, Saint N, Clantin B, Willery E, Lippens G, Locht C, Villeret V, Jacob-Dubuisson F. 2011. Substrate recognition by the POTRA domains of TpsB transporter FhaC. Molecular Microbiology 81:99-112. 10.1111/j.1365-2958.2011.07680.x.
93.Cotter SE, Surana NK, St. Geme JW. 2005. Trimeric autotransporters: a distinct subfamily of autotransporter proteins. Trends in Microbiology 13:199-205. 10.1016/j.tim.2005.03.004.
94.Linke D, Riess T, Autenrieth IB, Lupas A, Kempf VAJ. 2006. Trimeric autotransporter adhesins: variable structure, common function. Trends in Microbiology 14:264-270. 10.1016/j.tim.2006.04.005.
95.Guérin J, Bigot S, Schneider R, Buchanan SK, Jacob-Dubuisson F. 2017. Two-partner secretion: combining efficiency and simplicity in the secretion of large proteins for bacteria-host and bacteria-bacteria interactions. Frontiers in cellular and infection microbiology 7:148-148. 10.3389/fcimb.2017.00148.

96.Salacha R, Kovačić F, Brochier-Armanet C, Wilhelm S, Tommassen J, Filloux A, Voulhoux R, Bleves S. 2010. The *Pseudomonas aeruginosa* patatin-like protein PlpD is the archetype of a novel Type V secretion system. Environmental Microbiology 10.1111/j.1462-2920.2010.02174.x.
97.Casasanta MA, Yoo CC, Smith HB, Duncan AJ, Cochrane K, Varano AC, Allen-Vercoe E, Slade DJ. 2017. A chemical and biological toolbox for Type Vd secretion: Characterization of the phospholipase A1 autotransporter FplA from *Fusobacterium nucleatum*. Journal of Biological Chemistry 292:20240-20254. 10.1074/jbc.M117.819144.
98.da Mata Madeira PV, Zouhir S, Basso P, Neves D, Laubier A, Salacha R, Bleves S, Faudry E, Contreras-Martel C, Dessen A. 2016. Structural basis of lipid targeting and destruction by the Type V secretion system of *Pseudomonas aeruginosa*. Journal of Molecular Biology 428:1790-1803. 10.1016/j.jmb.2016.03.012.
99.Fairman James W, Dautin N, Wojtowicz D, Liu W, Noinaj N, Barnard Travis J, Udho E, Przytycka Teresa M, Cherezov V, Buchanan Susan K. 2012. Crystal structures of the outer membrane domain of Intimin and Invasin from enterohemorrhagic *E. coli* and Enteropathogenic *Y. pseudotuberculosis*. Structure 20:1233-1243. 10.1016/j.str.2012.04.011.
100.Oberhettinger P, Schütz M, Leo JC, Heinz N, Berger J, Autenrieth IB, Linke D. 2012. Intimin and Invasin export their C-terminus to the bacterial Cell surface using an inverse mechanism compared to classical autotransport. PLoS ONE 7:e47069-e47069. 10.1371/journal.pone.0047069.
101.Tsai JC, Yen M-R, Castillo R, Leyton DL, Henderson IR, Saier MH. 2010. The bacterial intimins and invasins: A large and novel family of secreted proteins. PLoS ONE 5:e14403-e14403. 10.1371/journal.pone.0014403.
102.Leo JC, Oberhettinger P, Chaubey M, Schütz M, Kühner D, Bertsche U, Schwarz H, Götz F, Autenrieth IB, Coles M, Linke D. 2015. The Intimin periplasmic domain mediates dimerisation and binding to peptidoglycan. Molecular Microbiology 95:80-100. 10.1111/mmi.12840.
103.Heinz E, Stubenrauch CJ, Grinter R, Croft NP, Purcell AW, Strugnell RA, Dougan G, Lithgow T. 2016. Conserved features in the structure, mechanism, and biogenesis of the inverse autotransporter protein family. Genome Biology and Evolution 8:1690-1705. 10.1093/gbe/evw112.
104.ur Rahman S, van Ulsen P. 2013. System specificity of the TpsB transporters of coexpressed two-partner secretion systems of *Neisseria meningitidis*. Journal of Bacteriology 195:788-797. 10.1128/JB.01355-12.
105.Chevalier N, Moser M, Koch H-G, Schimz K-L, Willery E, Locht C, Jacob-Dubuisson F, Müller M. 2004. Membrane targeting of a bacterial virulence factor harbouring an extended signal peptide. Microbial Physiology 8:7-18. 10.1159/000082076.
106.Mazar J, Cotter PA. 2006. Topology and maturation of filamentous haemagglutinin suggest a new model for two-partner secretion. Molecular Microbiology 62:641-654. 10.1111/j.1365-2958.2006.05392.x.

107.Heinz E, Lithgow T. 2014. A comprehensive analysis of the Omp85/TpsB protein superfamily structural diversity, taxonomic occurrence, and evolution. Frontiers in Microbiology 5 10.3389/fmicb.2014.00370.
108.Doyle MT, Bernstein HD. 2022. Function of the Omp85 superfamily of outer membrane protein assembly factors and polypeptide transporters. Annual Review of Microbiology 76:259-279. 10.1146/annurev-micro-033021-023719.
109.Simmerman RF, Dave AM, Bruce BD. 2014. Structure and function of POTRA Domains of Omp85/TPS superfamily, p 1-34.
110.ur Rahman S, Arenas J, Öztürk H, Dekker N, van Ulsen P. 2014. The polypeptide transport-associated (POTRA) domains of TpsB transporters determine the system specificity of two-partner secretion systems. Journal of Biological Chemistry 289:19799-19809. 10.1074/jbc.M113.544627.
111.Clantin B, Delattre A-S, Rucktooa P, Saint N, Méli AC, Locht C, Jacob-Dubuisson F, Villeret V. 2007. Structure of the membrane protein FhaC: A member of the Omp85-TpsB transporter superfamily. Science 317:957-961. 10.1126/science.1143860.
112.Sánchez-Pulido L, Devos D, Genevrois S, Vicente M, Valencia A. 2003. POTRA: a conserved domain in the FtsQ family and a class of β-barrel outer membrane proteins. Trends in Biochemical Sciences 28:523-526. 10.1016/j.tibs.2003.08.003.
113.Maier T, Clantin B, Gruss F, Dewitte F, Delattre A-S, Jacob-Dubuisson F, Hiller S, Villeret V. 2015. Conserved Omp85 lid-lock structure and substrate recognition in FhaC. Nature Communications 6:7452-7452. 10.1038/ncomms8452.
114.Guerin J, Botos I, Zhang Z, Lundquist K, Gumbart JC, Buchanan SK. 2020. Structural insight into toxin secretion by contact-dependent growth inhibition transporters. eLife 9 10.7554/eLife.58100.
115.Hodak H, Jacob-Dubuisson F. 2007. Current challenges in autotransport and two-partner protein secretion pathways. Research in Microbiology 158:631-637. 10.1016/j.resmic.2007.08.001.
116.Peterson JH, Tian P, Ieva R, Dautin N, Bernstein HD. 2010. Secretion of a bacterial virulence factor is driven by the folding of a C-terminal segment. Proceedings of the National Academy of Sciences 107:17739-17744. 10.1073/pnas.1009491107.
117.Renn Jonathan P, Junker M, Besingi Richard N, Braselmann E, Clark Patricia L. 2012. ATP-independent control of autotransporter virulence protein transport via the folding properties of the secreted protein. Chemistry & Biology 19:287-296. 10.1016/j.chembiol.2011.11.009.
118.Junker M, Besingi RN, Clark PL. 2009. Vectorial transport and folding of an autotransporter virulence protein during outer membrane secretion. Molecular Microbiology 71:1323-1332. 10.1111/j.1365-2958.2009.06607.x.
119.Szabady RL, Peterson JH, Skillman KM, Bernstein HD. 2005. An unusual signal peptide facilitates late steps in the biogenesis of a bacterial autotransporter. Proceedings of the National Academy of Sciences 102:221-226. 10.1073/pnas.0406055102.

120. Leyton DL, De Luna MdG, Sevastsyanovich YR, Tveen Jensen K, Browning DF, Scott-Tucker A, Henderson IR. 2010. The unusual extended signal peptide region is not required for secretion and function of an *Escherichia coli* autotransporter. FEMS Microbiology Letters 311:133-139. 10.1111/j.1574-6968.2010.02081.x.
121. Dautin N. 2021. Folding control in the path of Type 5 secretion. Toxins 13:341-341. 10.3390/toxins13050341.
122. C. Leo J, Linke D. 2018. A unified model for BAM function that takes into account type Vc secretion and species differences in BAM composition. AIMS Microbiology 4:455-468. 10.3934/microbiol.2018.3.455.
123. Ryoo D, Rydmark MO, Pang YT, Lundquist KP, Linke D, Gumbart JC. 2020. BamA is required for autotransporter secretion. Biochimica et Biophysica Acta (BBA) - General Subjects 1864:129581-129581. 10.1016/j.bbagen.2020.129581.
124. Baud C, Hodak H, Willery E, Drobecq H, Locht C, Jamin M, Jacob-Dubuisson F. 2009. Role of DegP for two-partner secretion in *Bordetella*. Molecular Microbiology 74:315-329. 10.1111/j.1365-2958.2009.06860.x.
125. Yan Z, Hussain S, Wang X, Bernstein HD, Bardwell JCA. 2019. Chaperone OsmY facilitates the biogenesis of a major family of autotransporters. Molecular Microbiology 112:1373-1387. 10.1111/mmi.14358.
126. Nelson KM, Young GM, Miller VL. 2001. Identification of a locus Involved in systemic dissemination of *Yersinia enterocolitica*. Infection and Immunity 69:6201-6208. 10.1128/IAI.69.10.6201-6208.2001.
127. Scarlato V, Aricò B, Prugnola A, Rappuoli R. 1991. Sequential activation and environmental regulation of virulence genes in *Bordetella pertussis*. The EMBO Journal 10:3971-3975. 10.1002/j.1460-2075.1991.tb04967.x.
128. Borlee BR, Goldman AD, Murakami K, Samudrala R, Wozniak DJ, Parsek MR. 2010. *Pseudomonas aeruginosa* uses a cyclic-di-GMP-regulated adhesin to reinforce the biofilm extracellular matrix. Molecular Microbiology 75:827-842. 10.1111/j.1365-2958.2009.06991.x.
129. Anderson MS, Garcia EC, Cotter PA. 2014. Kind discrimination and competitive exclusion mediated by contact-dependent growth inhibition systems shape biofilm community structure. PLoS Pathogens 10:e1004076-e1004076. 10.1371/journal.ppat.1004076.
130. Anderson MS, Garcia EC, Cotter PA. 2012. The *Burkholderia bcpAIOB* genes define unique classes of two-partner secretion and contact dependent growth inhibition systems. PLoS genetics 8:e1002877-e1002877. 10.1371/journal.pgen.1002877.
131. Garcia EC, Perault AI, Marlatt SA, Cotter PA. 2016. Interbacterial signaling via *Burkholderia* contact-dependent growth inhibition system proteins. Proceedings of the National Academy of Sciences 113:8296-8301. 10.1073/pnas.1606323113.
132. Aoki SK, Diner EJ, de Roodenbeke CtK, Burgess BR, Poole SJ, Braaten BA, Jones AM, Webb JS, Hayes CS, Cotter PA, Low DA. 2010. A widespread family of polymorphic contact-dependent toxin delivery systems in bacteria. Nature 468:439-442. 10.1038/nature09490.

133. Perault AI, Cotter PA. 2018. Three distinct contact-dependent growth inhibition systems mediate interbacterial competition by the cystic fibrosis pathogen *Burkholderia dolosa*. Journal of bacteriology 200 https://doi.org/10.1128/jb.00428-18.
134. Myers-Morales T, Oates AE, Byrd MS, Garcia EC. 2019. *Burkholderia cepacia* complex contact-dependent growth inhibition systems mediate interbacterial competition. Journal of bacteriology 201 10.1128/JB.00012-19.
135. Ruhe ZC, Subramanian P, Song K, Nguyen JY, Stevens TA, Low DA, Jensen GJ, Hayes CS. 2018. Programmed secretion arrest and receptor-triggered toxin export during antibacterial contact-dependent growth inhibition. Cell 175:921-933.e14. 10.1016/j.cell.2018.10.033.
136. Nikolakakis K, Amber S, Wilbur JS, Diner EJ, Aoki SK, Poole SJ, Tuanyok A, Keim PS, Peacock S, Hayes CS, Low DA. 2012. The toxin/immunity network of *Burkholderia pseudomallei* contact-dependent growth inhibition (CDI) systems. Molecular Microbiology 84:516-529. 10.1111/j.1365-2958.2012.08039.x.
137. Webb JS, Nikolakakis KC, Willett JLE, Aoki SK, Hayes CS, Low DA. 2013. Delivery of CdiA nuclease toxins into target cells during contact-dependent growth inhibition. PloS one 8:e57609-e57609. 10.1371/journal.pone.0057609.
138. Aoki SK, Malinverni JC, Jacoby K, Thomas B, Pamma R, Trinh BN, Remers S, Webb J, Braaten BA, Silhavy TJ, Low DA. 2008. Contact-dependent growth inhibition requires the essential outer membrane protein BamA (YaeT) as the receptor and the inner membrane transport protein AcrB. Molecular Microbiology 70:323-340. 10.1111/j.1365-2958.2008.06404.x.
139. Beck CM, Willett JLE, Cunningham DA, Kim JJ, Low DA, Hayes CS. 2016. CdiA effectors from uropathogenic *Escherichia coli* use heterotrimeric ssmoporins as receptors to recognize target bacteria. PLOS Pathogens 12:e1005925-e1005925. 10.1371/journal.ppat.1005925.
140. Ruhe ZC, Nguyen JY, Xiong J, Koskiniemi S, Beck CM, Perkins BR, Low DA, Hayes CS. 2017. CdiA effectors use modular receptor-binding domains to recognize target bacteria. mBio 8 10.1128/mBio.00290-17.
141. Lin H-H, Filloux A, Lai E-M. 2020. Role of recipient susceptibility factors during contact-dependent interbacterial competition. Frontiers in Microbiology 11 10.3389/fmicb.2020.603652.
142. Halvorsen TM, Garza-Sánchez F, Ruhe ZC, Bartelli NL, Chan NA, Nguyen JY, Low DA, Hayes CS. 2021. Lipidation of class IV CdiA effector proteins promotes target cell recognition during contact-dependent growth inhibition. mBio 12 10.1128/mBio.02530-21.
143. Elery ZK, Oates AE, Myers-Morales T, Garcia EC. 2022. Recipient cell factors influence interbacterial competition mediated by two distinct *Burkholderia dolosa* contact-dependent growth inhibition systems. Journal of Bacteriology 204 10.1128/jb.00541-21.
144. Koskiniemi S, Garza-Sánchez F, Edman N, Chaudhuri S, Poole SJ, Manoil C, Hayes CS, Low DA. 2015. Genetic analysis of the CDI pathway from

Burkholderia pseudomallei 1026b. PLOS ONE 10:e0120265-e0120265. 10.1371/journal.pone.0120265.
145. Ruhe ZC, Nguyen JY, Beck CM, Low DA, Hayes CS. 2014. The proton-motive force is required for translocation of CDI toxins across the inner membrane of target bacteria. Molecular Microbiology 94:466-481. 10.1111/mmi.12779.
146. Willett JLE, Gucinski GC, Fatherree JP, Low DA, Hayes CS. 2015. Contact-dependent growth inhibition toxins exploit multiple independent cell-entry pathways. Proceedings of the National Academy of Sciences of the United States of America 112:11341-11346. 10.1073/pnas.1512124112.
147. Myers-Morales T, Sim MMS, DuCote TJ, Garcia EC. 2021. *Burkholderia multivorans* requires species-specific GltJK for entry of a contact-dependent growth inhibition system protein. Molecular Microbiology 116:957-973. 10.1111/mmi.14783.
148. Diner EJ, Beck CM, Webb JS, Low DA, Hayes CS. 2012. Identification of a target cell permissive factor required for contact-dependent growth inhibition (CDI). Genes & Development 26:515-525. 10.1101/gad.182345.111.
149. Johnson PM, Beck CM, Morse RP, Garza-Sánchez F, Low DA, Hayes CS, Goulding CW. 2016. Unraveling the essential role of CysK in CDI toxin activation. Proceedings of the National Academy of Sciences 113:9792-9797. 10.1073/pnas.1607112113.
150. Jones AM, Garza-Sánchez F, So J, Hayes CS, Low DA. 2017. Activation of contact-dependent antibacterial tRNase toxins by translation elongation factors. Proceedings of the National Academy of Sciences 114 10.1073/pnas.1619273114.
151. Michalska K, Gucinski GC, Garza-Sánchez F, Johnson PM, Stols LM, Eschenfeldt WH, Babnigg G, Low DA, Goulding CW, Joachimiak A, Hayes CS. 2017. Structure of a novel antibacterial toxin that exploits elongation factor Tu to cleave specific transfer RNAs. Nucleic Acids Research 45:10306-10320. 10.1093/nar/gkx700.
152. Ruhe ZC, Wallace AB, Low DA, Hayes CS. 2013. Receptor polymorphism restricts contact-dependent growth inhibition to members of the same species. mBio 4 10.1128/mBio.00480-13.
153. Rojas CM, Ham JH, Deng W-L, Doyle JJ, Collmer A. 2002. HecA, a member of a class of adhesins produced by diverse pathogenic bacteria, contributes to the attachment, aggregation, epidermal cell killing, and virulence phenotypes of *Erwinia chrysanthemi* EC16 on *Nicotiana clevelandii* seedlings. Proceedings of the National Academy of Sciences 99:13142-13147. 10.1073/pnas.202358699.
154. Harding CM, Pulido MR, Di Venanzio G, Kinsella RL, Webb AI, Scott NE, Pachón J, Feldman MF. 2017. Pathogenic *Acinetobacter* species have a functional type I secretion system and contact-dependent inhibition systems. Journal of Biological Chemistry 292:9075-9087. 10.1074/jbc.M117.781575.
155. Mercy C, Ize B, Salcedo SP, de Bentzmann S, Bigot S. 2016. Functional characterization of *Pseudomonas* contact dependent growth inhibition (CDI)

systems. PLOS ONE 11:e0147435-e0147435. 10.1371/journal.pone.0147435.
156. Ruhe ZC, Townsley L, Wallace AB, King A, Van der Woude MW, Low DA, Yildiz FH, Hayes CS. 2015. CdiA promotes receptor-independent intercellular adhesion. Molecular Microbiology 98:175-192. 10.1111/mmi.13114.
157. Melvin JA, Gaston JR, Phillips SN, Springer MJ, Marshall CW, Shanks RMQ, Bomberger JM. 2017. *Pseudomonas aeruginosa* contact-dependent growth Inhibition plays dual role in host-pathogen interactions. mSphere 2 10.1128/mSphere.00336-17.
158. Harding CM, Hennon SW, Feldman MF. 2018. Uncovering the mechanisms of *Acinetobacter baumannii* virulence. Nature Reviews Microbiology 16:91-102. 10.1038/nrmicro.2017.148.
159. Choi K-H, Gaynor JB, White KG, Lopez C, Bosio CM, Karkhoff-Schweizer RR, Schweizer HP. 2005. A Tn7-based broad-range bacterial cloning and expression system. Nature methods 2:443-8. 10.1038/nmeth765.
160. López CM, Rholl DA, Trunck LA, Schweizer HP. 2009. Versatile dual-technology system for markerless allele replacement in *Burkholderia pseudomallei*. Applied and environmental microbiology 75:6496-503. 10.1128/AEM.01669-09.
161. Choi K-H, Mima T, Casart Y, Rholl D, Kumar A, Beacham IR, Schweizer HP. 2008. Genetic tools for select-agent-compliant manipulation of *Burkholderia pseudomallei*. Applied and Environmental Microbiology 74:1064-1075. 10.1128/AEM.02430-07.
162. Schmittgen TD, Livak KJ. 2008. Analyzing real-time PCR data by the comparative CT method. Nature Protocols 3:1101-1108. 10.1038/nprot.2008.73.
163. da Silva PRA, Vidal MS, de Paula Soares C, Polese V, Simões-Araújo JL, Baldani JI. 2016. Selection and evaluation of reference genes for RT-qPCR expression studies on *Burkholderia tropica* strain Ppe8, a sugarcane-associated diazotrophic bacterium grown with different carbon sources or sugarcane juice. Antonie van Leeuwenhoek 109:1493-1502. 10.1007/s10482-016-0751-0.
164. Jumper J, Evans R, Pritzel A, Green T, Figurnov M, Ronneberger O, Tunyasuvunakool K, Bates R, Žídek A, Potapenko A, Bridgland A, Meyer C, Kohl SAA, Ballard AJ, Cowie A, Romera-Paredes B, Nikolov S, Jain R, Adler J, Back T, Petersen S, Reiman D, Clancy E, Zielinski M, Steinegger M, Pacholska M, Berghammer T, Bodenstein S, Silver D, Vinyals O, Senior AW, Kavukcuoglu K, Kohli P, Hassabis D. 2021. Highly accurate protein structure prediction with AlphaFold. Nature 596:583-589. 10.1038/s41586-021-03819-2.
165. Mirdita M, Schütze K, Moriwaki Y, Heo L, Ovchinnikov S, Steinegger M. 2022. ColabFold: making protein folding accessible to all. Nature Methods 19:679-682. 10.1038/s41592-022-01488-1.
166. Varadi M, Anyango S, Deshpande M, Nair S, Natassia C, Yordanova G, Yuan D, Stroe O, Wood G, Laydon A, Žídek A, Green T, Tunyasuvunakool K, Petersen S, Jumper J, Clancy E, Green R, Vora A, Lutfi M, Figurnov M,

Cowie A, Hobbs N, Kohli P, Kleywegt G, Birney E, Hassabis D, Velankar S. 2022. AlphaFold protein structure database: massively expanding the structural coverage of protein-sequence space with high-accuracy models. Nucleic Acids Research 50:D439-D444. 10.1093/nar/gkab1061.
167. Pettersen EF, Goddard TD, Huang CC, Meng EC, Couch GS, Croll TI, Morris JH, Ferrin TE. 2021. UCSF ChimeraX: Structure visualization for researchers, educators, and developers. Protein Science 30:70-82. https://doi.org/10.1002/pro.3943.
168. Cavard D, Baty D, Howard P, Verheij H, Lazdunski C. 1987. Lipoprotein nature of the colicin A lysis protein: effect of amino acid substitutions at the site of modification and processing. Journal of Bacteriology:2187-2194.
169. Kim S, Malinverni JC, Sliz P, Silhavy TJ, Harrison SC, Kahne D. 2007. Structure and function of an essential component of the outer membrane protein assembly machine. Science 317:961-964. 10.1126/science.1143993.
170. Aschtgen M-S, Bernard CS, De Bentzmann S, Lloubes R, Cascales E. 2008. SciN Is an outer membrane lipoprotein required for Type VI secretion in Enteroaggregative *Escherichia coli*. The Journal of Bacteriology 190:7523-7523. 10.1128/JB.00945-08.
171. Grin I, Hartmann MD, Sauer G, Hernandez Alvarez B, Schütz M, Wagner S, Madlung J, Macek B, Felipe-Lopez A, Hensel M, Lupas A, Linke D. 2014. A trimeric lipoprotein assists in trimeric autotransporter biogenesis in *Enterobacteria*. Journal of Biological Chemistry 289:7388-7398. 10.1074/jbc.M113.513275.
172. Speare L, Woo M, Dunn AK, Septer AN. 2022. A putative lipoprotein mediates cell-cell contact for Type VI secretion system-dependent killing of specific competitors. mBio 13 10.1128/mbio.03085-21.
173. Hart EM, Silhavy TJ. 2020. Functions of the BamBCDE lipoproteins revealed by bypass mutations in BamA. Journal of Bacteriology 202 10.1128/JB.00401-20.
174. Castanié-Cornet M-P, Cam K, Jacq A. 2006. RcsF Is an outer membrane lipoprotein Involved in the RcsCDB phosphorelay signaling pathway in *Escherichia coli*. Journal of Bacteriology 188:4264-4270. 10.1128/JB.00004-06.
175. Nguyen HT, Wolff KA, Cartabuke RH, Ogwang S, Nguyen L. 2010. A lipoprotein modulates activity of the MtrAB two-component system to provide intrinsic multidrug resistance, cytokinetic control and cell wall homeostasis in *Mycobacterium*. Molecular Microbiology 76:348-364. 10.1111/j.1365-2958.2010.07110.x.
176. Göpel Y, Görke B. 2018. Interaction of lipoprotein QseG with sensor kinase QseE in the periplasm controls the phosphorylation state of the two-component system QseE/QseF in Escherichia coli. PLOS Genetics 14:e1007547-e1007547. 10.1371/journal.pgen.1007547.
177. Delhaye A, Laloux G, Collet J-F. 2019. The lipoprotein NlpE Is a Cpx sensor that serves as a sentinel for protein sorting and folding defects in the *Escherichia coli* envelope. Journal of Bacteriology 201 10.1128/JB.00611-18.

178.Simpson BW, Trent MS. 2019. Emerging roles for NlpE as a sensor for lipoprotein maturation and transport to the outer membrane in *Escherichia coli*. mBio 10 10.1128/mBio.01302-19.
179.Tokuda H, Matsuyama SI. 2004. Sorting of lipoproteins to the outer membrane in *E. coli*. Biochimica et Biophysica Acta - Molecular Cell Research 1693:5-13. 10.1016/j.bbamcr.2004.02.005.
180.Zückert WR. 2014. Secretion of bacterial lipoproteins: through the cytoplasmic membrane, the periplasm and beyond. BBA - Molecular Cell Research 1843:1509-1516. 10.1016/j.bbamcr.2014.04.022.
181.Inouye S, Franceschini T, Sato M, Itakura K, Inouye M. 1983. Prolipoprotein signal peptidase of *Escherichia coli* requires a cysteine residue at the cleavage site. The EMBO Journal 2:87-91. 10.1002/j.1460-2075.1983.tb01386.x.
182.Yakushi T, Tajima T, Matsuyama S, Tokuda H. 1997. Lethality of the covalent linkage between mislocalized major outer membrane lipoprotein and the peptidoglycan of *Escherichia coli*. Journal of Bacteriology 179:2857-2862. 10.1128/jb.179.9.2857-2862.1997.
183.Tanaka K, Matsuyama S-I, Tokuda H. 2001. Deletion of *lolB* , encoding an outer membrane lipoprotein, is lethal for *Escherichia coli* and causes accumulation of lipoprotein localization litermediates in the periplasm. Journal of Bacteriology 183:6538-6542. 10.1128/JB.183.22.6538-6542.2001.
184.Sankaran K, Wu HC. 1994. Lipid modification of bacterial prolipoprotein transfer of diacylglycerol moiety from phosphatidylglycerol. Journal Of Biological Chemistry 269:19701-19706.
185.Yamaguchi K, Yu F, Inouye M. 1988. A single amino acid determinant of the membrane localization of lipoproteins in *E. coli*. Cell 53:423-432. 10.1016/0092-8674(88)90162-6.
186.Schulze RJ, Zückert WR. 2006. *Borrelia burgdorferi* lipoproteins are secreted to the outer surface by default. Molecular Microbiology 59:1473-1484. 10.1111/j.1365-2958.2006.05039.x.
187.Narita S-I, Tokuda H. 2007. Amino acids at positions 3 and 4 determine the membrane specificity of *Pseudomonas aeruginosa* lipoproteins. The Journal of biological chemistry 282:13372-13378.
188.Lewenza S, Vidal-Ingigliardi D, Pugsley AP. 2006. Direct visualization of red fluorescent lipoproteins indicates conservation of the membrane sorting rules in the family *Enterobacteriaceae*. Journal of Bacteriology 188:3516-3524. 10.1128/JB.188.10.3516-3524.2006.
189.Seydel A, Gounon P, Pugsley AP. 1999. Testing the '+2 rule' for lipoprotein sorting in the *Escherichia coli* cell envelope with a new genetic selection. Molecular Microbiology 34:810-821. 10.1046/j.1365-2958.1999.01647.x.
190.Zhang D, de Souza RF, Anantharaman V, Iyer LM, Aravind L. 2012. Polymorphic toxin systems: Comprehensive characterization of trafficking modes, processing, mechanisms of action, immunity and ecology using comparative genomics. Biology Direct 7:18-18. 10.1186/1745-6150-7-18.
191.Ikryannikova LN, Kurbatov LK, Gorokhovets NV, Zamyatnin AA. 2020. Contact-dependent growth inhibition in bacteria: do not get too close!

International Journal of Molecular Sciences 21:7990-7990. 10.3390/ijms21217990.
192. James R, Penfold CN, Moore GR, Kleanthous C. 2002. Killing of *E. coli* cells by E group nuclease colicins. Biochimie 84:381-389. 10.1016/S0300-9084(02)01450-5.
193. Cavard D. 2004. Role of Cal, the colicin A lysis protein, in two steps of colicin A release and in the interaction with colicin A–porin complexes. Microbiology 150:3867-3875. 10.1099/mic.0.27160-0.
194. Cascales E, Buchanan SK, Duché D, Kleanthous C, Lloubès R, Postle K, Riley M, Slatin S, Cavard D. 2007. Colicin Biology. Microbiology and Molecular Biology Reviews 71:158-229. 10.1128/mmbr.00036-06.
195. Roussin M, Rabarioelina S, Cluzeau L, Cayron J, Lesterlin C, Salcedo SP, Bigot S. 2019. Identification of a contact-dependent growth inhibition (CDI) system that reduces biofilm formation and host cell adhesion of *Acinetobacter baumannii* DSM30011 strain. Frontiers in Microbiology 10 10.3389/fmicb.2019.02450.
196. Wäneskog M, Halvorsen T, Filek K, Xu F, Hammarlöf DL, Hayes CS, Braaten BA, Low DA, Poole SJ, Koskiniemi S. 2021. *Escherichia coli* EC93 deploys two plasmid-encoded class I contact-dependent growth inhibition systems for antagonistic bacterial interactions. Microbial Genomics 7 10.1099/mgen.0.000534.
197. Knowles TJ, Jeeves M, Bobat S, Dancea F, McClelland D, Palmer T, Overduin M, Henderson IR. 2008. Fold and function of polypeptide transport-associated domains responsible for delivering unfolded proteins to membranes. Molecular Microbiology 68:1216-1227. 10.1111/j.1365-2958.2008.06225.x.
198. Bernstein HD. 2010. Type V Secretion: the autotransporter and two-partner secretion pathways. EcoSal Plus 4 10.1128/ecosalplus.4.3.6.
199. Baud C, Guérin J, Petit E, Lesne E, Dupré E, Locht C, Jacob-Dubuisson F. 2014. Translocation path of a substrate protein through its Omp85 transporter. Nature Communications 5:5271-5271. 10.1038/ncomms6271.
200. Guérin J, Baud C, Touati N, Saint N, Willery E, Locht C, Vezin H, Jacob-Dubuisson F. 2014. Conformational dynamics of protein transporter FhaC: large-scale motions of plug helix. Molecular Microbiology 92:1164-1176. 10.1111/mmi.12585.
201. Renauld-Mongénie G, Cornette J, Mielcarek N, Menozzi FD, Locht C. 1996. Distinct roles of the N-terminal and C-terminal precursor domains in the biogenesis of the *Bordetella pertussis* filamentous hemagglutinin. Journal of Bacteriology 178:1053-1060. 10.1128/jb.178.4.1053-1060.1996.
202. Grass S, St. Geme JW. 2000. Maturation and secretion of the non-typable *Haemophilus influenzae* HMW1 adhesin: roles of the N-terminal and C-terminal domains. Molecular Microbiology 36:55-67. 10.1046/j.1365-2958.2000.01812.x.
203. Parkhill J, Sebaihia M, Preston A, Murphy LD, Thomson N, Harris DE, Holden MTG, Churcher CM, Bentley SD, Mungall KL, Cerdeño-Tárraga AM, Temple L, James K, Harris B, Quail MA, Achtman M, Atkin R, Baker S,

Basham D, Bason N, Cherevach I, Chillingworth T, Collins M, Cronin A, Davis P, Doggett J, Feltwell T, Goble A, Hamlin N, Hauser H, Holroyd S, Jagels K, Leather S, Moule S, Norberczak H, O'Neil S, Ormond D, Price C, Rabbinowitsch E, Rutter S, Sanders M, Saunders D, Seeger K, Sharp S, Simmonds M, Skelton J, Squares R, Squares S, Stevens K, Unwin L, et al. 2003. Comparative analysis of the genome sequences of *Bordetella pertussis*, *Bordetella parapertussis* and *Bordetella bronchiseptica*. Nature Genetics 35:32-40. 10.1038/ng1227.

204. Julio SM, Cotter PA. 2005. Characterization of the filamentous hemagglutinin-like protein FhaS in *Bordetella bronchiseptica*. Infection and Immunity 73:4960-4971. 10.1128/IAI.73.8.4960-4971.2005.
205. Tuanyok A, Leadem BR, Auerbach RK, Beckstrom-Sternberg SM, Beckstrom-Sternberg JS, Mayo M, Wuthiekanun V, Brettin TS, Nierman WC, Peacock SJ, Currie BJ, Wagner DM, Keim P. 2008. Genomic islands from five strains of *Burkholderia pseudomallei*. BMC Genomics 9:566-566. 10.1186/1471-2164-9-566.
206. De Gregorio E, Esposito EP, Zarrilli R, Di Nocera PP. 2018. Contact-dependent growth inhibition proteins in *Acinetobacter baylyi* ADP1. Current Microbiology 75:1434-1440. 10.1007/s00284-018-1540-y.
207. Allen JP, Hauser AR. 2019. Diversity of contact-dependent growth inhibition systems of *Pseudomonas aeruginosa*. Journal of Bacteriology 201 10.1128/JB.00776-18.
208. De Gregorio E, Zarrilli R, Di Nocera PP. 2019. Contact-dependent growth inhibition systems in *Acinetobacter*. Scientific Reports 9:154-154. 10.1038/s41598-018-36427-8.
209. Allen JP, Ozer EA, Minasov G, Shuvalova L, Kiryukhina O, Anderson WF, Satchell KJF, Hauser AR. 2020. A comparative genomics approach identifies contact-dependent growth inhibition as a virulence determinant. Proceedings of the National Academy of Sciences 117:6811-6821. 10.1073/pnas.1919198117.
210. Leonard-Rivera M, Misra R. 2012. Conserved residues of the putative L6 Loop of *Escherichia coli* BamA play a critical role in the assembly of β-Barrel outer membrane proteins, including that of BamA itself. Journal of Bacteriology 194:4662-4668. 10.1128/JB.00825-12.

VITA

Zaria K. Elery

Education

University of Kentucky **2018-Pres.**

Ph.D. Microbiology

Northern Kentucky University **2015-2018**

B.S. in Biological Sciences

Professional Experience

Graduate Research assistant **2019-Pres.**

Advisor: Dr. Erin Garcia — Department of Microbiology, Immunology, and Molecular Genetics, University of Kentucky, College of Medicine

Undergraduate Research assistant **2018**

Advisors: Dr. Michael Guy and Dr. John Carmen — Department of Biology, Northern Kentucky University

Undergraduate Research assistant **2016-2017**

Advisor: Dr. John Carmen — Department of Biology, Northern Kentucky University

Summer Research Fellow **2016**

Advisors: Dr. Ayman El-Baz and Dr. Ahmed Shalaby — Department of Bioengineering, University of Louisville, School of Engineering

Honors and Awards

ASM Young Ambassador to the State of Kentucky – 2023

ASM Young Ambassador to the State of Kentucky – 2022

Midwest Microbial Pathogenesis Conference (MMPC) Travel Award – 2021

Publications

Elery Z., Myers-Morales T., Phillips E., Garcia E.C., (2023). Relaxed specificity of BcpB transporters leads to interplay between *Burkholderia cepacia* complex bacteria contact-dependent growth inhibition systems. mSphere. https://doi.org/10.1128/msphere.00303-23.

Elery Z*., Oates A*., Myers-Morales T., Garcia E.C., (2022). Recipient cell factors influence inter-bacterial competition mediated by two distinct *Burkholderia dolosa* contact-dependent growth inhibition systems. Journal of Bacteriology. https://doi.org/10.1128/jb.00541-21. *Co-first author